Norsk Romsenter
NORWEGIAN SPACE CENTRE

NERSC

esa

→ SEASAR 2012

The 4th International Workshop on Advances in SAR Oceanography

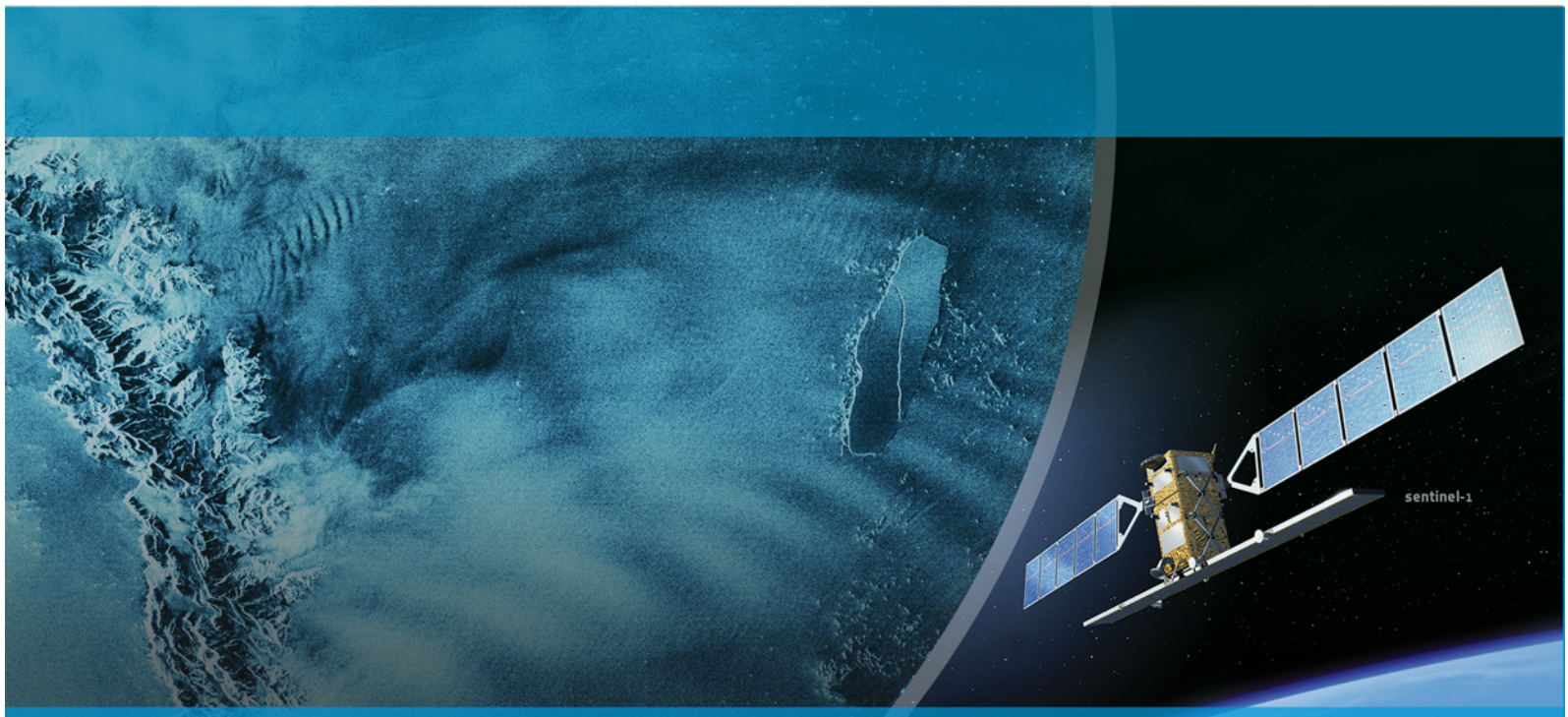

PROGRAMME & ABSTRACT BOOK

18-22 June 2012 | Tromsø, Norway

Programme & Abstract Book

SEASAR 2012

Advances in SAR Oceanography

18 - 22 June 2012

Tromsø, Norway

Table of Contents

Committees

Organising Committee

Yves-Louis Desnos (ESA)

Torbjørn Eltoft (University of Tromsø)

Johnny A. Johannessen (NERSC)

Harald Johnsen (NORUT)

Andrea Minchella (RSAC c/o ESA)

Jan-Petter Pedersen (KSAT)

Ann-Lisbeth Ruud (Norwegian Space Centre)

Per Erik Skrøvseth (Norwegian Space Centre)

Ulla Vayrynen (SERCO c/o ESA)

Scientific Committee

Prof. Werner Alpers (University of Hamburg, Germany)

Dr. Lotfi Aouf (MeteoFrance, France)

Dr. Camilla Brekke (University of Tromsø, Norway)

Dr. Bertrand Chapron (Ifremer, France)

Dr. Pablo Clemente Colon (NOAA, USA)

Dr. Fabrice Collard (CLS, France)

Dr. Jose da Silva (University of Porto, Portugal)

Dr. Knut-Frode Dagestad (NERSC, Norway)

Dr. Malcolm Davidson (ESA)

Dr. Daniel De Lisle (CSA, Canada)

Prof. Torbjørn Eltoft (University of Tromsø, Norway)

Dr. Dirk Geudtner (ESA)

Dr. Ben Holt (NASA, USA)

Dr. David Jackson (Canadian Ice Service, Canada)

Prof. Johnny A. Johannessen (NERSC, Norway)

Dr. Harald Johnsen (Norut, Norway)

Dr. Meng Junmin (FIO, China)

Prof. George Kallos (University of Athens, Greece)

Dr. Vincent Kerbaol (CLS, France)

Prof. Vladimir Kudryavtsev (NIERSC, Russia)

Dr. Susanne Lehner (DLR, Germany)

Dr. Joao Lorenzzetti (INPE, Brazil)

Mr. Nuno Miranda (ESA)

Dr. Francisco Ocampo-Torres (CICESE, Mexico)

Dr. Kim Partington (Polar Imaging, United Kingdom)

Dr. William A. Perrie (Fisheries and Oceans, Canada)

Dr. Simon Pinnock (ESA)

Mr. Pierre Potin (ESA)

Mrs. Betlem Rosich (ESA)

Prof. Stein Sandven (NERSC, Norway)

Mr. Ramon Torres (ESA)

Dr. Paris W. Vachon (Defence R&D Canada, Canada)

Dr. Christopher C. Wackerman (Veridian Systems, USA)

Dr. Jingsong Yang (SIO, China)

Programme

Day 1, Monday 18 June 2012

08:45 - 09:30 Registration and Poster mounting

Opening Session

09:30 - 09:50 Official Welcome (ESA, NSC)

Session: Future SAR missions (Sentinel-1, Radarsat Constellation Mission etc.)

Chairs: P.E. Skrøvseth, P. Potin

09:50 - 10:10 **Sentinel-1 Mission Operations Concept**
Pierre Potin [1], Siegfried Schmuck [1], Betlem Rosich [1]
[1]ESA / ESRIN, IT

10:10 - 10:30 **Sentinel-1 Instrument Overview**
Paul Snoeij [1], Ramon Torres [1], Dirk Geudtner [1], Michael Brown [1], Patrick Deghaye [1], Ignacio Navas-Traver [1], Allan Østergaard [1], Bjorn Rommen [1], Nicolas Floury [1], Malcolm Davidson [1]
[1]ESA, NL

10:30 - 10:50 **The Sentinel-1 core products and ground processor**
Nuno Miranda [1] et Al [1]
[1]ESA

10:50 - 11:20 *Coffee Break*

11:20 - 11:40 **A Marine Collaborative Ground Segment for the Sentinel-1 missions**
Fabrice Collard [1], Pierre Fabry [1], Alexis Mouche [1], Bertrand Chapron [2], René Garello [3]
[1]CLS, FR; [2]IFREMER, FR; [3]Telecom Bretagne, FR

11:40 - 12:00 **From RADARSAT-2 to RADARSAT Constellation Mission data continuity**
Daniel De Lisle [1]
[1]Canadian Space Agency, CA

12:00 - 12:20 **International Cooperation For Space-Based Global Maritime Awareness – The Next Step**
Harm Greidanus [1], Guy Thomas [2], Gordon Campbell [3], Karna Bryan [4]
[1]European Commission TP670, IT; [2]U.S. Coast Guard, USA; [3]ESA, IT; [4]NATO Undersea Research Centre, IT

12:20 - 12:50 **Round Table**

12:50 - 14:00 *Lunch*

Session: Methodology and techniques

Chairs: B. Chapron, L. Aouf

14:00 - 14:20 **Towards consistent inversion of wind, waves and surface current from SAR**
Bertrand Chapron [1], Vladimir Kudryavtsev [2], Fabrice Collard [3], Johnny Andre Johannessen [4], Alexis Mouche [3]
[1]Ifremer, FR; [2]NIERSC, RU; [3]CLS, FR; [4]NERSC, NO

14:20 - 14:40 **NEREIDS: New concepts in maritime surveillance for consolidating operational developments**
Gerard Margarit [1]
[1]GMV Idem, ES

14:40 - 15:00 **Toward automated classification of brightness fronts in RADARSAT-2 images of the ocean surface**
Christopher Jones [1]
[1]Dalhousie University Halifax, CA

15:00 - 15:20 **From 2D to 3D upper layer dynamics: The way forward**
Johnny Johannessen [1], Bertrand Chapron [2], Fabrice Collard [3], Vladimir Kudryavtsev [4], Annette Samuelsen [1]
[1]NERSC, NO; [2]Ifremer, FR; [3]CLS, FR; [4]NIERSC, RU

15:20 - 15:40 **Estimation of Underwater Topography using Satellite High Resolution Synthetic Aperture Radar Data**
Andrey L. Pleskachevsky[1], Susanne Lehner [1]
[1]German Aerospace Center, Remote Sensing Technology Institute, DE

15:40 - 16:10 **Round Table**

16:10 - 16:40 *Coffee Break*

Session: Wave mode processing algorithms, product validation and assimilation

Chairs: F. Collard, R. Romeiser

16:40 - 17:00 **On the impact of ASAR wave spectra in the operational wave model MFWAM**
Lotfi Aouf [1], Jean-Michel Lefèvre [1]
[1]Meteo France, FR

17:00 - 17:20 **Assimilation of ENVISAT ASAR Wave Mode Level 2 Product**
Saleh Abdalla [1], Peter Janssen [1], Jean-Raymond Bidlot [1]
[1]ECMWF, GB

17:20 - 17:40 **Application of SAR Wave Mode and Wide Swath Mode for Swell Tracking Across Ocean**
Fabrice Collard [1], Bertrand Chapron [2], Romain Husson [1], Fabrice Ardhuin [2]
[1]CLS, FR; [2]IFREMER, FR

17:40 - 18:00 **Global Numerical Wave Model Validation using ENVISAT ASAR Wave Mode and Radar Altimeter**
Data Xiaoming Li [1], Susanne Lehner [1], Thomas Bruns [2]
[1]German Aerospace Center (DLR), DE; [2]German Weather Service (DWD), DE

18:00 - 18:30 **Round Table**

18:30 - 19:50 *Welcome Cocktail*

Day 2, Tuesday 19 June 2012

Session: Wave retrievals and applications

Chairs: H. Johnsen, F. Ocampo-Torres

08:30 - 08:50 **The GLOBWAVE project**
Fabrice COLLARD [1], Geoff Busswell [2], Ellis Ash [3], Jean-Francois Piolle [4], Helen Snaith [5], Simon Pinnock [6]
[1]CLS, FR; [2]Logica, UK; [3]Satellite Oceanographic Consultants, UK; [4]IFREMER , FR; [5]National Oceanography Centre Southampton, UK; [6]ESA/ESRIN, IT

08:50 - 09:10 **SAR Wave Mode Processing – Improvements towards Sentinel-1 Mission**
Harald Johnsen [1], Fabrice Collard [2]
[1]Norut, NO; [2]CLS, FR

09:10 - 09:30 **Wave Rretrievals from ScanSAR Images under Tropical Cyclone Conditions**
Roland Romeiser [1], Hans Graber [1]
[1]University of Miami, US

09:30 - 09:50 **Sea State Measurements using TerraSAR-X Data**
Miguel Bruck [1], Susanne Lehner [1]
[1]DLR, DE

09:50 - 10:10 **Ocean Waves Inferred from X-Band Synthetic Aperture Radar Images of the Sea Surface**
Francisco Ocampo-Torres [1]
[1]CICESE, MX

10:10 - 10:30 **Wind and Wave Transformations in the Vicinity of Islands Employing SAR Precision Images**
Nelson Violante-carvalho [1]
[1]Coppe-ufrj, BR

10:30 - 11:00 *Coffee Break*

11:00 - 11:20 **Swell Emulation in Coastal Zone**
Fabrice COLLARD [1]
[1]CLS, FR

11:20 - 11:40 **Evaluation of High Resolution Wave Simulations with SAR-Observations and Estimation of the Wave Power Potential Spatiotemporal Distribution**
George Kallos [1], Christine Kalogeri [1], Alexandros Adam [1], George Galanis [1]
[1]University of Athens, GR

Session: Internal Waves

Chairs: W. Alpers, J. Da Silva

11:40 - 12:00 **A look at oceanic internal waves with TerraSAR-X along-track InSAR**
Roland Romeiser [1], Hans Graber [1], Steffen Suchandt [2]
[1]University of Miami, US; [2]DLR, DE

12:00 - 12:20 **On the origin of short internal waves trailing strong internal solitary waves observed on spaceborne SAR images acquired over the northern South China Sea**
Werner Alpers [1], Chuncheng Guo [2], Vasliy Vlasenko [2], Nataliya Stashhchuk [2], Xueen Chen [3]
[1]University of Hamburg, DE; [2]University of Plymouth, UK; [3]Ocean University of China, CN

12:20 - 12:40 **Airborne and SAR Sinergy reveals the 3D structure of air bubble entrainment in internal waves and fronts**
Jose Da Silva [1], Jorge Magalhaes [1], Miguel Batista [1], Louis Gostiaux [2], Theo Gerkema [3], Adrian New [4]
[1]University of Porto, PT; [2]Laboratoire des Ecoulements Géophysiques et Industriels, FR; [3]The Royal Netherlands Institute of Sea Research, NL; [4]NOCS European Way, UK

12:40 - 14:00 *Lunch*

14:00 - 14:40 **Round Table**

Session: Ocean current retrievals and applications

Chairs: B. Holt, J. Johannessen

14:40 - 15:00 **SAR observations of spiral eddies in the inner seas**
Svetlana Karimova [1]
[1]Space Research Institute of RAS, RU

15:00 - 15:20 **Monitoring the surface inflow of Atlantic Water to the Nordic Seas using Envisat ASAR**
Morten Wergeland Hansen [1], Johnny Johannessen [1], Fabrice Collard [2]
[1]NERSC, NO; [2]CLS, FR

15:20 - 15:40 **Surface Current Monitoring over Gulf Stream, Agulhas and North Brazilian Current**
Fabrice Collard [1], Bertrand Chapron [2], Johnny Johannessen [3], Vladimir Kudryavtsev [4], Alexis Mouche [1], Marjolaine Rouault [5]
[1]CLS, FR; [2]IFREMER, FR; [3]NERSC, NO; [4]NIERSC, RU; [5]CSIR, ZA

15:40 - 16:00 **High precision Doppler frequency estimation for ocean applications**
Harald Johnsen [1], Geir Engen [2]
[1]Norut, NO; [2]Norut Tromsø Earth Observation, NO

16:00 - 16:30 *Coffee Break*

16:30 - 16:50 **Results from the Submesoscale Experiment April 2011: In situ, aircraft, and satellite measurements of small eddies, fronts, and filaments in the Southern California Bight**
Benjamin Holt [1]
[1]Jet Propulsion Laboratory, USA

16:50 - 17:10 **Observations conditions and principle for ocean current front backscatter modulation**
Fabrice Collard [1], Bertrand Chapron [2], Frederic Nouguier [2]
[1]CLS, FR; [2]IFREMER, FR

17:10 - 17:30 **High Resolution Surface Velocity Monitoring with Wide Swath SAR: A User`s Guide to the Range Doppler Method**
Johnny Johannessen [1], Bertrand Chapron [2], Fabrice Collard [3], Alexis Mouche [3], Knut-Frode Dagestad [4], Morten Wergeland Hansen [1]
[1]NERSC, NO; [2]Ifremer, France; [3]CLS, FR; [4]Storm-Geo, NO

17:30 - 18:00 **Round Table**

18:00 - 20:30 **Visit to KSAT**

Day 3, Wednesday 20 June 2012

Session: Ship detection

Chairs: P. Vachon, G. Campbell

08:30 - 08:50 **Ship Detection and Sea Clutter Characterisation Using X&L – Band Full-Polarimetric Airborne SAR Data**
Sebastien Angelliaume [1], Philippe Martineau [1], Philippe Durand [2], Thibery Cussac [2]
[1]ONERA, FR; [2]CNES, FR

08:50 - 09:10 **Validating a Ship Detector Based on the Notch Filter with RADARSAT-2 Fine Quad-Pol Data**
Armando Marino [1], Nicholas Walker [2], Irena Hajnsek [3]
[1]ETH Zurich, CH; [2]EOsphere Ltd, UK; [3]ETH Zurich / DLR-HR, DE

09:10 - 09:30 **Operational Ship Detection in Canada Using RADARSAT: Present and Future**
Paris Vachon [1], Robert Quinn [2]
[1]Defence R&D Canada, CA; [2]DG Space, CA

09:30 - 09:50 **Ocean Clutter Modeling for Ship Detection**
Ding Tao [1], Stian Anfinsen [1], Camilla Brekke [1]
[1]University of Tromsø, NO

09:50 - 10:10 **Ship Detection and Motion Parameter Estimation with TanDEM-X in Large Along-Track Baseline Configuration**
Stefan Baumgartner [1], Gerhard Krieger [1]
[1]German Aerospace Center (DLR), DE

10:10 - 10:30 **Advanced Ship Detection and Classification**
Guillaume Hajduch [1], Nicolas Longépé [1], Jérome Habonneau [1], Jean-Yves Le Bras [2]
[1]CLS, Plouzané, FR; [2]CLS, Ramonville Saint-Agne, FR

10:30 - 11:00 *Coffee Break*

11:00 - 11:20 **MARISS - Near Real Time Ship Detection with TerraSAR-X**
Stephan Brusch [1], Susanne Lehner [1]
[1]German Aerospace Center Wessling, DE

11:20 - 11:40 **Ship Detection Using High Resolution Satellite Imagery and Space-Based AIS**
Tonje Nanette Arnesen Hannevik [1]
[1]Norwegian Defence Research, NO

Session: Oil spill detection

Chairs: C. Brekke, V. Kudryavtsev

11:40 - 12:00 **Analysis of the Deepwater Horizon Oil Spill Using Polarimetric L-Band UAVSAR Data AR Data**
Benjamin Holt [1]
[1]Jet Propulsion Laboratory, US

12:00 - 12:20 **Italian Coast Guard Integrated Maritime Surveillance in the Framework of Security, Anti-Pollution and Fisheries Control Activities**
Luigia Caiazzo [1], Dario Cau [1]
[1]Italian Coast Guard Rome, IT

12:20 - 12:40 **Oil Spill Detection and Modelling: Preliminary Results for the Cercal Accident**
Jose Da Silva [1], Ricardo Da Costa [2], Alberto Azevedo [2], Anabela Oliveira [2]
[1]University PORTO, PT; [2]LNEC, PT

12:40 - 14:00 *Lunch*

14:00 - 14:20 **Field Experiments on SAR Detection of Film Slicks**
Stanislav Ermakov [1], Jose Da Silva [2], Ivan Kapustin [1], Irina Sergievskaya [1]
[1]Institute of Applied Physics RAS, RU; [2]Porto University, PT

14:20 - 14:40 **Oil Spill Detection in Dual and Compact Polarimetry SAR Images**
Øystein Rudjord [1], Arnt-Børre Salberg [1], Anne H. S. Solberg [2]
[1]Norwegian Computing Center, NO; [2]University of Oslo, NO

14:40 - 15:00 **A Comprehensive Analysis of Polarimetric Features for Oil Spill Characterization**
Stine Skrunes [1], Camilla Brekke [1], Torbjørn Eltoft [1]
[1]University of Tromsø UiT, NO

15:00 - 15:20 **The "New Generation" of CleanSeaNet: the EU Remote Sensing Based Monitoring System for Oil Spill and Vessel Detection**
Sónia Pelizzari [1] , Olaf Trieschmann [1] ,
[1]European Maritime Safety Agency (EMSA), PT

15:20 - 16:00 **Round Table**

16:00 - 18:00 **Poster session**

Hosted Workshop dinner

Day 4, Thursday 21 June 2012

Session: Ocean Wind Retrievals and Applications

Chairs: K.-F. Dagestad, J. Horstmann

09:00 - 09:20 **SAR-Derived High-Resolution Operational Wind Products within NOAA CoastWatch**
William Pichel [1], Frank Monaldo [2], Christopher Jackson [3], John Sapper [4], Xiaofeng Li [5], Phillip Keegstra [6]
[1]NOAA/NESDIS, USA; [2]The Johns Hopkins University Applied Physics Laboratory, USA; [3]Global Ocean Associates, USA; [4]NOAA/NESDIS/OSPO, USA; [5]IMSG at NOAA/NESDIS, USA; [6]SP Systems, Inc., USA

09:20 - 09:40 **Estimating Winds From Synthetic Aperture Radar In Typhoon Conditions**
Chris Wackerman [1], Jochen Horstmann [2], Ralph Foster [3], Mike Caruso [4], Hans Graber [4]
[1]General Dynamics, USA; [2]NATO/NURC, IT; [3]Univerisity of Washington, USA
[4] University of Miami, US

09:40 - 10:00 **Validation of SAR Wind Retrieval at X-Band Using TERRASAR-X and COSMO-SKYMED Data**
Jochen Horstmann [1], Franck Monaldo [2], Michael Caruso [2], Salvatore Maresca [2]
[1]NATO Undersea Research Center, IT; [2]Johns Hopkins University Applied Physics Laboratory, USA

10:0 - 10:20 **Cross-Polarized SAR: a New Measurement Technique for Hurricanes**
Will Perrie [1], Biao Zhang [2]
[1]Bedford Institute of Oceanography BIO, CA; [2]Nanjing University of Information Sciences and Technology, CN

10:20 - 10:40 **Doppler Centroid, Normalized Radar Cross Sections and Sea Surface Wind**
Alexis Mouche [1], Fabrice Collard [1], Bertrand Chapron [2], Vladimir Kudryavtsev [3], Johnny Johannessen [4]
[1]CLS, FR; [2]Ifremer, FR; [3]NIERSC, FR; [4]NERSC, NO

10:40 - 11:10 *Coffee Break*

11:10 - 11:30 **Organized Multi-Km Surface Stress Convergence Lines in Tropical Cyclone Surface Wind Retrievals**
Ralph Foster [1]
[1]University of Washington, US

11:30 - 11:50 **Ocean Surface Winds Measurement Using X- and L-Band Polarimetric SAR**
Akitsugu Nadai [1], Toshihiko Umehara [2], Seiho Uratsuka [3]
[1]National Institute of Information and Telecommunications Technology, JP; [2]National Institute of Information and Communications Technology, JP; [3]Applied Electromagnetic Research Institute, JP

11:50 - 12:10 **Polar Lows and Ocean Wind Profiles**
Birgitte Furevik [1], Johannes Röhrs [1], Gunnar Noer [1], Harald Schyberg [1], Frank Tveter [1]
[1]Norwegian Meteorological Inst., NO

12:10 - 12:30 **High Resolution Wind Fields over the Black Sea Derived from Envisat ASAR Data Using an Advanced Wind Retrieval Algorithm**
Werner Alpers [1], Alexis Mouche [2], Andrei Ivanov [3], Burghard Bruemmer [1]
[1]University of Hamburg, DE; [2]Collecte Localisation Satellites Avenue La pérouse, FR; [3]P.P. Shirshov Institute of Oceanology, RU

12:30 - 12:50 **Dual-Polarized SAR Imaging of Meso-Scale Currents**
Vladimir Kudryavtsev [1], Fabrice Collard [2], Alexander Myasoedov [3], Bertrand Chapron [4], Johnny Andre Johannessen [5]
[1]RSHU/NIERSC, RU; [2]CLS, FR; [3]RSHU, RU; [4]Ifremer, FR; [5]NERSC, NO

12:50 - 14:00 **Lunch**

14:00 - 14:40 **Round Table**

Session: Sea ice retrievals and applications

Chairs: W. Dierking, T. Eltoft

14:40 - 15:00 **A Multi-Polarization Study of Arctic Sea Ice in C-Band and X-Band**
Torbjorn Eltoft [1], Ane Fors [1], Mari-Ann Moen [1], Angelika Renner [2], Anthony Doulgeris [1], Sebastian Gerland [2], Laurent Ferro-Famil [3]
[1]University of Tromsø DoPT, NO; [2]Norwegin Polar Institute, NO; [3]University of Rennes 1, FR

15:00 - 15:20 **Sea Ice Classification Using Radarsat-2 Dual-Polarisation Data**
Stein Sandven [1], Vitaly Alexandrov, Mohamed Babiker [2]
[1]Nansen Environmental and Remote Sensing Center, NO; [2]NERSC , NO

15:20 - 15:40 **Radar Polarimetry - Useful for Detection of Icebergs in Sea Ice**
Wolfgang Dierking [1], Christine Wesche [1]
[1]Alfred Wegener Institute, DE

15:40 - 16:00 **Iceberg Monitoring Service by Joint Use of Drift Model, SAR and Altimeter Data**
Nicolas Longepe [1], Franck Mercier [1], Jean Yves Lebras [1], Marion Sutton [1], Guillaume Hajduch[1]
[1]Collecte Localisation Satellites, FR

16:00 - 16:30 *Coffee Break*

16:30 - 16:50 **SAR Measurements of Sea Ice Drift in the Fram Strait and Bay of Bothnia**
Anders Berg (1), Leif Eriksson [1]
[1]Chalmers University of Technology, SE

16:50 - 17:10 **Sea Ice Concentration Retrievals by using Composite ScanSAR Features in a SAR Data Assimilation Process**
N. Gokhan Kasapoglu [1]
[1]University of Tromsø - Auroral Observatory, NO

17:10 - 17:30 **The SAR Ice Constellation Backscatter Simulation Tool and Sea Ice Signature Database**
Desmond Power [1], Dr. James Youden [1] , Nick Walker [2], Chris Williams [2] , Dr. David Barber [3] , Bruce Ramsay [4] , Kim Partington [5] , Matt Arkett [6] , Dr. Roger De Abreu [7] , Dr. Malcolm Davidson [8]
[1]C-CORE, CA, [2] eOsphere, UK, [3] University of Manitoba, CA, [4] Consultant,[5] Polar Imaging Limited, UK, [6] Canadian Ice Service, CA, [7] Canada Centre for Remote Sensing, CA, [8] ESA-ESTEC, NL

17:30 - 18:00 **Round Table**

Day 5, Friday 22 June 2012

Session: Session Summary

Chairs: P.E. Skrøvseth, Y.L. Desnos

09:00 - 09:20 **Future SAR missions (Sentinel-1, Radarsat Constellation Mission etc.)**

09:20 - 09:40 **Methodology and techniques**

09:40 - 10:00 **Wave mode processing algorithms, product validation and assimilation**

10:00 - 10:20 **Wave retrievals and applications**

10:20 - 10:40 **Internal Waves**

10:40 - 11:10 *Coffee Break*

11:10 - 11:30 **Ocean current retrievals and applications**

11:30 - 11:50 **Ship detection**

11:50 - 12:10 **Oil spill detection**

12:10 - 12:30 **Ocean wind retrievals and applications**

12:30 - 12:50 **Sea ice retrievals and applications**

12:50 - 13:10 **Closing**

Day 1, Monday 18 June 2012

Session: Future SAR missions (Sentinel-1, Radarsat Constellation Mission etc.)

Sentinel-1 Mission Operations Concept

Pierre Potin [1], Siegfried Schmuck [1], Betlem Rosich [1]
[1]ESA / ESRIN , IT

Abstract

SENTINEL-1 MISSION OPERATIONS CONCEPT Pierre Potin, Siegfried Schmuck, Betlem Rosich European Space Agency 1. INTRODUCTION As part of the European Global Monitoring for Environment and Security (GMES) program, the Sentinel-1 mission, based on a constellation of two SAR satellites, will ensure continuity of C-band SAR observations, building on ESA's and Canada's heritage on satellite SAR systems (ERS, Envisat and Radarsat). The first satellite is planned for launch in 2013, the second within the following two years. The Sentinel-1 mission operations concept follows the overall GMES Space Component operations concept, which covers the missions specifically developed for GMES, the Sentinels, as well as the so-called GMES contributing missions which have been developed for other purpose than GMES but which provide a valuable data set to GMES services and applications. 2. OVERVIEW OF THE SENTINEL OPERATIONS STRATEGY The main objectives of the Sentinel operations strategy is to provide data to GMES services and for use by ESA and EU Member States according to their specified requirements, ensuring systematic and routine operational activities with a high level of automation and, to the maximum extent possible, with pre-defined operations. The goal is to minimize the number of potential conflicts during operations, therefore solve anticipated conflicts a priori, in particular in the elaboration of pre-defined mission observation scenarios. 3. THE SENTINEL-1 MISSION OBSERVATION SCENARIO 3.1. Scope The application of the Sentinel operations strategy to the Sentinel-1 operations concept results in the definition of a baseline mission observation scenario, making optimum use of the SAR duty cycle within the technical constraints of the overall system, and aiming at satisfying the observation requirements from the GMES services and for the use by Member States, according to the GMES Space Component Programme Declaration. In addition, on a best effort basis and with lower priority, a secondary objective is to satisfy other SAR user communities and partners, ensuring continuity of ERS/ENVISAT, considering requirements from the science community, as well as from international partners. 3.2. High Level Sentinel-1 Observation Strategy Within the predefined observation plan, the Sentinel-1 mission shall ensure observations fulfilling the following two main categories of services: 1. Monitoring services related to oceans, seas and sea-ice: these services require quasi real time or near real time data, typically in less than 3 hours, and in some cases in less than 10 minutes. Quasi real time services or services requiring data within 1 hour from sensing require reception by local stations. Most of these monitoring types of services require systematic or very frequent (e.g. daily) observations. 2. Services / applications over land: these services or applications cover a wide range of different thematic domains. They do not require data in quasi real time, few of them require data in 3 hours near real time from sensing. Related data are most of the time planned to be recorded on-board and downloaded to the core ground station network. Products not required in near real time will be available within 24 hours from sensing. The high level Sentinel-1 observation strategy during full operations capacity is based on the following: · optimum use of SAR duty cycle (25 min/orbit), taking into account the various constraints (e.g. limitation in the number of X-band RF switches, mode transition times, maximum downlink time per orbit and maximum consecutive downlink time) · optimum use of single and dual polarisation acquisitions, in line with the available downlink capacity · Wave Mode (WV) continuously operated over open oceans, with lower priority versus the high rate modes · Interferometric Wide Swath (IWS) and Extra Wide Swath (EW) modes operated over pre-defined geographical areas: ◊ Over land: pre-defined mode is IWS ◊ Over seas and polar areas, and ocean relevant areas: pre-defined mode is either IWS or EWS. In exceptional cases only, emergency observation requests may alter the pre-defined observation scenario, with e.g. the use of the Strip Map (SM) mode. 4. PERSPECTIVES The oral presentation will further develop the Sentinel-1 mission observation strategy, providing an overview of the observation needs as well as more details in the way the mission will be operated (operational modes, polarisations, areas, revisiting etc.). This will provide the user communities with relevant information helping them to start their preparation to the exploitation of the mission. The process of collecting the Sentinel-1 observation needs (from GMES services, Member States, the scientific community, etc.) and defining the baseline observation scenario is currently on-going. While a good

knowledge on the topic is already available today, it is anticipated that at the time of SeaSAR 2012, more detailed and consolidated information will be available.

Sentinel-1 System Overview

Paul Snoeij [1], Ramon Torres [1], Dirk Geudtner [1], Michael Brown [1], Patrick Deghaye [1], Ignacio Navas-Traver [1], Allan Østergaard [1], Bjorn Rommen [1], Nicolas Floury [1], Malcolm Davidson [1]
[1]ESA , NL

Abstract

The forthcoming European Space Agency (ESA) Sentinel-1 (S-1) C-band SAR constellation will provide continuous all-weather day/night global coverage, with six days exact repetition time (near daily coverage over Europe and Canada) and with radar data delivery within 3 to 24 hours. These features open new possibilities for operational maritime services. The Sentinel-1 space segment has been designed and is being built by an industrial consortium with Thales Alenia Space Italia as prime contractor and EADS Astrium GmbH as C-SAR instrument responsible. It is expected that Sentinel-1A be launched in 2013. Data products from current and previous ESA missions including ERS-1, ERS-2 and ENVISAT missions form the basis for many of the pilot GMES services. Consequently Sentinel-1 data maintain data quality levels of the Agency's previous SAR missions in terms of spatial resolution, sensitivity, accuracy, polarization and wavelength. Nonetheless, the Sentinel-1 synthetic aperture radar (SAR) constellation represents a completely new approach to SAR mission design by ESA in direct response to the operational needs for SAR data expressed under the EU-ESA Global Monitoring for Environment and Security (GMES) programme. SAR is the primary source of data for information on the ocean and the arctic environment. The all-weather day-and-night observation capability, problems of access to open ocean and the harsh arctic environments often make radar the only reliable information source. Typical specific information products for the ice and snow services include monitoring glaciers and snow, icebergs, sea ice (floe edge) and the near shore ice complex. For the determination of the direction, wavelength and (extreme) heights of waves at the surface of the open ocean SAR imagettes are being used in near real time in conjunction with global ocean wave models. The extensive wave mode archive built up by the ERS and ENVISAT background mission is a critical resource for the analysis of regional wave climate and of extreme wave events. SAR is also the primary source of information for oil spill information services (such as surveillance, drift forecasting and decision support) and for ship detection services required for fisheries and security. The Sentinel-1 mission requirements ask for data products with different image characteristics, which require the implementation of four different measurement modes: Stripmap Mode, Interferometric Wideswath Mode, Extra-Wideswath Mode, and Wave Mode. Except for the Wave Mode, which is a single polarization per vignette mode (HH or VV), the SAR instrument has to support operation in dual polarisation (HH-HV, VV-VH), which requires the implementation of one transmit chain (switchable to H or V) and two parallel receive chains for H and V polarisation. In Stripmap mode the instrument has to provide an uninterrupted coverage with a high geometric resolution (5m x 5m) at a medium swath width of 80 km. Six overlapping swathes cover the required access range of 375 km. For each swath the antenna has to be configured to generate a beam with fixed azimuth and elevation pointing. The Interferometric Wideswath and Extra Wideswath modes are implemented as a ScanSAR mode with progressive azimuth scanning. This requires a fast antenna beam steering in elevation for ScanSAR operation, i.e. transmitting a burst of pulses towards a sub swath. In addition, fast electronic azimuth scanning has to be performed per sub swath (TOPS operation) in order to average the performance in along track direction (reduction of scalloping). The Interferometric Wideswath mode will allow combining a large swath width (250 km) with a moderate geometric resolution (5m x 20m). In Extra-Wideswath mode a swath width of more then 400 km will be covered with low resolution (20m x 40m). Finally, the Wave mode is composed of single stripmap (5m x 5m) operations with an alternating elevation beam (between 23° and 36.5° mid incidence angle) and a fixed on/off duty cycle, which results in the generation of vignettes of 20km x 20km size in regular intervals of 100 km. For the end-user of SAR imagery the radiometric resolution is a critical parameter as it defines the typical image noise in radar images caused by thermal noise and speckle. Image noise defines how well different surfaces (e.g. ice types, agricultural crops, soil moisture levels) can be classified. In its Extra-Wideswath mode Sentinel-1 offers 30% performance improvement with respect to ENVISAT while the Interferometric Wideswath mode of Sentinel-1 offers a further improvement by a factor of three. For the Sentinel-1 acquisition modes one type of L2 product is defined: OCeaN (OCN). The OCN product may contain the following components: Ocean SWell spectra (OSW), Ocean WInd field

(OWI), and/or Radial Surface VeLocity (RVL). The availability of a product component is depending on the acquisition modes as well as the type of the corresponding input Level-1 product. The L2 products to be expected in the future from collaborative centres include: · Wind: Use of combined cross section and Doppler shift for wind vector retrieval. · Waves: Retrieval of wave amplitude modulation on top of mean wave spectrum. Retrieval of wave spectra from IW-EW (TOPS) mode. · Current: Retrieval of radial surface current component from Doppler centroid shift. · Ship detection: used of dual-pol to better discriminate between targets and false alarms. The current project status sees a full compliance of the system to the very challenging requirements. It is important to mention that the Sentinel-1 project has represented a major European industrial effort since its kick-off phase and has implied for Thales Alenia Space Italia, acting as Prime Contractor, a number of very demanding tasks, including the need for an international industrial team coordination, the procurement of Sentinel-1A, -1B & -1C (expected) satellites for constellation performance improvement, the on-board accommodation of a third party Optical Communication Payload for space-to ground link improvement, and the very long satellite lifetime. The presentation will provide an overview of the Sentinel-1 system, the status and characteristics of the technical implementation. The key elements of the system supporting the maritime user community will be highlighted.

A Marine Collaborative Ground Segment for the Sentinel1 missions

Fabrice Collard [1], Pierre Fabry [1], Alexis Mouche [1], Bertrand Chapron [2], René Garello [3]
[1]CLS , FR
[2]IFREMER , FR
[3]Telecom Bretagne , FR

Abstract

MCGS (Marine Collaborative Ground Segment) is a project aimed at making the most of ESA 'Sentinels' satellites potential (Sentinel-1 and Sentinel-3) for downstream services. MCGS addresses the need of the European Space Agency to build up data processing centers in conjunction with the GMES Program for the provision of services to local and national, public and private European institutions or entities involved in marine activities. Coordination between MCGS and ESA is overseen by CNES. Based on experience gained through demonstration of ocean Level2 and Level3 ocean products for ASAR and to complement the Sentinel1 Level2 OCN product, the wind/wave/current MCGS platform will be developed in Brest by CLS, IFREMER and GIS Bretel to design, produce and deliver innovative Wind/wave/currents products and downstream services. This platform will have three major tasks, - to produce and demonstrate value added Level2 to Level4 wind/wave/current products in line with downstream services requirements. - to ensure delay time reprocessing and archiving of OCN products with the best auxiliary information not being available in near real time (model hindcast, precise orbits) - to ensure multi-mission inter calibration of Level2 Wind wave current products, and consistency in formats and quality assessment.

From RADARSAT-2 to RADARSAT Constellation Mission Data Continuity

Daniel De Lisle [1]
[1]Canadian Space Agency , CA

Abstract

The Government of Canada is has been providing C Band SAR data since 1995 with the launch of RADARSAT-1, still in operation, and RADARSAT-2 since 2008. There is also a commitment for data continuity with the RADARSAT Constellation Mission scheduled for 2016. This perennial data supply enables the Federal Departments to integrate this valuable source of information into their operational mandates. The Private Public Partnership (PPP) model of RADARSAT-2 with MacDonald Dettwiler and Associates (MDA) as proven effective; Image processing and dissemination have been centralized allowing better data sharing among Federal Departments and their partners. The Government investment of $446 M (CDN) of pre-paid imagery is managed by the Canadian Space Agency (CSA) to ensure provision during the 7 year life expectancy of RADARSAT-2. Use of SAR data within the Government of Canada is clearly growing. Consumption has risen from around 4,500 scenes annually in the RADARSAT-1 era to around 37,000 scenes for RADARSAT-2 from which 70% is dedicated to Marine applications. This is an excellent result and provides good justification for CSA's investment. It is also encouraging for the future use of the RADARSAT Constellation Mission (RCM). As new users prepare to become operational, utilization of RCM can be expected to exceed these numbers. The detailed design of the RADARSAT Constellation Mission is nearing completion, and the start of its implementation ("build" phase) is planned to overlap by a few months with the detailed design phase. The RADARSAT Constellation Mission will consist of three satellites flying in a constellation, which will be placed in orbit through two launches separated by 16 months in the middle of the current decade. The focus of the RADARSAT Constellation Mission is on meeting Government of Canada User Department's needs and requirements in three Core Use Areas: Maritime Surveillance, Disaster Management, and Ecosystem Monitoring. The constellation is designed primarily as a wide area monitoring system, offering medium resolution data on a daily basis, but it also offers high resolution imaging capabilities, including a Spotlight Mode, as well as multiple polarization including Compact Polarimetry and Experimental Quad-Polarization. This presentation will describe Canada's RADARSAT-2 current activities with an emphasis on maritime usage but also state the design of RCM space & ground segments as well as an overall project status. A summary on the programmatic and technical challenges and realizations, and activities surrounding application development and operational readiness will also be discussed.

International Cooperation For Space-Based Global Maritime Awareness – The Next Step

Harm Greidanus [1], Guy Thomas [2], Gordon Campbell [3], Karna Bryan [4]
[1]European Commission TP670, IT
[2]U.S. Coast Guard , USA
[3]ESA , IT
[4]NATO Undersea Research Centre , IT

Abstract

Issue
This paper aims to put forward for discussion a number of possible ways to promote international cooperation for global maritime awareness, in particular using space-based assets. Maritime awareness concerns the knowledge of human activities going on at sea, so for a large part equates to ship traffic detection and monitoring for safety, security and protection of resources and the environment. The essential benefits and challenges for cooperation, and related sharing of information, are recounted. Three concrete options for global cooperation that should be viable also in view of the challenges are proposed. A public discussion with global stakeholders should follow, leading to convergence on a mechanism that should be subsequently implemented.

Motivation
Maritime awareness is a necessary ingredient to establish safety, security and stewardship in the maritime domain. Authorities who want to address issues like safety of ship traffic and life at sea, piracy, irregular immigration, terrorism, pollution or management of fisheries, need a measure of maritime awareness. In the first instance, such authorities are concerned with their local area of responsibility. However, their "need to know" goes beyond that when it comes to protecting interests on the High Seas – think of piracy or protection of migrating fish stocks. Furthermore, ship traffic is not only present globally but also moves globally, so that potential threats that demand attention may easily go unnoticed if the authorities' field of view is only local – as in cross-border crime, terrorism or smuggling (narcotics, arms or people) between continents. But also many private commercial users who operate on the global market have a global interest. Given that government and private users in many countries need elements of the global ship traffic picture, it is obvious that there are benefits to some form of coordination in collecting such information. Space-based assets, i.e. observation and communication satellites, are characterised by global coverage, and they are therefore the logical first place to turn to for global awareness and its coordination.

History
Cooperation for maritime awareness is being actively sought and promoted for several years. The US Navy launched MSSIS (international AIS exchange), and the sharing of maritime information figures in several recent US strategies and plans. The EU under its Integrated Maritime Policy advocates maritime information sharing, as e.g. reflected in the 2010 Wise Pens paper, several European pilot projects (BlueMassMed, Marsuno, EUROSUR pilot) and the ongoing CISE initiative (Common Information Sharing Environment for the maritime domain). Many individual countries in the world subscribe to the value of international coordination and cooperation related to maritime awareness. The C-SIGMA (Cooperation in Space for International Global Maritime Awareness) in particular has been trying to mobilise the international community, and the present paper continues that process. Outside the maritime domain but in the area of international cooperation with global reach, the International Charter on Disasters has been very successful in providing access and increasing the use of space-based observation data for disaster recovery.

Information sharing
Any form of cooperation for maritime awareness using space-based assets will involve some level and amount of information sharing. The shared information can be either (a) ship positions, parameters and activities (derived from satellite data); (b) the data from which such information can be derived (e.g., satellite images); (c) meta-data, i.e. data describing attributes of the previous classes of data (e.g., times and locations when / where particular data are available); or (d) usage information (e.g., surveillance

plans; areas or ship types of interest). Because all of these classes of information have a value, and sometimes a sensitivity, the willingness to share them is not a given. The next paragraphs will discuss the main advantages and problems with sharing. These need to be well understood before any viable way forward for cooperation can be proposed.

Benefits of sharing

The benefits of sharing maritime awareness information have essentially been mentioned under 'Motivation', and they have been frequently discussed in recent papers and meetings. Nonetheless, it is helpful to consider at this point the different types of benefit. The main benefit of sharing information is increased efficiency and consequent cost saving. If two authorities need the same space-based data, it makes no sense to collect it twice. Indeed, entities needing some of the same data could number in the dozens. The second benefit is increased effectiveness. Increased availability of information as a consequence of sharing should lead to better results. But in addition to those two, a working international cooperation will lead to more streamlined access to data, which in turn should lead to increased usage and acceptance and a bigger market. This is a benefit to both users as well as suppliers; indeed, any workable strategy for cooperation and sharing should see to it that both these parties receive tangible benefits.

Challenges for sharing

It was mentioned that information has a value, which acts to inhibit its free exchange. Operators who receive information do so after they have incurred costs related to collection, transmission, analysis, etc. These costs need to be recuperated. Commercial operators therefore tend to sell their data, while government operators may provide them at reproduction cost, considering that the real costs will be repaid through societal benefits. However, even for government-operated systems, a price may be set for scheduling scarce assets such as satellite time (observation or communication), in order to properly allocate the economically optimal use. Similarly, archived data may carry a small price to avoid unnecessary access to the archive. Commercial operators frequently use a licensing model for the pricing of their data, which means that once bought, these data may not be given to others. However, this applies to the sold data itself (e.g., satellite images, or received AIS messages); derived information (e.g., ship positions extracted from the image) is subject to fewer restrictions. The latter, however, has taken effort to generate, and its producer may consider it unfair to part with it without any compensation. The above concerns prices set by the suppliers. But there is also another kind of value to the data, the one that enables the user to perform his task. In many cases, this value would be deleted if the information would be available to certain other parties – this is the case for security applications such as piracy, illegal fishing, smuggling, etc. Knowledge of when and where data will be collected (category 'd' mentioned above) can be sensitive, especially in police operations. Some information is therefore made classified and/or subject to legal restrictions. Also especially for private stakeholders, when considering the value of information in a globally competing world, the benefit of one may not always be parallel to the benefit of others. This situation is markedly different from e.g. disaster response, where general willingness for data sharing is more easily forthcoming. Finally, any framework for global operational cooperation will need some technical implementation, which implies some cost for setting up and running. All the above are challenges that need to be adequately covered if cooperation is to be successful.

Options

Even if everyone can see the advantages of cooperation (and data sharing), this is not enough to make it happen spontaneously. Some mechanism or framework needs to be set up, that can be followed and will lead to incremental benefits for its subscribers, resulting in steady development of international cooperation. Taking into account the considerations elaborated in the previous paragraphs, three possible options are proposed here. 1. To follow the model of the International Charter on Disasters, where satellite providers make a limited amount of data freely available when requested by an appointed authority, following an incident. 2. To set up a discovery service, where authorised users can see who of their global colleagues have space-based data from a time and place where they are also interested. 3. To set up a buyers' consortium that negotiates low prices for satellite data for authorised users over maritime regions, to exploit unused satellite capacity. Each of these options is attractive to both users (as their access to data is improved) but also to suppliers (as it is expected to lead to increased use and a bigger market). Further implementation details will need to address the identified challenges, but they

depend on the option; e.g. the sensitivity of data can be managed by defining user profiles and access rights.

Way ahead

The above ideas are now being put forward to the international community for discussion. The objective is to obtain input from the operational (and potential) stakeholders in maritime awareness on the acceptability of these options, and possibly alternative options. Options need to be fleshed out, also taking into account ongoing international (and national) coordination mechanisms and standards such as GEO/GEOSS, SDI/Inspire and CISE. This discussion is structured by presenting these ideas at appropriate international conferences, including this one, by organising dedicated meetings for actively interested stakeholders, and by providing a web forum to host an on-line discussion. When this public discussion converges on one (or maybe more) models for cooperation, the next step is to implement that. The exact nature of the implementation clearly depends strongly on the nature of the option chosen, but elements could include e.g. an MoU for participants to sign, a clearing house, some technical support staff, etc.

Notes

Day 1, Monday 18 June 2012

Session: Methodology and techniques

Towards Consistent Inversion of Wind, Waves and Surface Current from SAR

Bertrand Chapron [1], Vladimir Kudryavtsev [2], Fabrice Collard [3], Johnny Andre Johannessen [4], Alexis Mouche [3]
[1]Ifremer , FR
[2]NIERSC , RU
[3]CLS , FR
[4]NERSC , NO

Abstract

The synthetic aperture radar (SAR) technique has now successfully demonstrated its capacity to uniquely provide quantitative and valuable high-resolution products and information over a very wide range of marine applications: high resolution wind fields, global swell monitoring, coastal wave fields, mesoscale surface current and improved mean transport at regional scales, as well as oil-spill monitoring, ship detection, shallow-water bathymetry mapping, and sea-ice monitoring. This results, in particular, from the SAR capability to provide simultaneous quantitative information about the instantaneous sea surface roughness and motions under the combined action of surface wind, waves and current. While numerous investigations have been carried out to promote the combined analysis and interpretation of such a wealth of data and information, full consistent inversion schemes have yet to be developed and implemented. As it will be presented and discussed, advanced schemes shall especially be necessary to exploit future SAR missions, including polarization diversity, and possible interferometric capabilities, at finer spatial scales and resolution. In particular, we will insist on the polarization sensitivity that can already be analyzed to demonstrate very valuable wind speed and direction sensitivity, impacting both radar backscatter with its local modulations associated to underlying long wave and current variations, along with the associated Doppler signal properties. As such, future inversion schemes can certainly be anticipated to build on this polarization sensitivities to advance consistent wind/wave/current retrieval algorithms at very high resolution.

NEREIDS: New concepts in maritime surveillance for consolidating operational developments

Gerard Margarit [1]
[1]GMV Idem, ES

Abstract

The NEREIDS (New Service Capabilities for Integrated and Advanced Maritime Surveillance) project has been granted to GMV for the theme SPA.2010.1.1-05 SPA.2010.1.1-05 SPA] [Contributing to the "S" in GMES – Developing pre-operational service capabilities for Maritime Surveillance Contributing to the "S" in GMES – Developing pre-operational service capabilities for Maritime Surveillance Space within the FP7 Space 2010 call. NEREIDS is conceived to provide an integrated vision of maritime policy and maritime surveillance so that the different elements of the service become useful to the different maritime domains (Illegal trafficking, illegal immigration, fisheries control,...). The idea behind NEREIDS yields on developing a system of systems that permits solving some of the most challenging technological limitations that current services have to face on. This objective is completely aligned with what promoted by the EUROSUR program: "Awareness in the maritime domain requires monitoring the compliance of all activities, detecting with the help of surveillance and ship reporting system anomalies that may signal illegal (security threats) acts and generating intelligence that enables law enforcement authorities to stop unlawful entry into the EU area" In particular NEREIDS shall: ν Investigate on new SAR and optical satellite automatic processing capabilities together with new collaborative and non-collaborative data fusion techniques to make a best use of available space assets. ν Define an open architecture (toolbox) simplifying the process of implementing, testing and run into live demonstration new earth observation based capabilities for maritime surveillance. The service will have a kernel system (based on SOA architectures) that will manage the different resources while the processing capabilities will be added via external plug-ins. This avoids that errors or limitations in specific algorithms affect the rest of the system. Points of interest are: · Collection: diversified and large datasets shall be ingested in the most efficient way. New ICT technological state of the art solutions will be adopted for avoiding the typical bottleneck problems that appear when heavy images have to be downloaded. · Fusion: the information inferred from different sources of data shall be cross-correlated in order to reduce inaccuracies and to increase the sampling time of the reports that can be derived. · Analysis: Security sensitive analysis should be carried out separately. · Dissemination: Different tools and formats will be adopted in order to deliver the right information to the right decision maker at the right time. ν Contribute in reducing existing barriers for the users to adopt new technologies in particular in the maritime security domain where user's community is very fragmented with different cultures and priorities. ν Better understand maritime operator activities by analysing maritime anomalies and define how Earth observation can support in identifying such anomalies. ν Ensuring that key EU and national policy areas are addressed, such as border surveillance, search & rescue, traffic safety, fisheries control, environmental protection and monitoring of critical infrastructure such as oil platforms and sea ports. In summary, NEREIDS aims to enhance integrated, automatic and unsupervised ship monitoring service capabilities for maritime situational awareness and efficient decision making tools. This will be tackled by covering the following key technical objectives: ν A particular emphasis will be placed on improving the reliability of the detection small vessels and in high sea states. ν Improving the near-real-time speed with which information can be placed in the hands of decision makers without compromising the robustness of the information. ν Exploiting the enhanced capabilities (resolution, polarisation) of new sensors such as COSMO-Skymed, TerraSAR, and Radarsat2. ν Synergy between different sensors, including between optical and SAR sensors for: ν Improved detection performance. ν Reducing revisit times. ν Integrating satellite derived information with other data sources and information: ν Making use of inputs such as marine modelling and forecasting. ν Cooperative sensors, such as transponders (AIS). ν Route tracking and prediction, navigation analysis. ν Ensuring that information can be effectively integrated into decision support systems. The paper will present the main outcomes that have been achieved in NEREIDS up to current time. The two large measurement campaigns that are foreseen during project lifetime will also be tackled for stressing the importance of how a proper campaign design is essential for ensuring that user requirements are properly covered. The technical gaps that will be

filled with the system plug-ins will be reviewed in order to see the current state of the art and the status up to which NEREIDS aims to evolve them.

Toward Automated Classification of Brightness Fronts in RADARSAT-2 Images of the Ocean Surface

Christopher Jones [1]
[1]Dalhousie University Halifax, CA

Abstract

Images of the ocean surface captured by spaceborne SAR have long been known to exhibit spatial variations in surface roughness that corresponds to gradients in sea surface temperature (SST). Because SAR penetrates cloud cover, it represents a potential asset to the Canadian Forces Meteorology and Oceanography Center (MetOc) Halifax in its effort to provide a continual assessment of the location of tactically important SST features that are often obscured by clouds in passive radiometer images. As part of the research and development phase of the Spaceborne Ocean Intelligence Network (SOIN) project funded by the Canadian Space Agency, the objective of our study is to contribute toward an automated procedure to identify SST front signatures in RADARSAT-2 images acquired in the region of the Gulf Stream (GS), with particular interest in automated identification of the Gulf Stream North Wall (GSNW). A positive buoyancy flux on the warm side of an SST front typically forces a reduction in the stability of the surface layer of the marine atmospheric boundary layer (MABL), often manifested by convective processes that transport momentum from the upper MABL toward the surface. Moreover, the atmospheric temperature gradient often present across an SST front is itself often attended by a corresponding pressure gradient. Both of these processes enhance near-surface horizontal wind speed on the warm side the front, with concomitant intensification of surface roughness compared to the cold side. This sometimes results in a backscatter gradient in a SAR image that resembles the gradient of a collocated SST front. The above-described processes are, however, only two of many that render signatures in SAR images of the ocean surface. Signatures of atmospheric internal gravity waves, for example, often appear as a series of alternating dark and bright bands. Signatures produced by the entrainment of surfactants, and those produced by an enhancement in surface roughness in convergence zones associated with strong currents, commonly appears as dark and bright filaments, respectively. Patches of low backscatter that sometimes occur in the lee of a meander in the GS are consistent with the accumulation of cooler, biologically-ladened water originating from the continental shelf. Signatures of horizontal wind shear not forced by SST fronts appear as brightness fronts not necessarily aligned with nearby fronts evident in coincident SST images. The signatures of some processes can be readily identified by visual inspection alone. Furthermore, SST front signatures can sometimes be identified with high confidence without a validating SST image, for example by the presence of textures that indicate strong convection in the MABL. In the absence of such textures, however, an SST front signature can be easily confused for a signature of horizontal wind shear generated by a pure atmospheric process. We aimed to identify a set of textural and contextual measures that can discriminate between SAR signatures of SST fronts and similar long narrow SAR signatures of atmospheric horizontal wind shear not associated with gradients in SST. Our initial hypothesis was that strong divergence of winds in the cross-front direction, calculated by projecting wind vectors onto a curvilinear coordinate system centered on a computer-detected brightness front in a SAR image, would uniquely identify SST front signatures. For reasons not yet clear, it was the mean wind direction with respect to each brightness front that proved to have the greatest power to discriminate between SST front signatures and similar signatures produced by other processes. None of the textural measures included in the analysis contributed significantly to classification accuracy. Although the algorithm attained a classification accuracy of about 80 percent, our results indicated the possible necessity of an alternative approach to automated ocean feature classification. It is self-evident that a good classification algorithm should, as closely as possible, replicate the thought processes of an experienced analyst capable of accurate identification of ocean features in a SAR image. An analyst draws conclusions by noting various categorical cues and then making a decision based on auto-associations between sets of cues on the same image, as well as on associations between the cues and the processes that may have caused them consistent with past experience. This approach is in sharp contrast to the computation and comparison of local textural measures that was the mainstay of our analysis. Our results indicate that such measures are unlikely to be useful in the context of ocean feature classification, and indicate that a paradigm shift is called for. Artificial neural networks (ANN) comprise a class of statistical models that were designed specifically to

replicate human thought processes (Pinker 2009). Such models have been used extensively in the field of psychology as they provide a means to test hypothesis about the workings of the human brain. An auto-associated network is a special kind of ANN designed to make use of the co-occurrence of categorical inputs for discrete classes of objects, and may be well suited to mimic the thought processes of an analyst viewing a SAR image. In our presentation, we will first discuss our attempts to build an automated ocean feature detection and classification algorithm for RADARSAT-2 SCNA and SCWA VV images of the ocean surface, and show that traditional detection (Canny edge detector) and classification (logistic regression, maximum likelihood analysis, binary tree analysis) methods may not be appropriate because they do not mimic the thought processes of an experienced analyst. We will then propose a shift toward the use of an auto-associated artificial neural network is proposed, and will discuss our nascent efforts toward this.

From 2D to 3D upper layer dynamics: The way forward

Johnny Johannessen [1], Bertrand Chapron [2], Fabrice Collard [3], Vladimir Kudryavtsev [4], Annette Samuelsen [1]
[1]NERSC , NO
[2]Ifremer , FR
[3]CLS , FR
[4]NIERSC , RU

Abstract

The 3 dimensional dynamics within the ocean mixed-layer, embedded in a mesoscale to submesoscale eddy field at 1-30 km horizontal scales, are usually deviating from geostrophic balance. Moreover, the atmospheric forcing and intermittent air-sea fluxes in these conditions are highly variable. In general the knowledge of the dynamics and air-sea interaction at these scales are rather fragmented and insufficient due to lack of in-situ observations. The satellite data, on the other, are abundant but yet not fully explored and systematically used. For instance, in the presence of density fronts, internal waves, filaments and spiraling eddies, signatures of roughness variations are often expressed in high-resolution cloud independent radar satellite images. These are related to: - changes in the near-surface stability and surface stress; - impact of the ocean surface currents on the surface wind and waves; and - convective motion in the frontal zones triggering convergence and divergence. The SAR imaged expressions often strikingly match temperature patterns, such as strong meandering fronts and spiraling eddies, revealed at the 10 to 1 km scales from contemporaneous satellite images. Strategies should thus be refined to take optimum benefit of high-resolution multi-sensor satellite data. Specifically, synergy between near coincident cloud-free satellite IR-based sea surface temperature variability maps, sun glitter reflectance maps and chlorophyll concentration fields at 250 m to 1 km spatial resolution, as well as emerging capabilities to more directly estimate ocean surface velocity from SAR signals, already demonstrate the possibility to draw-out quantitative pictures of the 2-dimensional surface current dynamics. The major challenge is to further transform such rich 2-dimensional information, with the use of complementary sea level anomaly signals from altimetry and available in-situ data to fully diagnose 3 dimensional mesoscale to submesoscale mixed-layer dynamics. Guided by simulated fields from fine-resolution numerical ocean models, 2-dimensional satellite data can then help to uncover the 3-dimensional dynamics in the upper ocean. This is the rationale for proposing an innovative 2Dto3D analyses benchmark with a set of robust processing methods and tools for regular monitoring of the upper 200-500 m of the ocean based on high-resolution multi-sensor satellite observations.

Estimation of Underwater Topography using Satellite High Resolution Synthetic Aperture Radar Data.

Andrey L. Pleskachevsky[1], Susanne Lehner [1]
[1]German Aerospace Center, Remote Sensing Technology Institute, DE

Abstract

A method to obtain underwater topography for coastal areas using state-of-the-art remote sensing data and techniques worldwide is presented. The data from the new Synthetic Aperture Radar (SAR) satellite TerraSAR-X with high resolution up to 1m are used to render the ocean waves. As bathymetry is reflected by long swell wave refraction governed by underwater structures in shallow areas, it can be derived using the dispersion relation from observed swell properties. To complete the bathymetric maps, optical satellite data of the QuickBird satellite are fused to map extreme shallow waters, e.g., in near-coast areas. The algorithms for bathymetry estimation from optical and SAR data are combined and integrated in order to cover different depth domains. Both techniques make use of different physical phenomena and mathematical treatment. The optical methods based on sunlight reflection analysis provide depths in shallow water up to 20m in preferably calm weather conditions. The depth estimation from SAR is based on the observation of long waves and covers the areas between about 70- and 10-m water depths depending on sea state and acquisition quality. The depths in the range of 20m up to 10m represent the domain where the synergy of data from both sources arises. Thus, the results derived from SAR and optical sensors complement each other. In this study, a bathymetry map near Rottnest Island, Australia, is derived. QuickBird satellite optical data and radar data from TerraSARX have been used. The depths estimated are aligned on two different grids. The first one is a uniform rectangular mesh with a horizontal resolution of 150m, which corresponds to an average swell wavelength observed in the 10×10-km SAR image acquired. The second mesh has a resolution of 150m for depths up to 20m (deeper domain covered by SAR based technique) and 2.4 m resolution for the shallow domain imaged by an optical sensor. This new technique provides a platform for mapping of coastal bathymetry over a broad area on a scale that is relevant to marine planners, managers, and offshore industry.

Notes

Day 1, Monday 18 June 2012

Session: Wave Mode Processing Algorithms, Product Validation and Assimilation

On the Impact of ASAR Wave Spectra in the Operational Wave Model MFWAM

Lotfi Aouf [1], Jean-Michel Lefèvre [1]
[1]Meteo France, FR

Abstract

Satellite wave observations have provided a significant improvement in the physics of wave models. Since March 2011, the ASAR level 2 wave spectra and altimeters wave heights have been assimilated in the operational wave model MFWAM of météo France. The goal of this paper is to assess the performance of this new system after one year of operational use. Among this the contribution of ASAR wave spectra to correct the directional properties of the sea state is also brought to light. The validation of wave parameters such as the significant wave height, peak and mean wave periods is performed with independent wave data such as buoys or altimeters. The impact of the assimilation in the forecast period is also investigated. The use of ASAR level 2 wave spectra proved very effective in forecasting high waves generated by hurricanes and severe storms. The case of hurricane Katia in September 2011 is examined. In order to optimize the assimilation system the distribution of first guess errors is investigated for different ocean basins. Therefore, test runs are performed with an improved correlation model in the assimilation scheme.

Assimilation of ENVISAT ASAR Wave Mode Level 2 Product

Saleh Abdalla [1], Peter Janssen [1], Jean-Raymond Bidlot [1]
[1]ECMWF , GB

Abstract

The wave mode of the Synthetic Aperture Radar (SAR) provides a wealth of information regarding the detailed description of the surface sea state with global coverage. Unfortunately, SAR is not able to sense the whole spectrum of ocean waves especially in the azimuthal direction and misses quite a large range of short waves. Although this range usually carries the most energetic part of the ocean surface spectrum, the resolvable part of the spectrum can be very useful in a wide range of the oceanic applications including data assimilation in ocean wave models. The European Centre for Medium-Range Weather Forecasts (ECMWF) has been assimilating SAR Wave Mode (WM) Level 1b (L1b) product operationally since January 2003. This work started with the ERS-2 SAR WM L1b product. The corresponding product from ENVISAT replaced the ERS-2 product on the first of February 2006. WM L1b SAR spectrum product is inverted in-house using the iterative MPI-M (Max Planck Institute for Meteorology) nonlinear mapping scheme, which was developed by Hasselmann and Hasselmann (1991), to obtain the ocean wave spectra before assimilation. The assimilation of L1b product, both from ERS-2 and ENVISAT, proved to be beneficial. On the other hand, operational assimilation of ENVISAT ASAR WM Level 2 (L2) product has never been realised at ECMWF. Several experiments were carried out to assess the impact of assimilation of L2 product on wave model predictions. The obtained results were not encouraging. It seems that the information included in the BUFR (Binary Universal Form for the Representation of Meteorological data) template of the ASAR WM L2 product is not sufficient to carry out a proper quality control (QC) of product to achieve a successful data assimilation process. With the already available information in the BUFR template, relaxed QC criteria result in an adverse impact when WM L2 product is assimilated. Restricting the QC criteria improves the situation leading only to very limited impact which is mainly positive. The restricted QC criteria led to the rejection of most of L2 products, thus the limited impact. However, the negative impact, despite being very limited, in some areas could not be avoided. This prevented an operational assimilation of the product at ECMWF. The current plans of ESA for the future mission of Sentinel-1 do not accommodate the distribution of any Wave Mode Level 1b product. Therefore, it was decided to carry out a new series of ASAR assimilation experiments. Those experiments are planned to implement extra QC criteria using some information that is not available in the BUFR product. This work is based on the recommendations of Johnsen (2005) who suggested the use of the normalized image variance and the ambiguity factor. Both are not included in the BUFR product received at ECMWF. If positive impact is achieved, then a proposal to include those parameters in the BUFR template will be filed with the World Meteorological Organisation (WMO). The results obtained from the new series of experiments will be presented and discussed. An overview of the whole experience of ASAR WM L2 assimilation will also be presented.

Application of SAR Wave Mode and Wide Swath Mode for Swell Tracking Across Ocean

Fabrice Collard [1], Bertrand Chapron [2], Romain Husson [1], Fabrice Ardhuin [2]
[1]CLS , FR;
[2]IFREMER , FR

Abstract

Swell tracking from ASAR wave mode has been running for 5 years now which provides a global picture of the observed swell systems at global scale and at any time. An in depth comparison between SAR based swell tracking and in-situ observations by wave-rider buoys and seismometers will be presented to highlight the strength and limitations of this application. In view of recent availability of wave spectra from wide swath mode in north east Atlantic and upcoming Sentinel1 mission, analysis of SAR acquisitions mode (Wide swath, wave mode with or without leapfrog) and orbits (envisat vs. sentinel1) on swell system sampling will be discussed. Application of swell tracking for the deployment of “virtual buoys” at any locations in deep water will be presented. All propagated observations passing in the vicinity of this virtual buoy are merged to provide a time series of all swell systems at this location. A pilot service of swell monitoring and short term forecasting system for La Reunion island based on this "virtual buoy" concept, will be highlighted. Finally synthetic swell field reconstructed from all swell observations originating from the same storm source have been developed to drastically increase the assimilation impact of SAR wave spectral observations in sea state models.

Global Numerical Wave Model Validation Using ENVISAT ASAR Wave Mode and Radar Altimeter Data

Xiaoming Li [1], Susanne Lehner [1], Thomas Bruns [2]
[1]German Aerospace Center (DLR) , DE
[2]German Weather Service (DWD) , DE

Abstract

In the present study, the German Weather Service (DWD) forecast Global Sea wave Model (GSM) is validated using simultaneous measurements of the Advanced SAR ASAR and Radar Altimeter (RA) -2 from June 2006 to May 2007. The validation is on the one hand to systematically evaluate performance of the pure forecast wave model, and on the other hand to improve the assimilation criteria of satellite observations in the numerical wave model, particularly in high sea state. The ASAR and RA -2 are both mounted on board the ENVISAT platform to provide simultaneous surface wave measurements. RA yields the nadir sea surface measurements while the right-looking SAR and ASAR (ASAR is the Advanced SAR onboard the ENVISAT) measures at a ground distance of 300 km approximately from the RA. The empirical algorithm of CWAVE_ENV, an extension of the CWAVE, is proposed to derive integral wave parameters from the ENVISAT ASAR wave mode data for full sea state. This algorithm does not need any prior information while only using the calibrated ASAR image as an input for deriving integral wave parameters, e.g., SWH and mean wave period. Accuracy of the retrieved SWH is close to in situ buoy measurement with a bias of 0.06 m in deep water. The development of CWAVE_ENV algorithm makes the ASAR sensor be another independent observation of sea surface wave parameters in addition to the RA-2. Using both sensors for measuring sea state parameters brings a significant advantage. It increases spatial sampling over the open ocean and simultaneous observations reduce uncertainties of the measurement from a single instrument. This is of particular importance to evaluate performance of numerical wave models in high sea state, such as in the tropical and extra-tropical cyclones, which often exhibit significant spatial and temporal variations. When both sensors are used, it not only increases the opportunity to capture wind storms, but also is able to investigate the spatial variations of storm wave height as the parallel ground tracks have a ground distance of 300 km. In the present study, the overall performance of the DWD forecast Global Sea wave Model (GSM) is validated using the ASAR and the RA-2 measurements from June 2006 to May 2007. Evaluation of forecast storm wave height during winter season from December 2006 to February 2007 in the North Atlantic is particularly addressed. The annual validation shows that the forecast Significant Wave Height (SWH) of the GSM wave model has a fairly good agreement with both the satellite measurements over the globe with a slight underestimation of 2% to 3%. The monthly analysis shows that in the winter season of the North and South Hemisphere, the underestimation is 7% to 9%. Special emphasis is placed on evaluation of the GSM wave model in high sea state with SWH above 6 m in the North Atlantic during the winter season from December 2006 to February 2007. Both the case study and the statistical analysis show that the GSM wave model underestimate wave height by more than 12% for high sea state.

Notes

Notes

Day 2, Tuesday 19 June 2012

Session: Wave Retrievals and Applications

The GLOBWAVE Project

Fabrice COLLARD [1], Geoff Busswell [2], Ellis Ash [3], Jean-Francois Piolle [4], Helen Snaith [5], Simon Pinnock [6]
[1]CLS , FR
[2]Logica , UK
[3]Satellite Oceanographic Consultants , UK
[4]IFREMER , FR
[5]National Oceanography Centre Southampton , UK
[6]ESA/ESRIN , IT

Abstract

The primary objective of the GlobWave project is to improve the uptake of satellite-derived wind-wave and swell data by the scientific, operational and commercial user community. The project is a 3 year initiative funded by the European Space Agency, which aims to develop, operate and maintain an integrated set of information services based on satellite wave data. We are currently in the last year of the project. Wave data are available from in situ measurements, satellite altimeter and SAR instruments and are generated by an increasing number of wave models used in forecasting wave conditions. However, the use of wave data in a commercial, scientific and operational environment has been hampered the lack of harmonized integrated and homogeneously validated wave data. Merging and analysis of complementary satellite and in-situ measurements can deliver wave products with enhanced accuracy, spatial and temporal coverage, together with new types of higher-level products. This required the development of methodologies for complementary use of wave data from these different sources. The GlobWave project is providing : · A uniform, harmonised set of satellite wave data and ancillary information, in a common format from both SAR wave mode and altimeters · Reliable wave data based on multiple sensors and sources, which has been quality controlled, calibrated and validated with consistent characterisation of errors and biases. · Easy access to wave data products via a web portal and ftp server, regularly updated with near-real-time data. · A sustainable service that users can rely upon to meet their needs in the long term. The project was built on the knowledge and contacts of the consortium members, led by Logica UK, with support from CLS, IFREMER, SatOC and NOCS, to increase the value provided to GlobWave by parallel projects. The project User and Steering Groups provided direction and focus for the project, ensuring the widest range of activities were included and ensuring that user expectations were met. Sample of statistics that can easily be derived from GlobWave database will be highlighted, to demonstrate the potential of the developed system. online tools developed to browse the GlobWave database and perform basic satellite/in-situ data inter-comparisons will be presented

SAR Wave Mode Processing – Improvements Towards Sentinel-1 Mission

Harald Johnsen [1], Fabrice Collard [2]
[1]Norut , NO
[2]CLS , FR

Abstract

The Sentinel-1 level-2 (L2) ocean product (OCN) has been designed to deliver geophysical parameters related to the wind, waves and surface velocity to a large panel of end-users. Each L2 OCN product contains up to three geophysical components: the radial velocity (RVL), the ocean surface wind field (OWI) and the ocean swell wave spectra (OSW) components. The core algorithm of the Sentinel-1 Level 2 OSW component is an estimation of the cross-spectra and the corresponding inversion to an ambiguity free ocean wave spectra. The experiences with ASAR have shown the need to improve the modulation transfer functions (MTF), especially since the Sentinel-1 OSW processing will be performed over large range of incidence angles (S1 to S6) as well as for different polarizations (VV and HH). Large number of ASAR (WM and WSS) data collocated with model and in-situ data have been used to assess the MTF dependence on wind/wave conditions and instrument settings. The performance of wave spectra retrieval for different swaths and polarizations will be presented using an updated MTF, and perspectives for Sentinel-1 wave processing and retrieval will be discussed in relation to these findings.

Wave Retrievals from ScanSAR Images Under Tropical Cyclone Conditions

Roland Romeiser [1], Hans Graber [1]
[1]University of Miami , US

Abstract

Traditional techniques for retrieving ocean wave information from SAR images are based on the idea of inverting the processes that cause visible wave signatures in SAR images, i.e. tilt modulation and hydrodynamic modulation of the normalized radar backscattering cross section (NRCS) of the ocean surface and motion-related artifacts of the SAR imaging mechanism (velocity bunching). Due to the nonlinearity of the problem and speckle noise in all SAR images, typical wave retrieval algorithms work in the spectral domain and use some kind of iterative optimization to find the most likely solution for the ocean wave spectrum. Since the nonlinearities of the imaging mechanism are most pronounced for short waves, one can argue that these waves are not resolved by C-band ScanSAR images from ENVISAT or RADARSAT; therefore a simple linear inversion technique, using a modulation transfer function (MTF), may be appropriate for converting ScanSAR image spectra into ocean wave spectra. However, significant wave heights (SWHs) obtained by this approach cannot account for contributions of the unresolved waves at wavelengths shorter than approx. 100 m (RADARSAT) or even 150 m (ENVISAT). Furthermore, it is not clear if the known theoretical MTFs are valid under tropical cyclone conditions. In fact, many ScanSAR images of hurricanes and typhoons do not show any clear wave patterns in large regions – probably as a result of wave breaking and large amounts of foam and spray in the air, not because there are no waves. Inspired by empirical wind algorithms and by Schulz-Stellenfleth et al.'s empirical wave algorithm CWAVE for ASAR imagettes, we have developed an empirical wave algorithm for C-band ScanSAR images. Like the MTF-based approach, the proposed algorithm begins with the computation of image spectra, but instead of applying an MTF, it uses detected peak directions of signatures in the image as best estimates of ocean wave peak directions and applies an empirically derived relation to estimate ocean wave peak wavelengths. This is still limited to regions with detectable wave signatures, but in many cases it is possible to obtain a reasonable peak direction array for the whole image by interpolation. This is important for the following step. Like the peak wavelength conversion function, the proposed SWH retrieval algorithm was derived from a comparison of ScanSAR images of hurricanes and corresponding WAM model results. Consistent with Schulz-Stellenfleth's findings, we found a particularly strong correlation between SWH and mean backscattered power. Therefore, the proposed model function derives SWH values from mean NRCS values, and it depends on the local incidence angle and detected or estimated (through interpolation) peak direction. This way, it can provide SWH estimates for the entire ScanSAR image, including regions without visible wave patterns. In this presentation we will show results obtained for several RADARSAT-2 ScanSAR images of typhoons, which were acquired within the framework of the ONR-funded ITOP program in the fall of 2010. The proposed algorithm generates smooth SWH arrays that are found to be consistent with wave model results and available buoy data. A comparison with results of an MTF-based algorithm shows the advantages of the empirical algorithm, namely a much better coverage of the imaged scene with meaningful SWH estimates and more useful SWH magnitudes, which have been tuned (during the algorithm development phase) to represent the full SHW and not just the contributions of long waves whose signatures can be resolved by RADARSAT ScanSAR. Our future plans include the development of an empirical model function for X-band SAR images from TerraSAR-X and COSMO SkyMed and a more comprehensive comparison of wave results obtained from ScanSAR images, wave models, and in-situ instrumentation.

Sea State Measurements Using TerraSAR-X Data

Miguel Bruck [1], Susanne Lehner [1]
[1]DLR , DE

Abstract

Algorithms have been developed to extract meteo-marine information from the high-resolution TerraSAR-X (T-X)SAR data. The XWAVE algorithm for estimation of significant wave height and the XMOD algorithm for estimation of ocean surface wind speed.The XWAVE algorithm is based on Fourier analyses of TS-X data and uses a geophysical model function with coefficients that are found by fitting collocated hindcast wave model wave height results provided by the German Weather Center(DWD)and buoy in-situ measurements. Wind information provided by the XMOD algorithm is applied to improve the estimation of wave height from TS-X data. The integrated wave parameters derived from TS-X are compared to wave model results and buoy in-situ measurements for different locations. Wave peak direction of the SAR spectrum is also compared to Wave Peak direction obtained from directional buoys. Additionally the SAR integrated 1D spectrum is compared to 1D spectrum obtained from buoys measurements. TS-X data is particularly suitable for the characterization of sea state variability in the spatial domain in coastal areas. A study on sea state variability on coastal areas is presented using TS-X data. Changing sea state properties are investigated. Results are compared to wave spectral model designed for coastal applications and in-situ measurements where available.

Ocean Waves Inferred from X-Band Synthetic Aperture Radar Images of the Sea Surface

Francisco Ocampo-Torres [1]
[1]CICESE, MX

Abstract

A simple model is advanced to retrieve the wave spectrum from X-band radar images from the sea surface. A unique site is considered where well behaved swell travels near azimuth direction and a validation procedure is formulated. Direct wave measurements from sensors deployed near the coast allowed us to compare the results with those obtained from the retrieved SAR information. The effect of moderate to strong winds is analyzed in terms of the image formation mechanisms, and in particular, short wave directionality is studied. It is believed that short wave directionality might affect the imaged swell. A very detailed analysis of the swell modification as the waves propagate northward is performed. Some aspects of shorter waves are addressed as a signal associated with wind generated waves is detected in the SAR images.

Wind and Wave Transformations in the Vicinity of Islands Employing SAR Precision Images

Nelson Violante-carvalho [1]
[1]Coppe-ufrj, BR

Abstract

Wave attenuation can be caused by island blocking and a real challenge to the wave modelling community is to accurately represent the amount of wave energy that is attenuated. An important consideration in determining spatial resolution in global wave models is the need to properly resolve islands, and the option of simply increasing grid resolution does not appear to be computationally feasible. A common approach, used in general on small scales, consists of suppressing wave energy transport between grid points. One of the main difficulties in determining the amount of energy decrease lies in the spatial scales involved, since modifications can be discernible over a large area. The 100 km by 100 km area covered by a Synthetic Aperture Radar (SAR) image, when operating in the so called Precision Image (SAR PRI), turns out as an interesting technique to address this kind of problem. SAR has the capability of high-resolution imaging so that detailed distribution of wind vectors can be retrieved, along with reliable and spatially highly resolved directional wave spectra. In this ongoing work, several ERS-1&2 images acquired on the Southern California Bight yield the wind field and the wave spectra in the vicinity of the islands, leeward and windward sides. Spectral parameters, such as peak period and direction, significant wave height and directional spreading are compared to NDBC (National Data Buoy Center) buoys and WWIII estimates.

Swell Emulation in Coastal Zone

Fabrice COLLARD [1]
[1]CLS , FR

Abstract

Continuing efforts of ESA to open their data distribution policy and availability of growing archive of SAR data in coastal zone is opening a new era in coastal assessment of swell parameters. Not only statistics of swell parameters are now becoming available at high resolution along the coast but also machine learning is becoming possible to emulate the most likely coastal swell field given offshore swell parameters provided by sparse in-situ buoys or even global sea state models. Methodology of swell emulation will be described and demonstration will be presented over a test site. Performance of coastal swell emulation will be compared to coastal sea state model based on in-situ coastal wave rider measurements

Evaluation of High Resolution Wave Simulations with SAR-Observations and Estimation of the Wave Power Potential Spatiotemporal Distribution

George Kallos [1], Christine Kalogeri [1], Alexandros Adam [1], George Galanis [1]
[1]University of Athens, GR

Abstract

The use of numerical wave modeling systems for monitoring and estimating renewable energy resources is receiving increased attention as a result of the novel policies adopted in the energy market. In this framework, the MARINA Platform and the E-wave projects*, bridging leading European research groups and companies activated on the exploitation of renewable energy resources, provide novel products and methodologies for the estimation and exploitation of the wave power potential and the evaluation of multi-purpose platforms for marine renewable energy. One of the main outcomes of the above projects is a ten-year (2001-2010) data base of high resolution atmospheric and wave parameters that are used for monitoring the distribution of wind and wave power potential over different areas of the European coastline. Satellite measurements are of significant importance in this context since they can be utilized for the optimization and evaluation of model results. In the present work, the modeled results obtained within the framework of the MARINA and the E-wave projects are evaluated against SAR observations focusing mainly on the behavior of the wave parameters that directly or indirectly affect the wave energy potential as well as the stochastic distribution of the latter.

Notes

Day 2, Tuesday 19 June 2012

Session: Internal Waves

A Look at Oceanic Internal Waves with TerraSAR-X Along-Track InSAR

Roland Romeiser [1], Hans Graber [1], Steffen Suchandt [2]
[1]University of Miami , US
[2]DLR , DE

Abstract

Within the last few years, we have had several opportunities to acquire along-track interferometric SAR (along-track InSAR) images of river and ocean scenarios, some of which have been discussed in previous papers and presentations. A particularly interesting new example is a set of images of internal waves at the Dongsha atoll in the South China Sea from the Dual Receive Antenna mode (DRA mode) campaign in April 2010. To our knowledge, this is the first case of successful internal wave observations by along-track InSAR from a satellite, and we demonstrate that it is possible to derive meaningful orbital surface velocities from the data, which can be used to estimate the internal waves' amplitudes. The images were acquired in stripmap mode at an incidence angle of 31°, with a swath width of about 30 km and a full-resolution pixel spacing of 1.69 m in ground range x 2.05 m in azimuth direction. While we had ordered VV polarization, almost all ocean scenes of the DRA mode campaign were accidentally programmed in HH polarization, resulting in a significantly lower signal-to-noise ratio than what was hoped for. The effective along-track baseline is 1.20 m, which translates into a phase sensitivity to horizontal target velocities of approx. 2 deg per 1 m/s. Our main image of interest shows strong signatures of a very well-organized, coherent internal wave train in the image intensity (other images show more complex internal wave patterns that will require more refined data analysis techniques). Due to the short effective baseline and the relatively low signal-to-noise ratio, the corresponding interferometric phase signatures are quite noisy, but suggest that there is a correlation between image intensity and phase variations. To reduce the phase noise without losing much spatial resolution in the direction along the internal waves (i.e. across their crests), we apply strong directional filtering parallel to the leading internal wave signature, as determined from the intensity image. We obtain clear patterns of Doppler velocity anomalies (i.e. deviations from the large-scale mean) that vary between approx. −0.3 and +0.6 m/s over the first two solitons, where positive values indicate a forward velocity in their propagation direction. Using a simple squared hyperbolic secans parameterization of the surface current field over an internal soliton and a numerical model to compute hydrodynamically modulated surface wave spectra, Doppler spectra, and corresponding along-track InSAR signatures, we obtain relatively good agreement between observed and simulated intensity and phase signatures for internal soliton parameters within a range that is realistic for this test area. At the time of the conference, we may be able to present a comparison with in-situ data from Taiwanese scientists as well. Oceanic internal waves, which are governed by the same physical mechanisms as surface waves but propagate along pycnoclines inside the water body, are known to occur in stratified waters all over the world. They can carry large amounts of energy and momentum over long distances, and their orbital motions can make significant contributions to turbulence and mixing in the water column and to the resuspension of nutrients and other sediments from the bottom. Furthermore, the density and current variations associated with internal waves can be dangerous for submarines and for man-made structures in the ocean, such as oil platforms, and have strong effects on the propagation of sound signals. For these reasons, a lot of effort has been invested in the monitoring and theoretical understanding of internal waves, and the analysis of SAR images has made important contributions to this research since the launch of ERS-1 in 1991. If along-track interferometry can help to measure amplitudes of internal waves more accurately, its systematic utilization for this purpose can be another important step towards a comprehensive understanding and monitoring of internal waves.

On the Origin of Short Internal Waves Trailing Strong Internal Solitary Waves Observed on Spaceborne SAR Images Acquired over the Northern South China Sea

Werner Alpers [1], Chuncheng Guo [2], Vasliy Vlasenko [2], Nataliya Stashhchuk [2], Xueen Chen [3]
[1]University of Hamburg , DE
[2]University of Plymouth , UK
[3]Ocean University of China, CN

Abstract

Internal waves in the northern South China Sea (SCS) rank among the largest encountered in the World's ocean. They can have crest lengths of more than 200 km, and amplitudes of up to 170 m and phase speeds up to 2.9 ms-1. However, the internal wave field in the northern SCS is much more complex than in most other sea areas where strong internal waves are encountered. The large spatial and temporal variability of the internal wave field is a consequence of many factors, among them the complex bathymetry in the generation area (the Luzon Strait which separates the islands of Taiwan and Luzon (Philippines)), and the variability of the forcing barotropic current. This forcing current is mainly tidally driven, but modulated by non-tidal currents caused, e.g., by the often occurring intrusion of Kuroshio waters into the SCS. Many attempts have been made to explain this variability, but so far only with limited success. In this investigation we focus on an intriguing feature of the internal wave field which is frequently observed on synthetic aperture radar (SAR) images acquired over the northern SCS, but which has, to the best of our knowledge, has never been the subject of an investigation. This feature consists of sea surface signatures of strong solitary waves followed by short internal waves. We have compared these observation with results from numerical modeling which have been obtained recently by Vlasenko et al. (2010) using the MIT general circulation model (MITgcm). In their simulations they approximated the bathymetry of the Luzon Strait by a two-ridge structure and found that this bathymetry plays a crucial role in the generation of short internal waves trailing strong first mode internal solitary waves (ISWs) in the northern SCS. These short internal waves have typically wavelengths of 1.5 km and amplitudes of 20 m and ride on second mode ISWs. The existence of these short internal waves, which follow a first mode ISW, can be explained in terms of the Taylor-Goldstein equation that includes a shear in the background current associated with a second mode ISW. The simulations predict that the short internal waves occur in two distinct areas, one close to the Luzon Strait and the other further west. In the first area, they are generated by the disintegration of a baroclinic bore, which is generated by the interaction of the tidal current with the steep two-ridged topography in the LS. In the second area, they are generated when the faster first mode IW overtakes the second mode ISW of the previous tidal cycle. We have screened the ASAR archive of the European Space Agency (ESA) and found many SAR images acquired over the northern SCS showing sea surface signatures of such short internal waves trailing a strong first mode ISWs. The detailed analysis of six of these SAR images shows good correlation between modeled and observed internal wave fields. References Vlasenko, V., Stashchuk, N., Guo, C., and Chen, X. : "Multimodal structure of baroclinic tides in the South China Sea", Nonlinear Processes in Geophysics, 17 , 529-543, 2010.

Airborne and SAR Sinergy Reveals the 3D Structure of Air Bubble Entrainment in Internal Waves and Fronts

Jose Da Silva [1], Jorge Magalhaes [1], Miguel Batista [1], Louis Gostiaux [2], Theo Gerkema [3], Adrian New[4]
[1] University of Porto, PT
[2]Laboratoire des Ecoulements Géophysiques et Industriels , FR
[3]The Royal Netherlands Institute of Sea Research , NL
[4]NOCS European Way, UK

Abstract

Internal waves are now recognised as an important mixing mechanism in the ocean. Mixing at the base of the mixed layer and in the seasonal thermocline affects the properties of those water masses which define the exchange of heat and freshwater between the atmosphere and ocean. The breaking of Internal Solitary Waves (ISWs) contributes significantly to turbulent mixing in the near-surface layers, through the continual triggering of instabilities as they propagate and shoal towards the coast or shallow topography. Here we report some results of the EU funded project A.NEW (Airborne observations of Nonlinear Evolution of internal Waves generated by internal tidal beams). The airborne capabilities to observe small scale structure of breaking internal waves in the near-shore zone has been demonstrated in recent studies (e.g. Marmorino et al., 2008). In particular, sea surface thermal signatures of shoaling ISWs have revealed the turbulent character of these structures in the form of surface "boil" features. On the other hand, some in situ measurements of internal waves and theoretical work suggest subsurface entrainment of air bubbles in the convergence zones of ISWs. We conducted airborne remote sensing observations in the coastal zone off the west Iberian Peninsula (off Lisbon, Portugal) using high resolution imaging sensors: LiDAR (Light Detection And Ranging), hyperspectral cameras (Eagle and Hawk) and thermal infrared imaging (TABI-320). These measurements were planned based on previous SAR observations in the region, which included also near-real time SAR overpasses (ESA project AOPT-2423 and TerraSAR-X project OCE-0056). The airborne measurements were conducted from board the NERC (Natural Environmental Research Centre) Do 228 aircraft in the summer of 2010. The TABI-320 thermal airborne broadband imager can distinguish temperature differences as small as one-twentieth of a degree and operates in the spectral range 8-12 micrometers. With a nominal ground resolution of approximately 1.5 meters (at an altitude of 500 meters) it is capable to detect fine structure associated to turbulence. The LiDAR system that has been used is the Leica ALS50-II (1064nm) with a hit rate greater than 1 hit per square meter and a vertical resolution of approximately 15 cm. Both systems were available simultaneously, together with the hyperspectral system and the RCD105 39Mpx digital camera, integrated with the LiDAR navigation system. We analyse the airborne data together with a comprehensive dataset of satellite Synthetic Aperture Radar (SAR) that includes ENVISAT and TerraSAR-X images. In addition, in situ observations in the near-shore zone were obtained in a previous experiment (Project SPOTIWAVE-II POCI/MAR/57836/2004 funded by the Portuguese FCT) during the summer period in 2006. These included thermistor chain measurements along the water column that captured the vertical structure of shoaling internal (tidal) waves and ISWs close to the breaking point. The SAR and airborne images were obtained in light wind conditions, in the near-shore zone, and in the presence of ISWs. The LiDAR images revealed sub-surface structures (some 1-2 m below the sea surface) that were co-located with surface films. These film slicks were induced by the convergent fields of internal waves and upwelling fronts. Some of the sub-surface features were located over the front slopes of the internal waves, which coincides with the internal wave slick band visible in the aerial photos and hyperspectral systems. Our flight measurements revealed thermal features similar to "boils" of cold water within the wake of (admittedly breaking) internal waves. These features are consistent with the previous in situ measurements of breaking ISWs. In this presentation we will show coincident multi-sensor airborne and satellite SAR observations that reveal the 3D structure of air bubble

entrainment in the internal wave field and frontal zones. It is suggested that these bubble clouds are probably related with strong convergence and vertical downwelling in the front portion of the internal waves and fronts. This hypothesis is discussed according to coincident images in the thermal infrared and visible wavelengths, and available theoretical models of air bubbles and ISWs (Grimshaw et al., 2010).

Notes

Day 2, Tuesday 19 June 2012

Session: Ocean current retrievals and applications

SAR Observations of Spiral Eddies in the Inner Seas

Svetlana Karimova [1]
[1]Space Research Institute of RAS, RU

Abstract

A spiral eddy is a submesoscale (hereafter with a diameter less than approx. 20 km) vortical pattern on the sea surface with a distinct spiral structure. Spiral eddies on sea surface were first seen in 1968 on the Apollo Mission. They have been poorly studied since that. So there are still lots of uncertainties concerning this type of eddies such as their 3D structure, typical lifetime, mechanisms of generation, reasons of cyclonic asymmetry, etc. The dataset used in the present study included Envisat ASAR and ERS-2 SAR images with two-year time coverage (2009-2010) and pixel size of 75 m obtained in different parts of the Baltic, Black and Caspian seas. Total number of images exceeds 2000. Different mechanisms making hydrodynamic structures visible in SAR imagery were scrutinized. Among them there are ones due to surfactant films, wave/current interactions, thermal fronts and floating ice tracers. The most important of them were defined to be visualization by surfactant films presenting on the sea surface and wave/current interactions in the current shear zones. The first group of eddies (visible due to surfactant films) for the shortness sake was referenced as “black” eddies while the second one (visible due to wave/current interactions), as “white” eddies. The second task concerned an investigation of some individual characteristics of eddies, such as their lifetime, orbital and phase speeds, speed of eddy rotation, peculiarities of eddy evolution, properties of the surfactants visualizing eddies, width of eddy-visualizing slicks, fine eddy structure, eddy vertical dimension, etc. In every basin studied, some the most comprehensive eddy parameters both for “black” and “white” eddies were investigated. Among them there were number of eddies, frequency of their occurrence in SAR imagery, sign of vorticity and typical length scale. Totally about 14,000 vortical structures were detected. About 98% of them had a cyclonic rotation. As a whole, the numbers of the eddies detected in the different seas were proportional to the numbers of the images analyzed. Spatio-temporal parameters of the vortices were subjected to statistical analysis. Interannual and seasonal variabilities of the eddy parameters were traced. So the “black” eddies were detected mainly in the summer, spring and autumn seasons while the “white” ones were distributed rather evenly during all the seasons. Hypotheses explaining the variabilities revealed were proposed. For the most perfectly shaped 8500 eddies their spatial scale was defined. A diameter of the vortical structures detected varied from 1 to 75 km, while 99% of the eddies were within a range of 1-20 km. A characteristic size of the “black” eddies in all the basins was less than that of the “white” eddies. The values of the characteristic eddy size for the Baltic, Black and Caspian seas proved to be proportional to the values of the baroclinic Rossby radius of deformation typical for these basins. In order to define the regions of frequent eddy manifestation the generalized schemes of eddy spatial distribution were obtained. Spatial distribution were scrutinized separately for “black” and “white” eddies. The eddy density schemes were normalized by the number of SAR images covering every pixel. The analysis of the eddy spatial distribution showed that the “black” eddies were distributed rather evenly over the basins and did not demonstrate a significant connection with the basin- and meso-scale surface circulation. The most prominent spatial feature of the “white” eddies consisted in the location of the most of them along the western basin boundaries and (in the Baltic Sea only) in the elongated parts of the basin. So the “white” eddies seem to generate (manifest) in the regions with the highest wind speeds with resulting intense drift currents. Special attention was also paid to the mechanisms of spiral eddy generation. Earlier barotropic, baroclinic and inertial instabilities as well as specific atmospheric forcing and effects of convection were supposed to be potential reasons of spiral eddy generation. In the present study, a role of the different mechanisms mentioned above was clarified. This work was implemented within the framework of the Federal Target Program "Scientific and scientific-pedagogical

personnel of innovative Russia" in 2009-2013 and partly supported by the Russian Foundation for Basic Research (grants #10-05-00428, #11-07-12025). SAR data were obtained under the ESA grant #C1P.6342.

Monitoring the Surface Inflow of Atlantic Water to the Nordic Seas using Envisat ASAR

Morten Wergeland Hansen [1], Johnny Johannessen [1], Fabrice Collard [2]
[1]NERSC , NO
[2]CLS , FR

Abstract

Sea surface range Doppler velocities from nearly 5 years of Envisat Advanced Synthetic Aperture Radar (ASAR) acquisitions covering the Fram Strait, the Barents Sea, the Norwegian Sea, the North Sea, and the Skagerrak Sea, have been examined. After systematic corrections and combination of observations from varying instrument look directions, the zonal and meridional components of the inflow of Atlantic Water to the Nordic Seas are investigated. Distinct expressions of the sea surface flow are revealed with a clear manifestation of topographic steering, particularly along the 500 m isobath. At 70 degrees north, the Atlantic water separates into one branch entering the Barents Sea and one branch heading toward the Fram Strait. Along the Norwegian coast the Norwegian Coastal Current are also detected with time-averaged speed reaching up to 40 cm/s. At a spatial resolution of 10 km, the root mean square errors of the zonal velocities are estimated to be down to 2 cm/s. The range Doppler velocity retrievals are assessed and compared to other direct and indirect estimates of the upper ocean current, including surface Lagrangian drifters, moored recording current meter measurements, and surface geostrophic current inverted from several mean dynamic topography fields. The results are promising and demonstrate that the synthetic aperture radar based range Doppler velocity retrieval method is applicable to monitoring the temporal and spatial variations of ocean surface circulation, provided the imaging geometry is favorable.

Surface Current Monitoring over Gulf Stream, Agulhas and North Brazilian Current

Fabrice Collard [1], Bertrand Chapron [2], Johnny Johannessen [3], Vladimir Kudryavtsev [4], Alexis Mouche [1], Marjolaine Rouault [5]
[1]CLS , FR
[2]IFREMER , FR
[3]NERSC , NO
[4]NIERSC , RU
[5]CSIR , ZA

Abstract

Systematic ENVISAT ASAR wide swath acquisitions over selected supersites with strong currents are now available since 5 years opening to long term monitoring of such major ocean dynamic drivers. Outcome of this systematic monitoring are numerous including better assessment of surface current resolved scales, long term trend in water mass transport and observation of abnormal events such as Natal pulse or early retroflexion. Based on this long term archive, improvement of Mean Dynamic Topography in selected coastal areas where strong currents are stirred by significant bathymetry gradients is now possible and will be compared to state of the art MDT from altimetry and gravimetry. Finally, statistical comparison between the rotational of observed surface current and the presence of Cross sea favoring the formation of rogue waves will be presented, to demonstrate the capacity of SAR to monitor not only surface currents but also wave-current interactions.

High precision Doppler frequency estimation for ocean applications

Harald Johnsen [1], Geir Engen [2]
[1]Norut , NO
[2]Norut Tromsø Earth Observation, NO

Abstract

The Sentinel-1 level-2 (L2) ocean product (OCN) has been designed to deliver geophysical parameters related to the wind, waves and surface velocity to end-users. Each L2 OCN product contains up to three geophysical components: the radial surface velocity (RVL), the ocean surface wind field (OWI) and the ocean swell wave spectra (OSW) components. The core of the Sentinel-1 Level 2 RVL processing is a high-precision and high-resolution algorithm for estimation of Doppler frequency [Hz] and the corresponding standard deviation. The requirement from the user community is an accuracy of the surface current better than 0.3 m/s on a spatial resolution down to 1x1km2. This requires an accuracy of the estimated Doppler frequency of less than 5Hz. The Doppler frequency is estimated from a full-bandwidth processed SLC image with no windowing applied to the data enabling the correction for side-band effects (i.e. aliasing of energy from neighboring areas). The algorithm is based on modeling the expectation value of the azimuth spectra in terms of covariance coefficients over range of frequency bands taking into account the antenna coefficients, the true intensity and the white noise (thermal and quantization) contribution. The first order coefficient of the model is then solved simultaneously with respect to phase providing an estimate of Doppler offset, and to envelope providing an estimate of the unbiased (noise corrected) intensity. The model is also used to calculate the standard deviation of the Doppler estimate. The performance of the algorithm (both the Doppler estimate and the standard deviation) has been tested on ASAR SM data with varying signal-to-noise ratio. A standard deviation of less than 3Hz is achieved on a spatial resolution of 1.5km. Perspectives for Sentinel-1 Doppler estimation and performance will be discussed in relation to this. The Doppler estimation algorithm is easily extendable to TOPS mode data.

Results from the Submesoscale Experiment April 2011: In Situ, Aircraft, and Satellite Measurements of Small Eddies, Fronts, and Filaments in the Southern California Bight

Benjamin Holt [1]
[1]Jet Propulsion Laboratory, USA

Abstract

Benjamin Holt, Jet Propulsion Laboratory, California Institute of Technology Burkard Baschek and Jeroen Molemaker, UCLA George Marmorino and Geoff Smith, Naval Research Laboratory Carter Ohlmann, University California Santa Barbara Svein Vagle, Institute of Ocean Sciences Michelle Gierach, Jet Propulsion Laboratory, California Institute of Technology In order to truly resolve the small scales of submesoscale eddies and fronts, we have collected high-resolution (1-15m) in situ and aerial data during the submesoscale experiment SubEx1 in April 2011. The experiment took place near Catalina Island in the Southern California Bight, an area known to have extensive small-scale eddies. Repeat measurements every 15-30 min enabled us to observe significant changes over very short time scales and to investigate the temporal evolution of these features. Measurements were taken in a collaborative effort with aerial IR, hyperspectral, and SAR imagery from 3 planes, as well as in situ measurements with a Towed Instrument Array (TIA), drifters, currents, surfactants, and optical measurements. In addition, satellite observations were obtained from Envisat ASAR and MODIS sensors. The temperature and salinity data collected with the TIA have a vertical and horizontal resolution of 1-5m covering the upper 35m of the water column at a tow speed of 4-5m/s, demonstrating that the observed submesoscale features mostly occur within a shallow, 5-15m deep thermocline. Fronts are very sharp with temperature and density gradients of 1ÅãC and 0.2kg/m3over 5m. The observed features evolve over the course of a few hours. Rotational and advective velocities are 0.2-0.4 m/s resulting in a large Rossby number flow. This paper will focus on the repeat observations of small eddies obtained by NASA's UAVSAR aircraft system and Envisat ASAR. Small-scale eddies are detected by SAR in coastal environments by the appearance of surfactants which act as tracers of the underlying current field. Multiple repeat SAR observations were obtained approximately on hourly intervals that enable the tracking of the rapidly evolving eddy field and derivation of rotation velocity maps through feature tracking. These observations also included the detection of a recurring frontal feature off Catalina Island. This study will present preliminary results of eddy tracking from the combined SAR time series, and an interpretation of the surface features when compared with coincident high-resolution ocean surface temperatures, measured through airborne infrared observations, and in situ temperature transects. We will also present eddy tracking results from previously collected pairs of SAR-detected eddies obtained by Envisat ASAR and ERS-2 SAR.

Observations Conditions and Principle for Ocean Current front Backscatter Modulation

Fabrice Collard [1], Bertrand Chapron [2], Frederic Nouguier [2]
[1]CLS , FR
[2]IFREMER , FR

Abstract

Oceanic fronts at the boundary of meandering currents and eddies have been observed and models have been suggested to interpret the modulation of radar backscatter in terms of convergence and divergence zones. A new principle will be presented based on systematic collocation of radar backscatter modulation over oceanic fronts and surface winds highlighting the strong interraction of Eckman current with ageostrophic jet currents along the oceanic front location. Analysis of such backscatter modulation intensity in terms of wind conditions and observation geometry will be discussed. Complementary observations of the same principle on MERIS optical glitter derived sea surface roughness will be presented.

High Resolution Surface Velocity Monitoring with Wide Swath SAR: A User`s Guide to the Range Doppler Method

Johnny Johannessen [1], Bertrand Chapron [2], Fabrice Collard [3], Alexis Mouche [3], Knut-Frode Dagestad [4], Morten Wergeland Hansen [1]
[1]NERSC , NO
[2]Ifremer , France
[3]CLS , FR
[4]Storm-Geo , NO

Abstract

Doppler-derived ocean surface velocity monitoring from the European Space Agency`s (ESA) Envisat Advanced Synthetic Aperture Radar (ASAR) has emerged as unique method in the last decade. Operated as a "speed-gun" in space the ASAR Doppler shift anomalies manifest the range component of the surface current. Building on more than 10000 synoptic wide coverage acquisitions since 2007, new high-resolution gridded maps (10 km x 1o km) of intense surface current regimes have now been established. A broad range of examples will be given with coincident ASAR roughness, wind field and range Doppler velocity together with auxiliary data and information. Moreover we will demonstrate that the Doppler based method, in combination with surface drifter data, satellite altimetry and gravimetry, and sea surface temperature measurements, can resolve circulation patterns that have important implications for oceanographic and air-sea interaction research. The ASAR based surface velocity estimates that can be related to surface current are not error free, and they demand careful processing and correction for near surface wind speed effects and wave motions. We will also discuss this. Nevertheless, as also emphasized in another User`s Guide for high-resolution wind monitoring with wide swath SAR released in 2005, this Guide demonstrates the unique power of this new method, although the understanding of the signal formation and corrections are incomplete. With the launch of the Sentinel-1 missions in 2013 and 2015 a Doppler grid product will be made available. We are therefore expecting a significant growth in the research and application of the SAR based surface velocity estimation as was the case for the evolution of the wind retrievals in the last decade which has almost reached operational status today.

Notes

Day 3, Wednesday 20 June 2012

Session: Ship Detection

Ship Detection and Sea Clutter Characterisation Using X&L – Band Full-Polarimetric Airborne SAR Data

Sebastien Angelliaume [1], Philippe Martineau [1], Philippe Durand [2], Thibery Cussac [2]
[1]ONERA , FR
[2]CNES , FR

Abstract

Maritime surveillance and observation of non-cooperative ships become very important in the current context and spaceborne SAR systems could be used to detect and monitor them. As such, to allow observation of non-cooperative boats with temporal revisits compatible with the objectives of maritime surveillance responsiveness, the proposed solutions generally moved towards radar operating with a very wide swath, which implies acquisition at grazing angles. But the availability of experimental radar data acquired in such conditions is limited. With the contractual support of CNES, an acquisition campaign using SETHI, the airborne SAR system developed by ONERA - the French Aerospace Lab, took place in November / December 2011 in order to improve the understanding of radar backscattering, especially at grazing angles. The main objective of this dedicated campaign over the Atlantic Ocean, off the Brittany Coast of France, was to make very precise measurement of sea clutter and ship backscatter coefficient for numerous conditions of acquisition and to study the potentiality of SAR systems for boat detection. Full-polarimetric SAR data have been acquired with SETHI, at X and L – bands simultaneously; the total bandwidth is 300 MHz at X-band (range resolution of 0.5 m) and 100 MHz at L-band (range resolution of 1.5m). During the campaign, data have been acquired at three incidence angles: steep (60°), intermediate (70°) and grazing (80°). Moreover, specific passive reception at X and L-band have been made so has to study the efficiency of such acquisition to perform ship detection. Five flights during 6 days (from the 29th of November until the 04th of December 2011) have been realized over three different regions of interest so as to acquire data with different sea states. In order to validate the results obtained from the data analysis, a special effort has been made on ground truth for this campaign: in addition to having rented 6 different boats, AIS signal from boats present in the area was obtained from the SPATIONAV System, an optical camera has been set in one of the two PODs of the aircraft, we recorded the trajectory of the cooperative boats so as to perfectly know their position and direction during acquisition; meteorological information has been obtained form a lot of sources (buoys, institutional entities like Meteo France, ...). The planning of the airborne campaign was the following: ♣ Ushant traffic separation scheme (English Channel): Non-cooperative tankers / cargos o November 29, 2011 : sea state 5-6 o December 04, 2011 – morning : sea state 4-5 o December 04, 2011 – afternoon: sea state 5-6 o Available ground truth: AIS signal from non-cooperative boat ♣ 10 Nautical Miles South of the town of Le Guilvinec: 2 cooperative boats (15-20m) o November 30, 2011 : sea state 3-4 o Available ground truth: Tracking GPS for both cooperative ship and inertial central installed into one of both. AIS signal from the non-cooperative boat ♣ Bay of Quiberon: 4 cooperative boats (length less than 10m) o December 02, 2011 : sea state 2 o Speed equal to 15, 25, 35 and 45 knots o Available ground truth: Tracking GPS for all cooperative ship. AIS signal from the non- cooperative boat Finally, all the data collected during this campaign will allow us to study the influence of many parameters on sea clutter value and backscatter coefficient of boats: sea state (wind speed), frequency band, polarization state, incidence angle and more particularly in the grazing configuration, observation angle (compared to the orientation of the cooperative ship and the direction of waves), size of the boat, ... In this paper, we will first describe the SETHI sensor and its characteristics. Then we will detail the acquisition campaign: flight configuration and data acquisition, regions of interest, in-situ measurements and notes ... Finally, results obtained with the campaign will be presented in a third part: backscatter coefficient of ships, sea

clutter measurement and finally detection capability of a boat depending on the parameters of the acquisition.

Validating a Ship Detector Based on the Notch Filter with RADARSAT-2 Fine Quad-Pol Data.

Armando Marino [1], Nicholas Walker [2], Irena Hajnsek [3]
[1]ETH Zurich Schafmattstr. 6, CH
[2]EOsphere Ltd , UK
[3]ETH Zurich / DLR-HR , DE

Abstract

The monitoring of coastlines is a major topic for security and surveillance. In this context, satellite remote sensing with Synthetic Aperture Radar (SAR) has proven to be particularly beneficial because of its capability to acquire images with any-weather conditions and at night time. In recent years there have been a growing number of satellite borne SAR sensors that allow the possibility to attain the information related to the polarisation of the electromagnetic wave. Polarimetric information can be exploited to assist in the detection and classification of targets, since different targets and their surrounding background are likely to exhibit different backscattering characteristics when illuminated by different polarisations. This work concerns ship detection exploiting SAR polarimetric data using dual- and quad-polarimetric acquisition modes. Specifically, a new algebraic representation of polarimetric targets is introduced for the development of the detector. These are 6 dimensional complex vectors preserving all the information which exists in the polarimetric covariance matrix. The algorithm then performs a "perturbation analysis" in this vector space and measures the coherence between a target to detect and its perturbed version on the data. In order to adapt this approach to ship detection, the target to detect is defined as any vector lying in the orthogonal complement to the vector which represents the polarimetric signature of the sea. The actual procedure can be simply accomplished employing a Gram-Schmidt ortho-normalisation. In other words, the algorithm can be considered to be a notch (negative) filter focused on the sea. Consequently, all the features which have a polarimetric behavior different from the sea are detected (i.e. ships, icebergs, oil spills, etc). In order to make the algorithm applicable to any data and sea condition the polarimetric signature of the sea (the Null) and its amplitude are extracted locally from a region surrounding the pixel under consideration. Finally, a dual polarimetric version of the detector is developed, to be exploited in the circumstances where quad polarimetric data cannot be acquired, or in circumstances where it is desirable to have access to the wider swath widths that are possible with dual-pol data in comparison to quad-pol . In this work an accurate validation is performed exploiting 4 RADARSAT-2 Fine quad-pol images acquired during 2011, which have not been reported on previously. The acquisitions are accompanied by an accurate ground truth performed during the acquisition time. To identify large ships and vessels the AIS position was acquired. For smaller vessels which do not always use AIS photographic evidence of the area near the exit of Portsmouth harbour was acquired from the Spinnaker (Millennium) Tower of Portsmouth. The 4 acquisitions were all performed in ascending mode and represents a valuable data source with look angle varying from approximately 24 to 38 degrees (FQ5, FQ8, FQ14 and FQ18). In addition to the different look angles the weather conditions were also varying, which causes a corresponding variation in the backscatter from the background sea. The new data were compared with the other two RADARSAT-2 Fine quad-pol images acquired over the same region in 2010 (FQ3 descending and FQ18 ascending). Interestingly, the availability of two acquisitions with same orbital parameters (FQ18) with a time difference of one year makes it possible to reject most of the range and azimuth ambiguities (ghost targets), since these remain stable in the two acquisitions. The result of the analysis is that the detector seems to be able to obtain accurate detections within all the available conditions proving practically the results previously obtained (and presented) with a Monte Carlo simulation. Specifically, the notch filter seems able to detect targets of dimensions comparable (or even smaller in some instances) to the resolution cell. This is possible thanks to the processing performed by the notch filter which is able to

isolate the return coming from the sea and focus only on the rest. Finally, the quad polarimetric detection seems to outperform the dual polarimetric algorithm; however, the reduction is not very great and involves mainly small vessels.

Operational Ship Detection in Canada Using RADARSAT: Present and Future

Paris Vachon [1], Robert Quinn [2]
[1]Defence R&D Canada , CA
[2]DG Space , CA

Abstract

The Department of National Defence (DND) Polar Epsilon (PE) project has implemented operational ship detection using RADARSAT-2 data by constructing new receiving stations at Masstown (near Halifax) and Aldergrove (near Vancouver) and a central data processing facility at Aldergrove. RADARSAT-2 data are received at either of these sites, forwarded to Aldergrove if required, and processed to imagery. The imagery are then exploited for ship detection using the OceanSuite tool to generate ship detection reports, which are reviewed by an analyst prior to being forwarded to the Regional Joint Operation Centre (RJOC) Atlantic (Halifax) and RJOC Pacific (Esquimalt), both responsible for the DND/Canadian Forces global maritime domain awareness common operating picture. The system routinely delivers the ship detection reports within 10 minutes of downlink. The OceanSuite tool uses a K-distribution, Constant False Alarm Rate ship detection algorithm, followed by a fuzzy logic engine to reject image ambiguities and reduce false alarms. As part of PE, two new RADARSAT-2 ScanSAR modes have been implemented for maritime surveillance. Referred to as Maritime Satellite Surveillance Radar (MSSR), one mode is for detection of vessels while the other is for ocean surveillance. Both MSSR modes provide improved ship detection compared to heritage RADARSAT-2 modes, while the ocean surveillance mode should reduce acquisition conflicts, especially in the coastal zone. DND's incipient PE-2 project will focus on exploitation of data from the RADARSAT Constellation Mission (RCM), which is scheduled for launch starting in 2016. PE-2 will upgrade the PE capabilities for RCM compatibility, and will support the inclusion of an Automatic Identification System (AIS) receiver payload to provide nearly contemporaneous ship identification data, thereby improving RCM's utility for maritime surveillance.

Ocean Clutter Modeling for Ship Detection

Ding Tao [1], Stian Anfinsen [1], Camilla Brekke [1]
[1]University of Tromsø , NO

Abstract

1. Introduction: Ship detection based on polarimetric synthetic aperture radar (SAR) imagery can be achieved by applying a constant false alarm rate (CFAR) detector. To meet the specified false alarm rate, accurate statistical modeling of the ocean clutter becomes important. From previous studies [1], the product model is considered to be an appropriate statistical model for the ocean clutter. The scattering vector from the ocean clutter can be modeled as a product of a texture variable representing spatial variability of the reflectivity and a complex circular multivariate Gaussian vector representing the speckle. When the texture variable is gamma distributed, the scattering vector becomes multivariate K-distributed. Speckle, which is an inherent property of SAR data, can cause false alarms in ship detection. The polarimetric whitening filter (PWF) [2] applied in this study, processes the single look complex (SLC) polarimetric scattering vector into full-resolution pixel intensity and provides effective speckle reduction. This work considers the statistical modeling problem of covariance matrix estimation, which is a key part of the PWF process. The aim of this study is to investigate and compare three covariance matrix estimators: sample mean, fixed-point, and maximum likelihood. Their performances are examined under various texture conditions; ranging from high texture to non-textured cases with Gaussian clutter. Experiments are performed on simulated ocean clutter data with the specified covariance matrix obtained from real ocean clutter measurements in a Radarsat-2 quadrature polarimetric (quad-pol) SAR dataset. 2. Covariance matrix estimators: There are three covariance matrix estimators discussed in this study. The sample mean covariance matrix estimator is the computationally simplest. In many studies, the scattering vector is treated as Gaussian distributed by assuming a constant texture variable in the product model. In this case, the sample mean covariance matrix estimator is known to be complex Wishart distributed, and the PWF intensity output becomes Fisher distributed. The fixed-point covariance matrix estimator used in this study combines an estimator for the covariance matrix structure, introduced by Gini and Greco [3] and Conte et al. [4], with an estimator for the matrix scale proposed by Vasile et al. [5]. Compared with sample mean, the probability density function (pdf) of the fixed-point covariance matrix estimator is known to be asymptotically complex Wishart distributed also when the scattering vector has a non-Gaussian distribution. The PWF intensity output becomes compound gamma-Fisher distributed. The maximum likelihood covariance matrix estimator is defined by Gini and Greco in [3]. When the texture in the product model is assumed to be gamma distributed, shape parameter estimation becomes necessary. Hence, we have a compound estimation problem. The maximum likelihood covariance matrix estimator distribution function is unknown. 3. Preliminary results: Some preliminary experiments has been done to compare the covariance matrix estimation of the three estimators; sample mean, fixed-point, and maximum likelihood. Monte Carlo simulations are performed under various texture conditions and with different specified shape parameters. Large shape parameters correspond to low texture, and vice versa. Kullback-Leibler (KL) matrix distances are applied in the comparison of the three estimators. In summary, the maximum likelihood covariance matrix estimator provides the best estimation results (smallest KL matrix distances) under all texture conditions. The sample mean covariance matrix estimator shows the largest estimation errors under high textures, but it converges to the maximum likelihood under lower textures. The fixed-point covariance matrix estimation results are better than the sample mean under high textures. But under lower textures, it proves less accurate and does not converge to the maximum likelihood. The findings also confirm a previous theoretical study by Gini and Greco [3]. 4. Conclusions: Ship detection based on CFAR detection and the polarimetric whitening filter requires accurate statistical modeling of ocean clutter, especially the

covariance matrix estimation. This study addresses the problem of covariance matrix estimation, and three covariance matrix estimators are investigated and compared. The maximum likelihood covariance matrix estimator provides the most accurate estimation results under all texture conditions, but it requires a prior knowledge of the pdf of the texture in the product model. The sample mean and fixed-point covariance matrix estimators have good performance under lower texture and higher texture respectively. For subsequent statistical modeling of the PWF intensity output, the distribution function of the covariance matrix estimator is important to be studied. To the authors knowledge, the maximum likelihood covariance matrix estimator distribution function is unknown. The sample mean covariance matrix estimator is known to be complex Wishart distributed under the assumption of having Gaussian distributed scattering vector. The fixed-point covariance matrix estimator is known to be asymptotically complex Wishart distributed also when the scattering vector is non-Gaussian distributed. References: [1] E. Jakeman and P. Pusey, "A model for non-Rayleigh sea echo", Antennas and Propagation, IEEE Transactions on 24, pp. 806-814, Nov 1976. [2] L. Novak and M. Burl, "Optimal speckle reduction in polarimetric SAR imagery", Aerospace and Electronic Systems, IEEE Transactions on 26, pp. 293-305, Mar 1990. [3] F. Gini and M. Greco, "Covariance matrix estimation for CFAR detection incorrelated heavy tailed clutter", Signal Processing 82, pp. 1847-1859, 2002. [4] E. Conte, A. De Maio, and G. Ricci, "Recursive estimation of the covariance matrix of a compound-Gaussian process and its application to adaptive CFAR detection," Signal Processing, IEEE Transactions on 50, pp. 1908-1915, Aug 2002. [5] G. Vasile, F. Pascal, and J.-P. Ovarlez, "Heterogeneous clutter model for high resolution polarimetric SAR data parameter estimation", in Proc. 5th Int. Workshop on Science and Applications of SAR Polarimetry and Polarimetric Interferometry (POLinSAR2011), Frascati, Italy, 24-28 Jan 2011.

Ship Detection and Motion Parameter Estimation with TanDEM-X in Large Along-Track Baseline Configuration

Stefan Baumgartner [1], Gerhard Krieger [1]
[1]German Aerospace Center (DLR) Oberpfaffenhofen, DE

Abstract

Abstract: In the paper ship surveillance results obtained with the German TerraSAR-X / TanDEM-X radar satellite formation are presented. For processing a novel ground moving target indication (GMTI) algorithm applicable for dual-platform SAR systems is used. This algorithm enables high accurate estimation of the true geographical positions, the velocities and moving directions of the detected ships without the need of a priori knowledge. The algorithm is verified and evaluated using SAR data and ground truth reference data acquired during the commissioning phase of TanDEM-X in 2010. The results, which are discussed in detail in the paper, indicate that the obtained velocity estimation accuracy is in the order of 0.6 km/h and the position estimation accuracy is better than 20 m for ships end even better than 11 m for land moving vehicles. These figures are quite impressive; no other radar satellite system has ever achieved such accuracies, particularly without the use of a priori knowledge. Introduction: Surveillance of maritime traffic has evolved into an important security topic during the past years. Applications can be found in the military as well as in the civilian field. Among others the actual geographical positions, the velocities and moving directions of the ships are of interest. Larger international voyaging ships are already equipped with automatic identification systems (AIS). This enables the exchange of important navigation data with the aim to improve the guidance and to avoid accidents. However, so far no worldwide AIS coverage is reached. Signals from ships moving on the open sea often are too weak to be received by terrestrial AIS stations distributed along the coast lines. Even with future AIS spaceborne systems information about smaller ships carrying no AIS transceivers will not be available. Spaceborne synthetic aperture radar (SAR) systems provide an elegant solution for filling these information gaps, especially if the information is required on a non-regular basis as for instance in the case of major events and catastrophes. For detecting ships a single-channel SAR image is sufficient, as long as the sea surface is calm enough so that not clutter suppression is required. Impressive results obtained with single-channel TerraSAR-X data were published during the last years. If the ship is moving it appears displaced from its actual position in the SAR image. This effect often is denoted as “ship-of-the-wake effect”. The displacement in azimuth direction is proportional to the ship’s line-of-sight or across-track velocity, respectively. To give an example: an allegedly slowly ship moving in across-track direction with 17 kn (= 31.5 km/h) is already displaced by 600 m if a typical TerraSAR-X acquisition geometry with 45° incidence angle is considered. Thus, the objective of a SAR maritime traffic processor is to detect the ship and additionally to estimate its actual geographic position, its velocity and moving direction. With a single-channel SAR satellite the position and motion parameters are derived from the estimated Doppler parameters shift and slope, which are related to the ship’s across-track and along-track velocity components. However, especially for smaller ships or ships with low radar cross section the Doppler parameter estimation may be inaccurate. This may result in large position errors in the order of dozens or even hundreds of meters. With a dual-channel SAR system along-track interferometry (ATI) can be used. The ATI phase is proportional to the ship’s across-track velocity. Unfortunately the phase is negatively influenced by the receiver noise and the clutter. For the comparatively small along-track baselines available at state-of-the-art multi-channel SAR satellites, the ATI phase standard deviations are quite large resulting in large position and velocity estimation errors. For instance, the effective ATI baseline available at the TerraSAR-X satellite is only 1.2 m if the dual-receive antenna (DRA) mode is enabled. Even in the absence of clutter the position and velocity estimation accuracies for a ship signal with a signal-to-noise ratio (SNR) of 20 dB are in the order of 150

m and 5.5 km/h. For a weaker signal with SNR = 10 dB the accuracies are 490 m and 18 km/h. These accuracies might already be too worse for a lot of applications. Better accuracies can be achieved by using much larger along-track baselines. Since June 2010 the TerraSAR-X / TanDEM-X satellite formation is in orbit. The satellites fly in close formation with the opportunity to the select along- and across-track baselines nearly arbitrary. During the early commissioning phase the along-track baseline between both satellites was in the order of 20 km, corresponding to a time lag of approximately 2.5 seconds. This is just the time lag promising the best performance of the dual-platform GMTI algorithm used for maritime traffic monitoring. Therefore, during the commissioning phase several GMTI data takes over different test sites have been acquired with the satellite formation in pursuit monostatic mode, with the aim to evaluate and verify the dual-platform GMTI algorithm. The obtained results are impressive, especially if compared with the results obtained from state-of-the-art single-satellite SAR systems. For ships and land moving vehicles with SCNR values in the range of 10 to 23 dB position and velocity estimation accuracies smaller than 20 m and 0.6 km/h are achieved. In the final paper the GMTI processing scheme will be explained in detail and the obtained results will be presented and discussed.

Advanced Ship Detection and Classification

Guillaume Hajduch [1], Nicolas Longépé [1], Jérome Habonneau [1], Jean-Yves Le Bras [2]
[1] CLS, Plouzané, FR
[2] CLS, Ramonville Saint-Agne, FR

Abstract

SAR-based vessel detection has wide range of applications (traffic, fisheries monitoring, association with oil discharge…) with very diverse requirements in terms of detection performance, revisit time, etc. By choosing adapted modes, polarization and processing levels it is possible to improve in some extent the detection performances. Anyway, the improvement of the ship detection performance is generally not compatible with a systematic monitoring of large area with wide swath and low resolution products. The purpose of this paper is to present three ways of improvements allowing (1) a better estimation of the characteristics of detected ships (2) a better vessel detection by using polarimetric information (preliminary results) (3) a better ship detection of on high resolution product. The classical estimation of the characteristics of the detected vessel is based on the estimation of the geometric shape of the detected echo. On the other hand it has been shown that the Radar Cross Section (RCS) of the vessels may be expressed as a function of the ship length [R5]. We present here both an improvement of this RCS model and its application to the characterisation of the detected vessels. The forthcoming Sentinel-1 mission will be equipped with a dual polarization sensor that may be used in order to perform systematic monitoring of oceanic areas. The possibility to improve the vessel detection performances on such a dual polarization acquisition mode will be investigated. Finally, we will discuss the performances of ship detection on high resolution X-Band products from the CosmoSkyMed sensor. We will discuss the quality of the product, the backscattering of oceanic surface and X-Band and the radiometric contrast between sea and vessels. Acknowledgement These studies are partially funded by the European Commission under Framework Programme 7 (FP7) DOLPHIN project. Some Cosmo SkyMed products used in this study were provisioned through the ASI/CSK Principal Investigator program. References R1 G.Hajduch, “Ship Detection: from Processing to Instrument Characterization”, Proceedings of SeaSAR 2008 workshop R5 Vachon, P.W., J.W.M. Campbell, C.A. Bjerkelund, F.W. Dobson, et M.T. Rey. « Ship Detection by the RADARSAT SAR: Validation of Detection Model Predictions ». Candian Journal of Remote Sensing/Journal canadien de télédétection 23, n°. 1 (s. d.).

MARISS - Near Real Time Ship Detection with TerraSAR-X

Stephan Brusch [1], Susanne Lehner
[1]German Aerospace Center Wessling, DE

Abstract

Ship detection is an important application of global monitoring of environment and security. In order to overcome the limitations by other systems, surveillance with satellite synthetic aperture radar (SAR) is used because of its possibility to provide ship detection at high resolution over wide swaths and in all weather conditions. Results on the combined use of TerraSAR-X (X-Band) and ENVISAT (C-Band) ship detection, automatic identification system (AIS), and satellite AIS (SatAIS) in Near Real Time (NRT) is presented. The AIS system is an effective terrestrial method for tracking vessels in real time typically up to 40 km off the coast. SatAIS, as a space-based system, allows almost global coverage for monitoring of ships since not all ships operate their AIS and smaller ships are not equipped with AIS. The system is considered to be of cooperative nature. The quality of TerraSAR-X images with respect to ship detection is evaluated and the performance for ship detection is given. Results of Near Real Time applications in the framework of the ESA project MARISS are presented. Existing algorithms and Near Real Time capabilities can be adapted to the Sentinel Mission.

Ship Detection Using High Resolution Satellite Imagery and Space-Based AIS

Tonje Nanette Arnesen Hannevik [1]
[1]Norwegian Defence Research, NO

Abstract

The requirements for a national capability to monitor Norwegian waters increase with the increasing shipping and fishing along the Norwegian coast and in the Barents Sea. The Norwegian Defence Research Establishment (FFI) is developing capabilities using space borne sensors for monitoring ship traffic in the open ocean. Space borne Synthetic Aperture Radar (SAR) has been used operationally by the Norwegian Defence since 1998 to monitor the Norwegian economic and fisheries zones. Radar satellites increase the overview in vast areas and help the operative decision-making process. Traditionally, fairly coarse resolution SAR imagery from RADARSAT-1 and RADARSAT-2 ScanSAR mode (50 m resolution, 300 km swath width) have been used to support the Norwegian Coast Guard in fisheries monitoring. More recently, space-based AIS receivers have shown the possibility to monitor most of the world's ship traffic by different means. This allows the use of new approaches to obtain higher resolution data for selected areas of interest. New opportunities to use high resolution radar sensors (Radarsat-2, TerraSAR-X and Cosmo-Skymed) and also optical data from satellites such as Worldview-1 and GeoEye open up. In this paper we present a trial carried out in the Malangen area close to Tromsø city in the north of Norway in September 2010. High resolution Synthetic Aperture Radar (SAR) images from RADARSAT-2 were used to analyse how high-resolution SAR images and cooperative reporting can be combined. Data from the Automatic Identification System (AIS), both land-based and space-based, have been used to identify detected vessels in the SAR images. The paper presents results of ship detection in high resolution RADARSAT-2 Standard Quad-Pol images, and how these results together with land-based and space-based AIS can be used. Norway and FFI has launched an AIS transponder on a satellite on July 12th 2010 to receive AIS signals in space. AISSat-1 is a demonstration mission focusing on vessel detection in waters north of the Arctic Circle. This includes an AIS instrument on a satellite. AISSat-1 gives new opportunities for monitoring ship traffic and also to track ships outside the coastal land-based AIS chain (outside 40 nautical miles). An example is shown in the paper.

Notes

Day 3, Wednesday 20 June 2012

Session: Oil Spill Detection

Analysis of the Deepwater Horizon Oil Spill Using Polarimetric L-Band UAVSAR Data AR Data

Benjamin Holt [1]
[1]Jet Propulsion Laboratory, US

Abstract

Benjamin Holt and Cathleen Jones, Jet Propulsion Laboratory, California Institute of Technology Brent Minchew, California Institute of Technology On June 22-23, 2010, NASA deployed the airborne UAVSAR platform to the Gulf of Mexico to study the polarimetric radar properties of the Deepwater Horizon (DWH) oil spill, gather data for improved discrimination and characterization of oil slicks, and evaluate the environmental impact of oil in coastal ecological areas by tracking oil incursion into wetlands and monitoring the impact and recovery of marshland vegetation. We have analyzed the UAVSAR data collected over the main oil slick near the Deepwater Horizon rig site to address the first two of these science goals. Our analysis is used specifically to demonstrate the applicability of the fully-polarimetric L-band UAVSAR radar to oil spill detection and more generally to determine the scattering properties of polarimetric L-band radar from oil. The broad extent of the Deepwater Horizon oil slick has allowed characterization of radar backscatter for a very large range of incidence angles, from 27º - 64º. Along with the fine spatial resolution of 1-5 m, the low noise floor of the UAVSAR radar allowed detection of radar returns in both co-polarized (HH and VV) and cross-polarized (HV) channels across most of the swath, permitting a full characterization of the scattering mechanism through polarimetric decomposition analysis. Previous studies of oil slicks have been limited in their ability to measure the cross-polarized channel returns, either because the instrument did not have quad-pol capability or because the cross-polarization returns were below the instrument noise floor. Using the two UAVSAR data sets obtained directly over the main oil slick, plus an area of the Louisiana coast impacted by oil, we analyzed and compared the radar backscatter for all of the polarization channels (HH, VV, and HV) and decomposed the data using the Cloude-Pottier eigenvector decomposition for several areas of known oil contamination and for areas of clean water. The usefulness of the different polarization-dependent parameters for discriminating oil from water and for identifying variations within the oil of the slick was evaluated in order to determine the best parameters upon which to base an oil slick identification and classification algorithm. UAVSAR data from DWH demonstrated sensitivity to oil slick thickness especially emulsions [Jones et al 2011; Minchew et al., 2012], a capability not previously achieved despite SAR's well-known oil detection capability. Besides oil damping of ocean surface waves, additional radar backscatter reduction is attributed to oil-water emulsions that effectively alter the dielectric response, providing a unique signature. The polarimetric analysis showed the scattering mechanism to be predominantly Bragg surface scattering in all areas of both unslicked sea surface and oil-slicked surface within the main slick over a range of incidence angles from 27º to 60º. In addition to the damping of the ocean wave spectral components by the oil, damping also results from an effective reduction of the ocean dielectric constant from a mixture of 65-90% oil with water in the surface layer. Measurement of the reduction in effective dielectric constant requires a relatively thick emulsified layer and is not measurable for thin oil sheens where the oil affects the radar backscatter only through alteration of the ocean wave spectra. The high spatial resolution of the UAVSAR enabled the characterization of very near-shore oiling of vegetation in the marshlands affected by the DWH oil spill. UAVSAR returns from unslicked water in the Gulf and Barataria Bay in Louisiana were similar and much higher than oil slick returns in either the main slick or Barataria Bay at all incidence angles. Furthermore, oil slick returns from the main slick were significantly higher than oil sheen returns in Barataria Bay, indicating sensitivity in the UAVSAR data to varying oil properties including thickness and weathering. These studies have concluded that the L-band radar backscatter intensity is the most reliable radar indicator of oil slicks, affecting both co-polarized and

cross-polarized channels. The largest variations within the oil slick related to the intensity and the anisotropy decomposition parameter (indicative of small-scale surface roughness), although measurement of the latter requires a low-noise instrument with cross-polarization capability, like the UAVSAR. This indicates that a critical requirement in UAVSAR detection of varying oil slick characteristics (e.g., thickness, coverage, emulsification) is a low instrument noise floor, which allows accurate measurement of cross-polarization return for oil slicks [Jones et al. 2011; Minchew et al. 2011]. References Jones, C.E., Minchew, B., Holt, B., & Hensley, S. (2011). Studies of the Deepwater Horizon oil spill with the UAVSAR radar. In Y. Liu, A. MacFadyen, Z.-G. Ji, & R.H. Weisberg (Eds.), Monitoring and Modeling the Deepwater Horizon Oil Spill: A Record-Breaking Enterprise, Geophysical Monograph Series, vol. 195 (pp. 33-50) Washington, D.C.: AGU Minchew, B., Jones, C., & Holt, B. (2012). Polarimetric analysis of backscatter from the Deepwater Horizon oil spill using L-band synthetic aperture radar. Transactions of Geosciences Remote Sensing, in press.

Italian Coast Guard Integrated Maritime Surveillance in the Framework of Security, Anti-Pollution and Fisheries Control Activities

Luigia Caiazzo [1], Dario Cau [1]
[1]Italian Coast Guard Rome, IT

Abstract

The operational use of satellite data in maritime applications, in support of the Italian Coast Guard activities, integrated with maritime traffic monitoring systems, in order to improve the "Maritime Picture" . Data cross check and data integration represent, at the moment, the only way to identify "non-cooperative targets" on the scene (illegal fishing vessels, illegal migrants boats). The use of Earth Observation (EO) integrated with other data is very promising. EO enables the detection of targets in open sea waters, beyond the range of coastal monitoring and identification systems in support to tactical monitoring and integrated surveillance of illegal activities such as intentional environmental pollution, trafficking of people, goods, drugs, weapons. New generation satellites, as well as innovative processing tools allow to increase the systems capability in terms of data availability, resolution, coverage and time-revisit in order to better satisfy the Operational Users, as Italian Coast Guard is, needs in the framework of the Integrated maritime surveillance. The satellite observations of naval maritime traffic are used to collect information on the position, speed (where the wake is visible) and dimensions of the ships detected, on their time of passage through a given area and, by interpolating between successive observations, on the routes used to cross territorial waters. Ship identification is possible only by ship reporting systems (AIS, VMS e LRIT) data and satellite image cross-check and integration. While the EO sensors are non-cooperative systems, meaning that they detect all vessels sailing the observed area, almost the totality of non-EO vessels identification systems are cooperative and could be manipulated. Therefore, only by integrating these two sources of information it is possible to detect suspect vessels' behaviours or activities. Some preliminary feedbacks from the service providers and Italian Coast Guard (as user) were obtained. The results are mainly based on the outcomes of R&D projects and services set up at a pan-European and International level, such as LIMES (Land and Sea Integrated Monitoring for EU Security) European Commission Integrated Project and MARISS (European Maritime Security Services) and then MARISS Scaling-Up, MARCOAST, became EMSA CleanSeaNet service, SeAU, DOLPHIN and finally, in the framework of GMES, G-MOSAIC. Earth Observation data, both SAR (Synthetic Aperture RADAR) and optical, are also considered as a valuable support for the Fisheries and aquaculture Control and Management activities, in particular in the IUU fisheries contrast. The detection of oil pollution at sea is an European effective operational service since 2007 and Earth Observation based ship detection services are retained to be at an operational phase. The Oil and Gas Maritime needs in case of emergency situation drove the Service Providers to further develop their operational capabilities and technology in order to satisfy the operational Users' requirements: to require satellite acquisition with a very short advance (1 day), to receive the Oil spill Detection reports up to 30 minutes from Satellite pass and a monitoring capability that is independent from weather conditions and daytime. Taking the above into account, the capability for efficient response in case of an emergency is linked not only to the time the data are received by the Ground Segment, but to several other components of the response systems that will be analysed as: · Tasking time of the satellites · Revisit time of the different satellites · Location of the Ground Segments Reception capabilities · 24h emergency and data access availability Keywords: Earth Observation, Ship Detection, Illegal activities, cooperative/non-cooperative systems, fisheries.

Oil Spill Detection and Modelling: Preliminary Results for the Cercal Accident

Jose Da Silva [1], Ricardo Da Costa [2], Alberto Azevedo [2], Anabela Oliveira [2]
[1]University PORTO , PT
[2]LNEC , PT

Abstract

Oil spill research has significantly increased mainly as a result of the severe consequences experienced from industry accidents. Oil spill models are currently able to simulate the processes that determine the fate of oil slicks, playing an important role in disaster prevention, control and mitigation, generating valuable information for decision makers and the population in general. On the other hand, satellite Synthetic Aperture Radar (SAR) imagery has demonstrated significant potential in accidental oil spill detection, when they are accurately differentiated from look-alikes. The combination of both tools can lead to breakthroughs, particularly in the development of early warning systems. This paper presents a hindcast simulation of the oil slick resulting from the Motor Tanker Cercal oil spill, listed by the Portuguese Navy as one of the major oil spills in the Portuguese Atlantic Coast. The accident took place nearby Leixoes Harbour, North of the Douro River, on the 2nd of October 1994. The oil slick was segmented from available ERS SAR images, using an algorithm based on a simplified version of the K-means clustering formulation. The image-acquired information, added to the initial conditions and forcings, provided the necessary inputs for the oil spill model. Simulations were made considering the tri-dimensional hydrodynamics in a cross-scale domain, from the interior of the Douro River Estuary to the open-ocean on the Iberian Atlantic shelf. Atmospheric forcings (from ECMWF – the European Centre for Medium-Range Weather Forecasts and NOAA – the National Oceanic and Atmospheric Administration), river forcings (from SNIRH – the Portuguese National Information System of the Hydric Resources) and tidal forcings (from LNEC – the National Laboratory for Civil Engineering), including baroclinic gradients (NOAA), were considered. The lack of data for validation purposes only allowed the use of the two-dimensional surface plume transport model VOILS with the oil spreading formulation enabled. The remaining oil weathering processes (evaporation, emulsification, dispersion and dissolution in the water column) and shoreline retention were disregarded. The computational structure of the model is based on Eulerian-Lagrangian formulations, horizontal unstructured mesh discretization and it is soft-coupled with the tri-dimensional hydrodynamic model SELFE that uses hybrid sigma-Z coordinates in the vertical. The preliminary results of this hindcast simulation for the Cercal oil spill are presented and compared with available satellite SAR images. The forcings used play an important role in the final results. During the late stage spreading phases of the oil, about one month after the spill, the Douro River outflow is best seen in the SAR images. The morphology of the river outflow is discussed according to traditional coastal dynamics, and compared with model results. In addition to several interesting physical features that were identified, we report on the generation of Internal Solitary Waves in the vicinity of the Douro River plume. It is well known that trains of short-period internal waves can be generated by river plumes (such as the Columbia River). The internal structure of the observed internal waves (elevation waves or mode-2 versus mode-1 internal waves) is discussed based on the SAR signatures and available stratification. The present work has been conducted under an FCT/MCTES (PIDDAC) funded project entitled PAC:MAN – "Pollution accidents in coastal areas: a Risk management system" (PTDC/AAC-AMB/113469/2008).

Field Experiments on SAR Detection of Film Slicks

Stanislav Ermakov [1], Jose Da Silva [2], Ivan Kapustin [1], Irina Sergievskaya [1]
[1]Institute of Applied Physics RAS, RU
[2]Porto University, PT

Abstract

Experiments on SAR detection (TerraSAR-X) of oil slicks simultaneous with measurements of radar backscatter using an X-band scatterometer on board a ship were carried out on the Gorky Water Reservoir in the summer of 2011. The experiments were performed with artificial slicks (oleic acid films) with known physical parameters (the surface tension and the film elasticity) at different wind velocity and wind directions, including rather high winds (about 10 m/s). Radar contrasts characterizing the radar intensity depression in slicks were obtained, and the contrast values both for the SAR and X-band scatterometer were found to be comparable in magnitude with each other, although in some cases the scatterometer contrasts were higher than for SAR. The measured contrast values are found to be consistent with those obtained in our previous experiments of 2008-2009 with TerraSAR-X. Theoretical analysis of radar contrasts using a composite radar imaging model and a hydrodynamic model of wind wave damping due to films was carried out in order to describe the experiment, theory and experiment are in satisfactory agreement. The experimental results are also compared with data of previous platform and boat experiments, in particular, experiments on the Black Sea on slick detection using Envisat ASAR and ERS-2 SAR. X-band SAR contrasts are obtained to be higher than C-band contrasts, so that TerraSAR-X band can be used as a very effective tool for detection of oil film slicks.

Oil Spill Detection in Dual and Compact Polarimetry SAR Images

Øystein Rudjord [1], Arnt-Børre Salberg [1], Anne H. S. Solberg [2]
[1]Norwegian Computing Center, NO
[2]University of Oslo, NO

Abstract

Introduction During the last decade polarimetric SAR has been investigated in several oil spill detection studies (Gade et al., 1998; Lobardo and Oliver, 2000; Migliaccio et al., 2009b; Zhang et al. 2011). It has been demonstrated that the use of polarimetric SAR increases the oil spill detection performance (Lombardo and Oliver, 2000), and makes it possible to discriminate oil slicks from biogenic slicks (Migliaccio et al., 2009b). It is in particular the co-polarized phase difference (CPD) between the VV and HH channels that provides additional discrimination power to the oil spill detection problem (Migliaccio et al., 2009b). While many of the studies have focused on the SIR-C data obtained by the space shuttle in April and October 1994 (Gade et al., 1998; Migliaccio et al., 2009b), some also considered L-band ALOS PalSAR (Miglicaccio et al., 2009a) , Radarsat-2 quad-pol (Zhang et al., 2011) and TerraSAR-X dual-pol VV/HH (Kim et al., 2010) SAR data. However, none of these images are suitable for operational oil spill monitoring. Regarding the frequency, it is broadly recognized that C-band SAR data provides better detection capabilities than L-band SAR (Migliaccio et al., 2009). When considering C-band SAR data, the quad-pol mode on Radarsat-2 has only a spatial coverage of 25 km2. Envisat ASAR also offers a dual-pol VV/HH SAR data mode, but this is an alternating polarization mode without the needed CPD information. The VV/HH dual-pol is only available for Stripmap mode on TerraSAR-X, which has only a swath width of 15 km and a nominal length of 50 km. The X-band Cosmo-SkyMed also offers polarized SAR data, but the swath width is only 30km for the Ping-Pong mode. Due to these reduced capabilities for operational use of polarimetric SAR based oil spill detection using VV/HH or quad-polarization, we investigate other possibilities using dual-polarization. Methods Dual-pol entropy/alpha decomposition The first method we investigate is based on dual VV/VH or HH/HV polarization. Entropy/alpha decompositions have been applied extensively in radar polarimetry, also in oil spill detection (Migliaccio et al., 2007). However, all studies using the entropy/alpha decomposition in oil spill detection consider full polarimetric data. In this paper, we investigate the entropy/alpha decomposition for dual-pol SAR data proposed by Cloude (2007). In particular, we show that in some cases the mean scattering angle (alpha) may provide additional oil spill discrimination capabilities. The major benefit of using these dual-pol SAR data is that they are delivered in ScanSAR modes for both Radarsat-2 and Envisat ASAR, and thereby suitable for operational use. This is expected to be the case for the coming Sentinel-1 satellite as well. Compact polarimetry The other method we investigate for polarimetric oil spill detection is based on compact polarimetry (Raney, 2011. The objective of compact polarimetry is to realize many (but not all) benefits of quad-polarization, without the reduced swath width (Raney, 2011). Zhang et al. (2011) has demonstrated that the conformity index constructed from LL and RR polarized data may be used enhance performance of the oil spill detection. In this paper we will investigate the use of compact polarimetric data transmitted with: (i) 45o polarization angle, (ii) circular left polarization and (iii) circular right polarization, and received on both horizontal and vertical channels. From the compact polarimetry data, we will estimate the full coherency and covariance matrices and from these we construct several features for oil spill detection in quad-pol SAR data, The coming Radarsat Constellation Mission will be particularly tailored to compact polarimetry, offering e.g. maritime imaging mode with a swath width of 350 km and a resolution of 50 m, or a low noise mode with the same swath width and a resolution of 100 m. Experiments To demonstrate oil spill detection using compact polarimetry images, we analyse a Radarsat-2 quad-pol image. The image covers an oil-in-sea exercise in Norwegian waters, and contains three oil spills: plant oil, emulsion and crude oil. The image also contains a dark patch which is of

unknown status, but not oil. First we convert the quad-pol data to dual-pol compact polarimetry through a synthesis using PolSARPro. On the transmitter side we consider a linear polarization (45o polarization angle) and a left circular polarization. The reception is in the horizontal and vertical channels. The 3×3 coherency matrix is then reconstructed assuming rotation symmetry for the linear polarization and rotation and reflection symmetry for the left circular polarization. From the coherency matrix, the depolarization index is computed . From the depolarization index images we observe that the different oil spills appears with unequal contrast, which is not the case in the VV-image. We also find that when using a left circular transmit-polarization, only the crude oil is clearly visible in the image. Conclusions Currently, there is no satellite-based SAR sensor that provides quad-polarization or dual-pol VV/HH that may be used for operational oil spill monitoring (e.g. to provide input to services like EMSA's CleanSeaNet). The spatial coverage of existing quad-pol and dual-pol VV/HH images are too small. We have demonstrated that compact polarimetry may be an attractive imaging mode for oil spill detection. Since the planned Radarsat Constellation Mission is planned with a compact polarimetry mode with a spatial coverage of 350 km2 oil spill detection based on compact polarimetry may be used in operational services. The demonstration shows that compact polarimetry offers additional discrimination possibilities compared to single-pol. However, the results depend strongly on the synthesis and reconstruction method selected. Further research is needed in order to understand all properties of oil spill detection in compact polarimetric images.

References Cloude, S., 2007. The dual polarization entropy/alpha decomposition: A PalSAR case study. In Proc. 3rd Int. Workshop Science Applications SAR Polarimetry and Polarimetric Interferometry. PolInSAR, 2007; 22-26 January, ESA-ESRIN, Frascati, Italy. Gade , M., Alpers, W., Masuko, H. & Kobayashi, T., 1998. Imaging of biogenic and anthropogenic ocean surface films by the multifrequency/multipolarization SIR-C/X-SAR. J. Geophysical Research, 103(C9), pp. 18851-18866. Kim, D.-j., Moon, W. M. & Kim, Y.-S., 2010. Application of TerraSAR-X Data for Emergent Oil-Spill Monitoring. IEEE Trans. Geosci. Remote Sens., 48(2), pp. 852-863. Lombardo, P. & Oliver, C. J., 2000. Optimum detection and segmentation of oil-slicks using polarimetric SAR data. IEE Proc. -Radar, Sonar Navig., 147(6), pp. 309-321. Migliaccio, M., Gambardella, A. & Tranfaglia, M., 2007. SAR polarimetry to observe oil spills. IEEE Trans. Geosci. Remote Sensing, 45(2), pp. 506-511. Migliaccio, M., Gambardella, A., Nunziata, F., Shimada, M., and Isoguchi, O., 2009a. The PALSAR polarimetric mode for sea oil observation. IEEE Trans. Geosci. Remote Sens., 47(12), pp. 4032-4041. Migliaccio, M., Nunziata, F. & Gambardella, A., 2009b. On the co-polarized phase difference for oil spill observation. Int. J. Remote Sensing, 30(6), pp. 1587-1602. Raney, R. K., 2001. A perspective on compact polarimetry. IEEE Geosci. Remote Sens. Newlett.,no. 160, Sept., pp.12-18. Vespe, M. et al., 2011. Oil spill detection using COSMO-SkyMed over the Adriatic Sea: The operational potential. Vancouver, Canada, Proc. IEEE Int. Geosci. Remote Sens. Symp. (IGARSS), pp. 4403-4406. Zhang, B., Perrie, W., Li, X. & Pichel, W. G., 2011. Mapping sea surface oil slicks using Radarsat-2 quad-polarization SAR image. Geophys. Res. Lett., Volum 38, pp. L10602, doi: 10.1029/2011GL047013.

A Comprehensive Analysis of Polarimetric Features for Oil Spill Characterization

Stine Skrunes [1], Camilla Brekke [1], Torbjørn Eltoft [1]
[1]University of Tromsø UiT, NO

Abstract

INTRODUCTION Single-polarization (VV or HH) C-band synthetic aperture radar (SAR) sensors have conventionally been utilized in remote sensing of marine oil pollution. Over the last years, more advanced commercial SAR satellites have become available, providing dual- or quad-polarization data. The added information in multi-polarization measurements may increase the ability to characterize oil spills and to discriminate mineral oil from natural phenomena with similar appearance in SAR images. In this study, we address this issue through a large scale oil-on-water exercise conducted in Norwegian waters in June 2011 by the Norwegian Clean Seas Association for Operating Companies (NOFO). In this exercise, a unique data set was obtained, including quasi-simultaneous Radarsat-2 and TerraSAR-X data, containing the same three slicks with different chemical properties. Multi-polarization features are computed based on the two scenes, and evaluated in terms of their characterization and discrimination potential. A K-means classification is applied to a subset of the features. The analysis shows a potential for discrimination between mineral oils and biogenic slicks. Within-slick zones are revealed, possibly related to thickness variations. Currently, an analysis of multi-polarization features related to surface roughness and dielectric constant are pursued. The extraction of these properties could be valuable for the discrimination between oil and sea, and between different types of slicks. DATA SET From 6-9 June 2011, NOFO conducted their annual oil-on-water exercise in the North Sea. During the controlled discharges of oil at sea for the purpose of equipment and procedure testing, three different slicks, i.e. oil emulsion, crude oil and plant oil, were formed and imaged by SAR. One quad-polarization Radarsat-2 scene and one dual-polarization (HH,VV) TerraSAR-X scene were acquired with a temporal difference of only 16 minutes. Both scenes contain all three slicks. Wind speeds of ~1-3 m/s were measured in conjunction with the acquisitions. MULTI-POLARIZATION FEATURES In this study, multi-polarization features are extracted from the quasi-simultaneous Radarsat-2 and TerraSAR-X data. The analysis includes common multi-polarization features such as entropy, mean scattering angle, anisotropy, mean radar backscatter and co- and cross-polarization ratio. In addition, several features that have previously been found useful for oil spill purposes have been extracted, including co-polarized phase difference and the correlation between HH and VV channels [3] [4] [5]. The preliminary results show that several of the features show interesting variations, both between different regions within the slicks and also between the three different slick types. Initial classifications of the scenes have been done based on a subset of three of the features, i.e. mean radar backscatter, standard deviation of co-polarized phase difference, and the correlation between HH and VV. The classifications show a potential for distinguishing the plant oil slick from the two mineral oil spills, especially in the Radarsat-2 scene. For this sensor, the classifications also reveal interesting zones along the edges of the crude oil and oil emulsion. The zones could be related to slick thickness, which is expected to be low for the plant oil and decrease towards the edges of the mineral oils. As the emulsion have been on the surface for the longest amount of time, it is interesting to note that it's properties are more similar to the crude oil than to the plant oil. This may indicate that the differences we see are related to the type of slick (mineral vs biogenic) and the properties they have, e.g. monomolecular vs thicker layer etc. The TerraSAR-X scene does not show this zoning to the same extent as the Radarsat-2 scene. Photographs taken of the spills from boats and aircrafts will be used in the interpretations of the features. Currently, multi-polarization features related to physical properties of scattering media are evaluated for oil spill purposes. According to the reflection symmetry hypothesis, for natural media, the correlation between co- and cross-polarized channels is assumed to be zero. The Non-Ordered in Size (NOS) eigenvalues can then be derived, and used to extract

different parameters useful for describing a natural media. The single bounce eigenvalue relative difference (SERD) is useful for describing the scattering mechanisms in media with large entropy values, while the double bounce eigenvalue relative difference (DERD) variations are very sensitive to surface roughness [2]. A new alpha angle related to the dielectric constant [1] will also be extracted. The sensitivity of these parameters to natural media characteristics have previously been found useful for quantitative inversion of bio- and geo-physical parameters for terrestrial applications [2]. An analysis of the applicability of these features for oil spill information retrieval is ongoing. CONCLUSION AND FURTHER WORK Experimental data from the oil-on-water exercise in June 2011, including quasi-simultaneous multi-frequency data, are investigated in terms of multi-polarization features. Variations in the features are seen, both within the individual slicks, and between the different types of oil. These findings are especially pronounced in the Radarsat-2 data. A classification is performed on a subset of the features, and a potential in discriminating between biogenic and mineral oils is found for both sensors. However, Radarsat-2 seems to give more distinct results. The classification results of Radarsat-2 reveal slick zones possibly related to thickness variations. In the further work, features that have previously been related to physical parameters such as surface roughness and dielectric constant, will be thoroughly investigated and evaluated for oil spill characterization purposes.

ACKNOWLEDGEMENT Thanks to Total E&P Norge AS for funding this study, thanks to NOFO for letting us participate in the exercise, and thanks to KSAT, InfoTerra and The Norwegian Meteorological Institute for providing the Radarsat-2, TerraSAR-X and weather data respectively.

REFERENCES [1] Allain, S., Ferro-Famil, L. and Pottier, E., "Surface parameters retrieval from polarimetric and multi-frequency SAR data", Proc. of IEEE Int. Geosc. and Rem. Sens. Symp., 2003 [2] Allain, S., Lopez-Martinez, C., Ferro-Famil, L. and Pottier, E., "New Eigenvalue-based Parameters for Natural Media Characterization", Proc. of IEEE Int. Geosc. and Rem. Sens. Symp., 2005 [3] Migliaccio, M, Nunziata, F. and Gambardella, A., "On the co-polarized phase difference for oil spill observation", Int. J. of Rem. Sens., vol. 30, no. 6, p. 1587-1602, 2009 [4] Nunziata,F., Gambardella,A. and Migliaccio,M., "On the Mueller Scattering Matrix for SAR Sea Oil Slick Observation", IEEE Geosc. and Rem. Sens. Letters., vol. 5, no. 4, p. 691-695, 2008 [5] Velotto, D., Migliaccio, M., Nunziata, F. and Lehner, S., "Dual-Polarized TerraSAR-X Data for Oil-Spill Observation", IEEE Trans. on Geosc. and Rem. Sens., vol. 49, no. 12, p. 4751-4762, 2011

The "New Generation" of CleanSeaNet: the EU Remote Sensing Based Monitoring System for Oil Spill and Vessel Detection

Sónia Pelizzari [1] , Olaf Trieschmann [1] ,
[1]European Maritime Safety Agency (EMSA), PT

Abstract

Discharge of oil from ships, oil platforms and other sources causes significant damage to our coasts and to the marine environment in general. The monitoring of European waters is particularly challenging as the EU is an inundated peninsula with an extensive external coastline and several significant semi-enclosed seas. Currently, monitoring is undertaken by Member States with the support of the European Maritime Safety Agency (EMSA), via the CleanSeaNet service. CleanSeaNet is a Near Real Time (NRT), distributed, operational satellite monitoring oil and vessel detection system, which is in place since April 2007.

CleanSeaNet supplies Synthetic Aperture Radar (SAR) analysed images, from data provided by the European Space Agency's ENVISAT (now discontinued) and Canada's RADARSAT satellites, to 26 Coastal States. The downloading, processing and analysis of the data and the supply of the results is carried out by four European companies. An important scope of the service is also, whenever possible, to provide a first indication of the potential polluter, taking into consideration AIS data.

Since February 2011, a "new generation" of the CleanSeaNet service is available. The new system has been developed with the key concept of interoperability of services and data: it is OGC standard compliant and follows the INSPIRE directives. The system is hosted at EMSA premises and provides a number of extra functionalities and configuration capabilities to the users. As an indication of the volume of processed data, more than 2000 SAR images are processed per year.

The presentation will describe the technical setup of the service, the main features of the new generation and will provide examples of use-case.

Corresponding author email address:
sonia.pelizzari@emsa.europa.eu
olaf. trieschmann@emsa.europa.eu

Notes

Day 4, Thursday 21 June 2012

Session: Ocean Wind Retrievals and Applications

SAR-Derived High-Resolution Operational Wind Products within NOAA CoastWatch

William Pichel [1], Frank Monaldo [2], Christopher Jackson [3], John Sapper [4], Xiaofeng Li [5], Phillip Keegstra [6]
[1]NOAA/NESDIS, USA
[2]The Johns Hopkins University Applied Physics Laboratory, USA
[3]Global Ocean Associates, USA
[4]NOAA/NESDIS/OSPO, USA
[5]IMSG at NOAA/NESDIS, USA
[6]SP Systems, Inc., USA

Abstract

After 12 years of experimental production, SAR-derived winds are transitioning from research to operations in the United States National Oceanic and Atmospheric Administration (NOAA) during 2012. The first routine experimental near-real-time SAR winds products were generated by the NOAA, National Environmental Satellite, Data, and Information Service (NESDIS), Center for Satellite Applications and Research (STAR) and the Johns Hopkins University Applied Physics Laboratory in 1999. After a number of years of trial use, the utility of these products were recognized by the NOAA National Weather Service (NWS) Alaska Region which requested in 2008 that the SAR winds be transitioned to operations. During the operational implementation process, which started in 2009, many improvements were made in the capabilities of the SAR wind processing system. These include: (1) SAR input from all the readily available SAR satellites (ENVISAT is currently the primary source) using C-, L-, or X-band SAR data, (2) use of an improved land mask (Global Self-consistent Hierarchical High-resolution Shoreline), (3) ability to chose from multiple model inputs for a priori wind direction information (the NWS Global Forecast System is the primary source), (4) ability to choose from multiple SAR wind geophysical model functions (CMOD5 is the current algorithm for ENVISAT), (5) ability to choose from various HH/VV polarization ratio algorithms so that VV geophysical model functions can be used with HH data (the Mouche polarization ratio will be used initially), (4) addition of new wind product formats compatible with the NOAA CoastWatch products system (NetCDF4, HDF-5, png, kmz, GeoTiFF, shapefile), (5) product archival by the NOAA National Oceanographic Data Center (NODC) with on-line access through the NOAA Comprehensive Large Array-data Stewardship System (CLASS), (6) full operational documentation including a SAR Wind Algorithm Theoretical Basis Document, (7) parallel processing in product production to be able to quickly process an increasing volume of SAR images, (8) a real-time operational monitoring and error-tracking system to track the product production process and respond to processing errors, and (9) a comprehensive validation module that provides monthly statistics of matches between SAR winds and model, buoy, or scatterometer winds. User requirements for SAR wind products include an accuracy (bias) of 1 m/s or better over a wind-speed range of 3-15 m/s, product delivery within 1-2 hours (3-4 hours still useful), a resolution of 1 km or better (SAR winds are calculated at 500 m resolution), and coverage of selected U.S. coastal regions. In the operational winds processing system, a SAR image from any available satellite source is processed to normalized radar cross section and stored in a standard internal format, along with a matching land mask and metadata for the image. This standard image file is then processed to wind speed employing forecast model wind directions and the CMOD5 algorithm. Finally, standard output products are created and distributed by the NOAA CoastWatch program and archived by NODC. Daily statistics of the comparison of the SAR winds with model winds are derived for system stability monitoring; and once a month, a validation program generates statistics of SAR wind matches with buoy and scatterometer winds for product quality monitoring. In one study matching buoy with ENVISAT ASAR winds, 431 SAR-buoy comparisons had a bias of 0.14 m/s and a standard deviation of 1.41 m/s. In another study matching ASCAT scatterometer winds with ASAR winds, 23,692 ASAR-ASCAT comparisons had a bias of 0.58 m/s and a standard deviation of 1.31 m/s. Based on over 12 years of experience with using SAR winds to understand and improve the forecasting of coastal meteorological conditions in areas with rugged coastal topography, the operational availability of these products will, without doubt, save lives and property. With the eventual availability of Sentinel-1 and RADARSAT Constellation Mission operational SAR imagery, SAR winds should become available routinely for many more coastal regions and with a higher frequency of repeat coverage, increasing their value to the marine forecaster.

Estimating Winds From Synthetic Aperture Radar In Typhoon Conditions

Chris Wackerman [1], Jochen Horstmann [2], Ralph Foster [3], Mike Caruso [4], Hans Graber [4]
[1]General Dynamics , USA
[2]NATO/NURC , IT
[3]Univerisity of Washington , USA
[4] University of Miami , USA

Abstract

For accurate predictions of the path and intensity of a typhoon/hurricane it is essential to have accurate initial conditions of the winds and waves within the storm. It is often unpractical to fly aircraft through every storm, so the Office of Naval Research (ONR) has launched the Integrated Typhoon Observations in the Pacific (ITOP) Program which has as one component to determine if satellite-based Synthetic Aperture Radar (SAR) imagery can be used to generate accurate initial conditions for the winds and waves within typhoons/hurricanes. Under this program an end-to-end system has been developed to derive wind and wave fields under typhoon conditions from SAR imagery. The eventual goal is for the system to be completely automated, however to date user interaction is required to fine-tune the location of the eye of the storm. The standard set of tools for estimating moderate winds with SAR imagery [1,2,5] need to be modified to handle the high wind conditions of typhoons. There appears to be a bias in direction between SAR image features around the storm and the actual surface wind as measured by the QuickSCAT scatterometer. The standard geophysical model functions (e.g. CMOD5N) generate "hourglass" artifacts around the eye of the storm that need to be corrected. Due to the large number of X-band SAR satellites, the geophysical model function for these wavelengths needs to be developed for high winds. All of these are being addressed within the system. To remove SAR image artifacts and to impose a more globally physical constraint on the resulting wind fields, the raw SAR wind vector estimates are masked out in regions where the uncertainty of the result is too high and then used as inputs into a boundary layer model for tropical cyclones [6,7] which acts as a spatial filter to smooth the estimates and fill in any holes in a physically consistent manner. Since typhoon models often have coarser resolutions than the SAR wind estimates, further smoothing can be done either by using the SAR-derived winds as inputs into the H*wind tool [8] or by using very large scale smoothing functions derived from a Holland model [9]. The overall system works as follows: · The user indicates the location of the storm eye. · Two different methods for estimating wind direction are used, a local gradient method [3] and a projection-based method [1], or used to estimate wind direction and then merged to reduce outliers in each method. · The wind speed is estimated using the wind direction and CMOD5N [4] or wind direction with a geophysical model function that attempts to correct the "hourglass" artifacts. · Uncertainty masks are generated for the SAR product and the winds are used as inputs to an iterative boundary layer model to generate new wind vectors as well as an estimate of the pressure field. · The winds are then heavily smoothed via H*wind or large-scale spatial filters. System performance has been estimated using 17 historical Radarsat-1 SAR images of hurricanes containing storm eyes for both Atlantic and Pacific storms that were co-located with QuikSCAT wind speed and direction estimates, and with overflights of the aircraft-based Stepped Freqeuncy Microwave Radiometer (SFMR) wind speed estimates. Wind direction RMSE was 21 degrees, wind speed RMSE versus SFMR was 4.1 m/s, and wind speed RMSE versus QuikSCAT was 5.9 m/s. In addition, in the fall of 2010 the ONR ITOP Program ran a series of in situ experiments in the Pacific that covered a number of typhoons passing through the region with primary focus on Typhoon Malakas and Typhoon Megi. Coincident SAR imagery was also collected with near-simultaneous dropsondes and SFMR flights to estimate wind speed. For Typhoon Malakas, wind speed RMSE versus dropsondes was 3.0 m/s and versus SFMR was 3.9 m/s. Overall the system is estimating wind direction for typhoon conditions with a RMSE of 21 degrees and wind speeds with a RMSE of ~ 4 m/s compared to dropsondes and SFMR, and 6 m/s compared to QuikSCAT.

References [1] Wackerman, C.C., W.G. Pichel, and P. Clemente-Colon, "A projection method for automatic estimation of wind vectors with RADARSAT SAR imagery", Proc. 2nd Workshop on Coastal and Marine Applications of SAR, Svalbard, Norway, ESA SP-565, p. 55, 2003. [2] Horstmann, J., and W. Koch, "Comparison of SAR wind field retrieval algorithms to a numerical model utilizing ENVISAT ASAR data", IEEE Journal of Oceanic Engineering, 30 (Iss.3), 508-515, doi 10.1109/JOE.2005.857514, 2005. [3]

Horstmann J., W. Koch, S. Lehner, and R. Tonboe, "Ocean winds from RADARSAT-1 ScanSAR", Can. J. Remote Sens., Vol. 28(3), pp. 524-533, 2002. [4] Hersbach, H., "Comparison of C-Band Scatterometer CMOD5.N Equivalent Neutral Winds with ECMWF", J. Atmos. Oceanic Technol., 27, 721–736, 2010. [5] Monaldo F., D. Thompson, R. Beal, W. Pichel, and P. Clemente-Colon, "Comparison of SAR derived wind speed with model predictions and ocean buoy measurements", IEEE Trans. Geosci. Remote Sens., vol. 39, no. 12, pp. 2587–2600, 2002. [6] Patoux, J., R. Foster, R. Brown, "An evaluation of scatterometer-based oceanic surface pressure fields," J. Applied Meteor. Climate., vol. 47, 835-852, March 2008. [7] Foster, R., "Boundary-layer similarity under an axisymmetric gradient wind vortex," Bound-Layer Meteorol., 131:3, 321-344, 2009. [8] Powell, M.D., S.H.Houston, L.R. Amat, N. Morisseau-Leroy, "The HRD real-time hurricane wind analysis system," J. Wind Engineer and Indust. Aerodyn., 77 & 78, 53-64, 1998. [9] Holland, G.J., "An analytic model of the wind and pressure profiles in hurricanes," Monthly Weather Review, vol. 108, 1212-1218, August 1980.

Validation of SAR Wind Retrieval at X-Band Using TERRASAR-X and COSMO-SKYMED Data

Jochen Horstmann [1], Franck Monaldo [2], Michael Caruso [2], Salvatore Maresca [2]
[1]NATO Undersea Research Center , IT
[2]Johns Hopkins University Applied Physics Laboratory , USA

Abstract

In the last decade, C-band synthetic aperture radar (SAR) imagery from ERS-1/2, Radarsat-1/2 and Envisat have been used very successfully to retrieve high resolution wind fields (e.g. Monaldo et al., 2002 and Horstmann et al., 2005). Generally, wind directions are extracted by estimating the orientation from wind-induced phenomena which are visible in the SAR images and are aligned in the wind direction (Horstmann et al., 2002, Wackerman et al., 2003). Wind speeds are retrieved from the normalized radar cross section (NRCS) using the wind direction, SAR imaging geometry and validated C-band geophysical model function (GMF), originally developed for scatterometry (Hersbach, 2010). The availability of X-band SAR imagery from TerraSAR-X and Cosmo-SkyMed has encouraged the development of X-band GMFs, which are well suited for retrieving wind speed from these new sensors (Thompson et al., 2012). These GMFs have been derived in both theoretical and empirical approaches. The theoretical model relies on first principles: model the short ocean surface wave spectrum and then compute backscattering from the surface. The empirical approach is based on the interpolation between validated GMFs at C-band and Ku-band to estimate the X-band GMF. The processing chain, which is required to obtain high resolution wind fields from both TerraSAR-X and Cosmo-Skymed SAR data, consists of several steps. In the first step, SAR data are converted into calibrated NRCS imagery, which are corrected for scalloping (Romeiser et al., 2010) and beam seams. These are typical artifacts for ScanSAR imagery, particularily with respect to wind direction retrieval. For the next step, wind directions are extracted from the wind induced streaks via the Local Gradient Method, (LG-Method; Horstmann et al., 2002). Therefore, SAR image is sequentially smoothed and binned to reduced resolutions of 100, 200, and 400 m. From each of these smoothed images, local directions, defined by the normal to the LG-Method, are computed on the different scales and the most frequent directions in a predefined grid cell are selected. Wind speeds are than retrieved via the X-band GMF's (Thompson et al., 2012), using the SAR retrieved wind direction, NRCS and imaging geometry. Examining a number of TerraSAR-X images, we found that both the composite and empirical GMF work well at VV-polarization. However, at HH-polarization only the empirical GMF produced credible results, while the theoretical GMF significantly overestimated the wind speeds. Comparison of about 40 VV-polarized Cosmo-SkyMed images to a numerical weather prediction model showed a standard deviation of 2.3 m/s and a bias of -2.3 m/s, were SAR-retrieved winds were underestimating the wind speeds. Besides the bias, which could be reduced to 0.1 m/s by adding a constant to the NRCS, these are reasonable results considering numerical model results. We are also investigating the capabilities of X-band SAR under extreme wind conditions. An in depth investigation is ongoing, in particular in comparison to measurements and collocated C-band SAR data, which we will present at the workshop.

References Hersbach, H., "Comparison of C-Band Scatterometer CMOD5.N Equivalent Neutral Winds with ECMWF", J. Atmos. Oceanic Technol., 27, 721–736, 2010. Horstmann J., W. Koch, S. Lehner, and R. Tonboe, "Ocean winds from RADARSAT-1 ScanSAR", Can. J. Remote Sens., Vol. 28(3), pp. 524-533, 2002. Horstmann, J., and W. Koch, "Comparison of SAR wind field retrieval algorithms to a numerical model utilizing ENVISAT ASAR data", IEEE Journal of Oceanic Engineering, 30 (Iss.3), 508-515, doi 10.1109/JOE.2005.857514, 2005. Monaldo F., D. Thompson, R. Beal, W. Pichel, and P. Clemente-Colon, "Comparison of SAR derived wind speed with model predictions and ocean buoy measurements", IEEE Trans. Geosci. Remote Sens., vol. 39, no. 12, pp. 2587–2600, 2002. Romeiser, R., J. Horstmann and H. Graber, "A new scalloping filter algorithm for ScanSAR images", in Proc. IGARSS, pp. 4079-4082, 2010. Thompson, D.R., J. Horstmann, A. Mouche, N. S. Winstead, R. E. Sterner, and F. M. Monaldo, "Comparison of high-resolution wind fields extracted from TerraSAR-X SAR imagery with predictions from the WRF mesoscale model", J. Geophys. Res., in press, 2012. Wackerman, C.C., W.G. Pichel, and P. Clemente-Colon, "A projection method for automatic estimation of wind vectors with RADARSAT SAR imagery",

Proc. 2nd Workshop on Coastal and Marine Applications of SAR, Svalbard, Norway, ESA SP-565, p. 55, 2003.

Cross-Polarized SAR: a New Measurement Technique for Hurricanes

Will Perrie [1], Biao Zhang [2]
[1]Bedford Institute of Oceanography BIO, CA
[2]Nanjing University of Information Sciences and Technology, CN

Abstract

Forecasting hurricane intensities and tracks is important to protect coastal infrastructure and people. For reliable wind measurements, the state-of-the-art is airborne Stepped-Frequency Microwave Radiometer (SFMR). Averaged (10s) winds from SFMR are within 4m/s RMS error to dropwindsonde near-surface estimates (Uhlhorn et al. 2007). However, SFMR only measures along the aircraft flight track. Wind speeds from SAR images are routinely estimated from an empirical GMF, such as CMOD4 or CMOD5, derived from C-band scatterometer data, relating wind vectors to measured normalized radar cross sections (NRCS) in VV polarization and radar incidence angles. With wind direction, incidence angle and the NRCS, wind speed can be obtained via the GMF at any pixel. SAR data are accurate to 1~2 m/s for low ~ moderate winds via CMOD4. SAR wind speed retrieval accuracy is affected by errors in wind directions, which can be inferred from SAR data streaks, weather predictions, or scatterometer data. These have limitations. Streaks can be biased by other processes. Weather forecasts are low resolution. Scatterometer data has biases near coasts. While conventional optical satellites cannot see through clouds, C-band SAR can, at high resolution. Recently, hurricane winds have been retrieved from C-band RADARSAT-1 and ENVISAT images, with CMOD5 giving better results than CMOD4 (Horstmann et al. 2005). However, CMOD5 tends to underestimate the highest winds, biased by heavy rain and high sea states. Just as the drag coefficient and sea surface roughness have limiting values as winds exceed hurricane threshold, >33 m/s (Donelan et al. 2004), so also, airborne C-band NRCS data in VV polarization stops increasing, in these sea states (Fernandez et al. 2006), the ambiguity problem. Recently, C-band cross-polarized ocean backscatter was shown to be insensitive to wind direction and radar incidence angle, in wind speed retrievals (Zhang et al. 2011). Here, we establish a C-band Cross-Polarization Ocean Backscatter (C-2PO) model for high wind retrievals, > 20 m/s. Winds derived from C-2PO and CMOD5.N (Hersbach, 2010), using 2 RADARSAT-2 dual-polarization (VV, VH) SAR images over hurricane Earl is compared with SFMR, buoy data, and H*Winds (6km resolution). We show that C-2PO does not need external wind directions or radar incidence angles, and that it is simpler to use than CMOD5.N. Also, in available data, the SAR-observed NRCS in cross-polarization linearly increases, even for winds up to 26 m/s.

Doppler Centroid, Normalized Radar Cross Sections and Sea Surface Wind

Alexis Mouche [1], Fabrice Collard [1], Bertrand Chapron [2], Vladimir Kudryavtsev [3], Johnny Johannessen [4]
[1]CLS , FR
[2]Ifremer , FR
[3]NIERSC , FR
[4]NERSC , NO

Abstract

In weak to moderate ocean surface current environment, the SAR Doppler centroid is dominated by the directionality and strength of wave-induced ocean surface displacements. In this study, we show how this sea state signature can be used to improve surface wind retrieval from SAR. Doppler shifts of C-band radar return signals from the ocean is thoroughly investigated by co-locating wind measurements from the ASCAT scatterometer with Doppler centroid anomalies and normalized radar cross sections retrieved from Envisat ASAR. An empirical geophysical model function (CDOP) is derived, predicting Doppler shifts at both VV and HH polarizations as function of wind speed, radar incidence angle, and wind direction with respect to radar look direction. This function is used into a Bayesian inversion scheme in combination with wind from a priori forecast model and the normalized radar cross section (NRCS). The benefit of Doppler for SAR wind retrieval is shown in complex meteorological situations such as atmospheric fronts or low pressure systems. The interest of using the Doppler centroid anomaly for scatteromters is also discussed. This method is very promising with respect of future SAR missions, in particular Sentinel-1, where the Doppler Centroid Anomaly will shall be more robustly retrieved.

Organized Multi-Km Surface Stress Convergence Lines in Tropical Cyclone Surface Wind Retrievals

Ralph Foster [1]
[1]University of Washington , US

Abstract

Organized Multi-Km Surface Stress Convergence Lines in Tropical Cyclone Surface Wind Retrievals Ralph Foster Our research into using surface pressure data to improve Tropical cylcone surface wind retrievals produced an unexpected result. We found a new level of organization in the near-surface boundary layer. Throughout the images, we find organized bands, roughly aligned with the mean wind, of near-surface wind convergence at wavelengths on the order of 10 km. We are unaware of any direct observation of organization on this scale and further research is necessary to verify that the signature is a processing artifact. At present we believe it is not an artifact. However, these results must be considered preliminary. We hypothesize that the convergence bads are induced by multi-km wavelength roll vortices in the tropical cyclone boundary layer. We present evidence for these structures and some preliminary analysis of the mechanisms by which they might form. Previous research had documented that low aspect ratio (wavelength/PBL depth) PBL-spanning roll vortices are a very common feature of hurricane and typhoon boundary layers. Foster (2005) presented a theoretical explanation why they ought to be the expected state of the boundary layer. These rolls would form at small angles to the mean PBL wind and have typical wavelengths of about 2.5 to 4 times the PBL depth, or nominally 1500 to 2500 m. Hence, their effects should not be resolved in th 1-km pixel wind speed images that we have produced. (Note however that their imprint can be resolved in the raw 10 to 25 m SAR pixels. This imprint is used to make the first guess at wind directions in the wind speed retrieval process.) Although the strongest direct effect of the rolls is a period enhancement and reduction of the mean azimuthal winds in the radial direction, there is an associated overturning circulation that induces alternating bands of ne3ar-surface convergence and divergence, with the same 1.5 to 2.5 km spacing, in the surface wind field. One major benefit of the scene-wide, SLP-filtered wind retrievals is that it is possible to make sensible calculations of wind vector gradients. Figure 1 shows surface wind convergence fields calculated from SAR images of six hurricanes and typhoons. They all show a high degree of organization on multi-km scales ~10 km spacing. we find such patterns in all of the images that we have analyzed. These patterns are roughly aligned along the surface wind direction and hence bear a lot of similarity to the PBL rolls seen in observations (Wurman and Winslow Morrison et al., 2005; Lorsolo et al. 2008; Zhang et al. 2008; Ellis and Businger, 2010) and theoretically derived in Foster (2005). What remains to be explained is their very large aspect ratio (wavelength divided by PBL depth), which is on the order of 5 to 10. Possible explanations are coupling with tropospheric gravity waves, nonlinear roll-roll interactions and coupling to convection. Their dynamical role is also unknown. They may contribute to nonlocal (i.e. non-gradient) fluxes of enthalpy and momentum across the PBL or they might precondition the PBL and lower troposphere for future convection bands. We recently became aware of some numerical modeling studies that find similar structures and attributes them to a mechanism similar to that described in Foster (2005) (Prof. Gregory Tripoli, pers. comm.). It should be noted that the theory in Foster (2005) does indeed predict that nonlinearly stable, large aspect ratio rolls (~10) are possible. Figure 2 reproduces Figures 4 and 7 from Foster (2005). The interpretation of Figure 13a is that a wide range of wavenumbers with a range of orientation angles are unstable. All of these instabilities are roll vortices; they vary primarily in wavelength and orientation relative to the mean wind. The most unstable modes agree with the low aspect ratio rolls that have been documented in a large number of observational studies. However, large aspect ratio rolls (corresponding to wavenumbers, α, near 0.25 are unstable. Furthermore, Figure 13b shows that all unstable modes are nonlinearly stable – that is, the exponential growth is checked by self-modification and modifications of the mean flow in a manner that equilibrates into a new mean state with finite non-local fluxes of heat and momentum. So, large aspect ratio rolls that could match the structures seen in the SAR in the convergence fields are consistent with theory of Foster (2005). However, the large aspect ratio modes grow more slowly than the basic roll modes and, all things being equal, might not survive the "competition" for extracting mean flow energy against the faster low aspect ratio modes. However, Mourad and Brown (1990) demonstrated that nonlinear roll-roll interactions are a viable mechanism for developing large aspect ratio (~10) rolls in, for example, cold-air

outbreaks. A similar mechanism may be in play in the hurricane boundary layer. We will discuss these possibilities. These features are an unexpected result of this research and future research efforts will focus on developing a dynamical explanation for their formation and maintenance and on uncovering what role they play in typhoon physics.

Ocean Surface Winds Measurement Using X- and L-Band Polarimetric SAR

Akitsugu Nadai [1], Toshihiko Umehara [2], Seiho Uratsuka [3]
[1]National Institute of Information and Telecommunications Technology, JP
[2]National Institute of Information and Communications Technology , JP
[3]Applied Electromagnetic Research Institute , JP

Abstract

Synthetic Aperture Radar (SAR) is one of the powerful tools to investigate the earth surface. Usually, SAR is utilized to observe features on land surface, like classification of land use, volcano monitoring, biomass measurement, etc. Moreover, using the interferometric techniques, the 3-D information is able to be extract from pair of SAR observation data, as digital elevation model. SAR is also one of the powerful tools to investigate the ocean surface features. In this paper, some examples of utilization of SAR on ocean surface feature are presented.Ocean surface winds are important factor to determine environment related to ocean currents in coastal area. Because land topography strongly influences to wind field around it, the ocean wind field near the coast changes with small spatial scale. To measure the small scale change of ocean wind field is difficult by traditional method. The high spatial resolution of SAR agrees well with this requirement. The estimation of ocean wind vector needs at least two measurements. In recent years, the ocean wind estimation using the normalized radar cross section (NRCS) with external information of wind direction has been investigated. However, the spatial resolution of the external information influences on the accuracy of estimates. In this paper, the dependency of the NRCS on wind direction is compared between parallel polarizations. The difference of dependency suggests the possibility of ocean winds measurement with high spatial resolution using a polarimetric SAR. The dependency of probability distributions of NRCS on ocean winds may also be discussed.

Polar Lows and Ocean Wind Profiles

Birgitte Furevik [1], Johannes Röhrs [1], Gunnar Noer [1], Harald Schyberg [1], Frank Tveter [1]
[1]Norwegian Meteorological Inst. , NO

Abstract

The Polar Regions are known for their cold air outbreaks and polar lows that often spin off during these events. A task within the STARS project (http://stars.wiki.met.no) is to collect available Envisat ASAR scenes over registered polar low events in an open data base (STARS-DAT) together with other satellite remote sensing data. Polar lows in Norwegian areas have been registered by the Norwegian Meteorological Institute (met.no) for more than 10 years. This list has been extended to the Greenland Sea and the Northern North Atlantic within STARS and in total now contains information about the date and track of 180 polar lows during the last 10 years. So far, around 300 ASAR Wide Swath Mode (WSM) and Global Monitoring (GM) passes are included in STARS-DAT, covering 5 years of polar low cases. About 15 of the polar lows have been observed in the SAR images, and some of them can be tracked by ASAR over 1-2 days. The processes of polar low formation, development and decay are not fully understood and are often poorly captured by numerical weather forecast models. Comparing SAR radar backscatter with scatterometer and model simulated backscatter, the amount of details from SAR which are not included in the model and scatterometer can be quantified. In parallel with this work, analysis of 10 years of rawinsonde data obtained at the weather ship Polarfront (66N 2E) in the Norwegian Sea has revealed a relatively frequent appearance of negative wind profiles, i.e. situations where the wind speed in 10m above the sea surface (asl) is stronger than higher up in the boundary layer (up to 150m asl). It turns out that these negative wind profiles mainly are associated with slightly unstable situations (difference in virtual potential temperature between 150m and 10m of -0.5degrees) and occurs predominantly when the winds are from the North. This indicates that those situations may be related to cold air outbreaks with downstream rain cells which are common in the Norwegian Sea and calls for an analysis of the upstream history of development of the near-surface boundary layer. Satellite data are unique for this purpose. Brümmer and Pohlmann (2000) "Wintertime roll and cell convection over Greenland and Barents Sea regions: A climatology", Journal of Geophysical Research, vol 105 (D12), showed that organised convective patterns (rain cells and atmospheric boundary layer roll vortices) are present 60% of the time in infrared images over an ocean area starting 200km North of Polarfront. Thus, in order to know if rain cells are present at the time of rawinsonde launch, infrared images and in particular SAR can be very useful. The advantage of SAR when working with near-surface wind profiles is that it shows the wind imprint on the sea surface, and this way gives direct evidence if the winds from the organised convective patterns actually reach the surface. Preliminary results from comparing rawinsonde wind profiles with Envisat ASAR images tend to confirm the hypothesis that the negative wind profiles are caused by organised convective phenomena. The presentation will include case studies of polar lows and analysis of ocean wind profiles from Polarfront.

High Resolution Wind Fields over the Black Sea Derived from Envisat ASAR Data Using an Advanced Wind Retrieval Algorithm

Werner Alpers [1], Alexis Mouche [2], Andrei Ivanov [3], Burghard Bruemmer [1]
[1]University of Hamburg, DE
[2]Collecte Localisation Satellites Avenue La pérouse, FR
[3]P.P. Shirshov Institute of Oceanology, RU

Abstract

The Black Sea is a sea area surrounded by mountains of differing heights with valleys opening to the sea and by flat planes. Local winds blowing onto the sea over coastal mountains or through valleys as well as meso-scale atmospheric eddies are often encountered over the Black Sea. Thus it is an ideal area to study complex wind systems and their interactions. Local winds, like foehn winds, gap winds, katabatic winds, and atmospheric eddies interact with synoptic-scale winds or with each other and thus give rise to wind fronts in which often rain cells are embedded (Alpers et al., 2010, 2011). Synthetic aperture radar (SAR) is an ideal sensing means to study fine-scale structures of near-surface wind fields over water surfaces. In contrast to scatterometers, which measure near-surface wind speeds and directions with a spatial resolution of the order of ten kilometres, SARs can measure it with a resolution of the order of 100 meters. However, the retrieval of two-dimensional wind fields from SAR data is not as straightforward as from scatterometer data, since SAR cannot measure wind directions directly. In most previous investigations the wind direction was obtained either from 1) atmospheric models or from 2) linear features visible on the SAR images, which are assumed to be aligned in wind direction. In this investigation we apply a new wind retrieval algorithm, which uses for wind direction retrieval also the Doppler shifts induced by motions of the sea surface (Mouche et al., 2011). The extraction of Doppler shifts from SAR data requires a special analysis of the complex SAR data. This new wind retrieval algorithm uses all three sources of information on wind direction (model, linear features, and Doppler shift) and combines them using the Bayesian method. In this investigation we apply this new algorithm to four complex wind events with winds blowing from opposite directions. The near-surface wind field is retrieved from SAR data acquired in 2011 by the Advanced SAR (ASAR) onboard the Envisat satellite over the Black Sea. It is demonstrated that the new wind retrieval gives much better results than the conventional wind retrieval algorithms. The Envisat ASAR data are compared with model winds and with in-situ measured meteorological data. Furthermore, we use in our interpretation of the wind events also Radarsat SAR images and MODIS and MERIS cloud images. References Alpers, W., A.Yu. Ivanov, and K.-F. Dagestad, "Observation of local wind fields and cyclonic atmospheric eddies over the Eastern Black Sea using Envisat synthetic aperture radar images", Issledovanie Zemli iz Kosmosa, 5, 1-13, 2010. Alpers, W., A.Yu. Ivanov, and K.-F. Dagestad, "Encounter of foehn wind with an atmospheric eddy over the Black Sea as observed by the synthetic aperture radar onboard Envisat", Mon. Wea. Rev., 139, 3992-4000, doi:10.1175/MWR-D-11-00074.1, 2011. Mouche, A., K.-F. Dagestad, F. Collard, G. Guitton, B. Chapron, J. Johannessen, V. Kerbaol, and M. W. Hansen, 2011: On the use of Doppler shift for sea surface wind retrieval from SAR, IEEE Trans. Geosci. Remote Sens., in press.

Dual-Polarized SAR Imaging of Meso-Scale Currents

Vladimir Kudryavtsev [1], Fabrice Collard [2], Alexander Myasoedov [3], Bertrand Chapron [4], Johnny Andre Johannessen [5]
[1]RSHU/NIERSC , RU
[2]CLS , FR
[3]RSHU , RU
[4]Ifremer , FR
[5]NERSC , NO

Abstract

Analysis of the dual-polarized (VV and HH) Radarsat-2 SAR images over the Gulf of Lion and the Agulhas Current are presented and discussed. These images possess distinct features that can be treated as SAR image manifestations of meso-scale surface currents, surface slicks (presumably oil slicks) and near surface wind field variability. Although the shape of VV and HH images are very similar, the magnitudes of the image anomalies are remarkably different. We argue that the departures of VV and HH NRCS anomalies for each of the observed phenomena can be interpreted as distinct contribution of the different scattering mechanism to the SAR imaging. The Radar Imaging Model (RIM) is invoked to support the interpretation of these observations.

Notes

Day 4, Thursday 21 June 2012

Session: Sea ice retrievals and applications

A Multi-Polarization Study of Arctic Sea Ice in C-Band and X-Band

Torbjorn Eltoft [1], Ane Fors [1], Mari-Ann Moen [1], Angelika Renner [2], Anthony Doulgeris [1], Sebastian Gerland [2], Laurent Ferro-Famil [3]
[1]University of Tromsø DoPT, NO
[2]Norwegin Polar Institute , NO
[3]University of Rennes 1 , FR

Abstract

The emergence of dual-polarization and fully polarimetric (quad-pol) space-borne SAR systems gives prospects for enhancement in the amount of information about sea ice properties that can be obtained from satellite borne sensors. A system is denoted fully polarized if it simultaneously measures all combinations of linear polarizations, i.e. VV, VH, HH, and HV. The interpretation of satellite-derived signatures of sea ice requires a thorough understanding of the interaction of electromagnetic radiation with the snow and ice layers (and ocean), and of how this interaction depends on both surface properties, such as roughness and salinity, and imaging parameters such as frequency, incidence angle, and polarization. This paper presents preliminary results from a study of polarimetric properties of synthetic aperture radar (SAR) signals scattered from Arctic sea ice. The SAR images analyzed are quad-pol C-band images from the Canadian system Radarsat 2 and dual-polarimetric X-band data from TerraSAR-X. These data were collected over the same area during field campaigns North of Svalbard in March/April 2011, and from the Fram Strait in August/September the same year. In addition to multi-polarization SAR images, an extensive set of validation data were also collected. The ground truth data included snow data such as; depth, stratigraphy, grain size, temperature, density, salinity, and sea ice data such as; thickness, salinity, temperature, conductivity, and freeboard height. In addition, helicopter flights were performed to measure sea ice thickness along certain transects using an EM-Bird instrument. Optical photos of the sea ice surface were also acquired during these helicopter flights. The analysis of the data has been conducted in several steps. Initially, the SAR images are segmented into distinct classes using an unsupervised classification algorithm, which incorporates both polarimetric and statistical signal features. The algorithm has built in contextual information through Markov Random Field modeling, and determines automatically the number of segments supported by the data through a goodness-of-fit testing. The resulting classes are unlabeled, but are separated using statistical and polarimetric properties representative of different sea ice types. The image segments are subsequently classified into ice types. In this labeling, ice properties obtained from in-situ measurements, combined with signal signatures derived from the PolSAR data, are used. The initial segmentation is the starting-point for the successive detailed polarimetric analysis of the data. It is well known that quad-pol data provide information about physical scattering mechanisms. It is also noted that some polarimetric parameters are directly related to surface properties such as roughness and the dielectric constant. Through various decomposition strategies, we generate a multitude of polarimetric parameters, and analyze their significance in the discrimination between sea ice types, and their sensitivity to surface properties. Dual-pol images are subsets of fully polarimetric data. Dual-pol data allow for more limited polarimetric analysis. On the other hand, sea ice will in most instances comply with the assumptions of reciprocity and reflection symmetry. This allows for a decoupling of the volume scattering effects and the surface scattering effects in the polarimetric coherence matrix. Surface scattering mechanisms are predominantly characterized by properties of the signals in the co-pol channels (HH-VV), whereas volume scattering manifests itself in the cross-pol channels (HV-VH). The TerraSAR-X scenes include the HH-VV combination, and hence our collected data sets allow for inter-comparisons between C- and X-band with respect to how surface scattering mechanisms influence some relevant polarimetric features. The current paper gives an overview of research scopes and methods, and reports on some preliminary results. Future work will go more deeply into the analysis and interpretations of the various findings.

ACKNOWLEDGEMENT: The project is funded by the Fram Centre, the Norwegian Ministry of Foreign Affairs, and Troms Fylke (RDA).

Sea Ice Classification Using Radarsat-2 Dual-Polarisation Data

Stein Sandven [1], Vitaly Alexandrov, Mohamed Babiker [2]
[1]Nansen Environmental and Remote Sensing Center , NO
[2]NERSC , NO

Abstract

The objective if this study is to investigate Radarsat2 signatures of various sea ice types and features in dual polarization images in different modes, for development of algorithm that can be used in ice classification and support to operational sea ice monitoring. During 2011 a set of ScanSAR Wide, Fine Mode and dual-polarisation (HH and HV) were collected for the area north of Svalbard. The images have been calibrated and range-normalized for the typical ice conditions in the area which includes level and deformed firstyear ice, multiyear ice, nilas and young ice, and open water in leads and in the marginal ice zone. The backscatter relation between HH and HV polarization has been analyzed for the different ice types. The possibility to improve ice classification by use of dual-polarisation SAR compared to single polarization has been assessed. Preliminary results suggest that combined use of HH and HV data gives better discrimination between ice and open water, especially between calm open water and level firstyear. Also multiyear and deformed firstyear ice can be better discriminated by use of HH and HV data. Methods for validation of the classification results are investigated using high-resolution optical images, aerial photographs, and in situ observations. The long-term goal is to implement and validate automated algorithms for ice-water discrimination and ice type classification of SAR images from Sentinel-1 and other planned SAR missions. Automated algorithms are needed to process the large amount of SAR data that will be available under GMES for use in operational ice monitoring and forecasting services.

Radar Polarimetry - Useful for Detection of Icebergs in Sea Ice?

Wolfgang Dierking [1], Christine Wesche [1]
[1]Alfred Wegener Institute, DE

Abstract

The presentation is focused on Radarsat-2 C-band data acquired in polarimetric mode over sea-ice covered regions with drifting and grounded icebergs. The dominant backscattering mechanisms of icebergs are deduced from different polarimetric parameters. Cross-polarization ratios, the correlation coefficient between HH- and VV-polarized signals, and the entropy/alpha decomposition reveal strong indications of volume scattering. The phase difference between HH- and VV-polarization is explained by the dielectric anisotropy of the ice. Observations of phase patterns over icebergs show that radar reflections from the sea ice towards the sidewall of an iceberg may propagate through the ice bulk to its surface and influence its radar signature. How effective single mechanisms are depends on ice properties and environmental conditions. The radar intensities of some icebergs overlap partly considerably with those of sea ice. The tested polarimetric parameters did not show a potential to reduce these ambiguities indicating that scattering mechanisms in sea ice and icebergs are similar in such cases.

Iceberg Monitoring Service by Joint Use of Drift Model, SAR and Altimeter Data

Nicolas Longepe [1], Franck Mercier [1], Jean Yves Lebras [1], Marion Sutton [1], Guillaume Hajduch [1]
[1]Collecte Localisation Satellites , FR

Abstract

With the increase of maritime transports at high latitude region, iceberg monitoring has become increasingly important. Sea routes along the edges of the Arctic Ocean are to be opened as a result of climate changes: these routes yield potential for saving cost for transportation companies. This concerns not only goods shipping but also transport of natural resources such as oil or gas extracted in the Arctic. However, icebergs would represent a potential danger of oil spills and pollution for the sensitive wilderness areas. Round-the-world sailboat races also navigate around icebergs in Antarctica. Iceberg monitoring is of high interest to optimize routes and warn sailboats of infested areas. This paper presents a new operational iceberg monitoring service based on a joint use of drift model, SAR and altimeter data. Following the Vendée Globe race (hereafter mentioned as VG) in 2008, SAR-based detection combined with drift modeling appears as a very efficient and reliable system for iceberg tracking in Antarctica (Lebras et al. 2010). Nonetheless, a massive amount of SAR images was used (for instance 250 ENVISAT SAR images) which could be detrimental for the future operational use of such a satellite-based monitoring system. Recently, it was demonstrated that targets in open water can be detected by using high-rate altimeter waveforms (Tournadre et al. 2008). This approach has been successfully adapted and applied to Jason 1, Jason 2 and Envisat data for iceberg detection in Antarctica (Mercier et al. 2011). The main drawback of altimetry missions for iceberg detection is that the ground track coverage is directly link to the orbital characteristics since the measurement is limited to the nadir direction. The area that actively contributes to the leading edge of the waveform is limited to a few kilometers around the nadir position (a 2- to 5 km ray circle depending on sea state condition). As a result, altimeter data is used to produce cumulative iceberg maps over long time periods (at least 10-15 days) enabling the identification of potential iceberg fields. The acquisitions of SAR images can be hence scheduled only when the ships/sailboats supposedly are in the vicinity of infested iceberg waters. In addition, a drift model is used to forecast the location of EO-based detected icebergs. In this paper, the following topics will be outlined: · Some quantitative assessments of the previous VG 2008 are shown. SAR-based iceberg detection has been analyzed depending on incidence angle and wind speed. · The capabilities of this new concept combining altimeter, SAR and drift model is demonstrated based on the operational service carried out during the solo round the world record attempt by Sodebo in January 2011. A new demonstration is also foreseen for the coming VG in December 2012. · Icebergs can also represent a potential danger for oil platforms in the Arctic region. A dedicated methodology based on these 2 radar technologies coupled to the drifting model is currently under development in the Barents Sea. The detection of icebergs either free or trapped in the ice floe is of interest: preliminary results will be shown. These studies are partially funded by the European Commission under Framework Programme 7 (FP7) SIDARUS project no. 262922 and by the GEP (Groupement des entreprises parapétrolières et paragazières) under the CITEPH research program.

References: Lebras J.Y., V. Kerbaol, G. Hajduch, L. Mesnier and E. Grenier, “Iceberg detection service for sailing races: the 'Vendee-Globe 2008-2009' experience”, oral presentation - SeaSAR symposium, 2010 Tournadre, J., K. Whitmer, and F. Girard-Ardhuin, “Iceberg detection in open water by altimeter waveform analysis”, J. Geophys. Res. 113, C08040, doi:10.1029/2007JC004587 Mercier F., Tournadre J. and Kouraev A. “Iceberg detection and continental lake-ice thickness estimation using altimeter waveforms”, 2nd SARAL-Altika science workshop, 2011.

SAR Measurements of Sea Ice Drift in the Fram Strait and Bay of Bothnia

Anders Berg (1), Leif Eriksson [(1)]
[(1)]Chalmers University of Technology, SE

Abstract

A sea ice drift algorithm has been implemented and utilized for two different regions; the Fram Strait between Greenland and Svalbard, and the Bay of Bothnia in the northernmost part of the Baltic Sea. The algorithm is based on an algorithm published by M. Thomas in 2008 that uses phase correlation of two sequential SAR images that cover the same area. Phase correlation is a fast frequency-domain method that corresponds to normal cross-correlation in spatial domain. An initial, rough estimate of the motion field is first computed with large search windows. The motion field is then refined by using smaller and smaller search windows. For each iteration the most recent motion field will be used to properly match the two images, thus avoiding problems with ice drifting out of the search windows. The algorithm has been extended with a module that attempts to resolve the rotation of the ice. The module makes use of the Fourier-Mellin transform which effectively converts rotation to a linear shift. It is activated when phase correlation gives a too weak signal or no signal at all. If any rotation can be resolved, the second image window will be rotated back to match the first image window, and phase correlation is repeated. The algorithm has been applied to horizontally polarized wide swath SAR images from the C-band SAR satellite ENVISAT. It has been evaluated with reference data that was obtained during a field campaign conducted in the Bay of Bothnia in spring 2010. An ice buoy developed by the Swedish Meteorological and Hydrological Institute (SMHI) was deployed on a large ice floe in the center of Bay of Bothnia. The buoy can be tracked remotely as it transmits data over a satellite link. It is equipped with a GPS receiver, an interior thermometer and two exterior thermometers. The GPS receiver was working as expected with the exception of a three week interruption in the beginning of the campaign. The temperature data shows how the sea ice surface melts during day and freezes again at night, until the buoy finally floats in water. Warm weather conditions with melting sea ice are quite challenging for the ice drift algorithm and a clear sensitivity to temperature can be observed. The sea ice is very dynamic during the last period of the campaign and the ice floes change their shape, shrinks and break up into smaller floes from one day to the next. The results from the field campaign show high accuracy of the algorithm within the pack ice with a root-mean-square error of five percent for the ice speed. A long time series of wide swath SAR images have been collected over the Fram Strait during 2011. The images have been processed by the algorithm and the result can be used to determine the Arctic sea ice export through the Fram Strait during summer. The drift and rotation computed by the algorithm has been validated with measurements made by manual tracking of ice floes in the images with promising results.

Sea Ice Concentration Retrievals by using Composite ScanSAR Features in a SAR Data Assimilation Process

N. Gokhan Kasapoglu [(1)]
[(1)]University of Tromsø - Auroral Observatory, NO

Abstract

Sea ice analysis based on synthetic aperture radar (SAR) observations for high analysis accuracy and with less analysis bias is often a difficult task because of the ambiguities mostly related to both wind and open water interaction and variation of the radar backscatter along the range direction (i.e., incidence angle effect). In this study, instead of assimilation of ScanSAR features for a whole range, individual features for specific incidence angle intervals are selected, combined and assimilated in order to degrease analysis bias and reach more accurate and detailed sea ice concentration information. SAR is an active remote sensing sensor which has been widely and successfully used for operational sea ice applications for many years. ScanSAR data is the most convenient SAR beam mode with its sufficient coverage for making sea ice analysis for operational purposes. Conventionally, sea ice analysis has been done manually by image analysis experts and analysis can be strongly depended on experience of the experts and contains some bias. Therefore automated sea ice analysis systems are needed to produce timely and qualitative analysis. Availability of dual polarized ScanSAR data (e.g., cross polarized HV) reduces some of the limitations of ScanSAR co polarized channel (e.g., ScanSAR HH) and make possible to develop automated sea ice analysis systems. Geophysical parameters such as ice concentration are continuous variable and this requirement may not be covered by the conventional pattern recognition algorithms. In the literature some supervised and unsupervised pattern recognition techniques have been proposed for sea ice analysis. Mostly pure pixel type (e.g., ice, no ice) assumption is made for these pattern recognition methods but pure pixel assumption may not be true for all cases and may not be completely applicable for geophysical parameter retrievals. Such methods based on region growing are very promising but has heavy computational cost [1]. SAR data has been successfully assimilated in a zero dimensional variational (0D-Var) data assimilation system to make sea ice analysis [2]. The data assimilation system compares the predicted and the observed (i.e., assimilated) SAR features and minimizes the errors through an optimization of the desired sea ice features (i.e., ice concentration). The result is an improved sea ice analysis. In this error minimization process, appropriate estimation of both observation and background error covariance matrices is essential. Sometimes assimilation of correlated ScanSAR features reduces the performance of the assimilation process. Additionally, when the number of assimilated features increases, then proper estimation of observation error covariance matrix can be problematic. Therefore assimilated features should be statistically independent [3]. Data assimilation can be defined as a fusion process of previous analysis and current observation. To map previous analysis into observation feature space (e.g., SAR feature space) a SAR forward model is employed [4]. For observations, the tonal based features, i.e., the backscattering coefficients (sigma nought) from HH and HV channels, and the first and second order co-occurrence based texture features that are extracted from HH and HV sigma nought have been identified [5, 6]. 0D-Var system produces an independent analysis at each observation location (i.e., using only one observation and one background state value). Sea ice analysis based only on passive microwave data (e.g., SSMI, AMSR-E) has been used as the background state which represents the previous analysis [2, 4]. With this experiment, impact of the SAR data on passive microwave based analysis has been shown. Because of the variation of the radar backscattering coefficients along the range direction, observation error covariance matrix is not constant for every incidence angle intervals. Therefore, in this study, ScanSAR features are selected for specific incidence angle intervals to obtain optimum sea ice analysis with the reasonable number of assimilated composite

feature. With this, lower analysis bias and accurate sea ice analysis were obtained by assimilating lower number of composite ScanSAR features.

References: [1] Q. Yu and D.A. Clausi, "SAR sea-ice image analysis based on iterative region growing using semantics," IEEE Transactions on Geoscience and Remote Sensing, Vol. 45, No. 12, Part 1, pp. 3919-3931 Dec, 2007. [2] N. G. Kasapoglu, "Synthetic aperture radar data assimilation for sea-ice analysis," IEEE Geoscience and Remote Sensing Symposium, In the proceedings of IGARSS 2011, pp. 4435-4438, Vancouver, Canada. [3] N. G. Kasapoglu, "Synthetic aperture radar feature selection for dual polarized ScanSAR data," Recent Advances in Space Technologies (RAST), pp. 370 - 374, Istanbul, Turkey, 9-11 June 2011. [4] N. G. Kasapoglu, "Synthetic aperture radar and passive microwave analysis fusion," Recent Advances in Space Technologies (RAST), pp. 360-364, Istanbul, Turkey, 9-11 June 2011. [5] R.M. Haralick, K. Shanmugam and I. Dinstein, "Textural features for image classification," IEEE Trans. Systems, Man and Cybernetics, vol. 3, no.6, pp. 610-621, Nov. 1973. [6] N. G. Kasapoglu, I. Papila, S.Kent and B. Yazgan,"Segmentation and Classification of SAR Data with Co-Occurrence Matrix for Texture Features," p. 717, 4th European Conference on Synthetic Aperture Radar (EUSAR'2002), Cologne, Germany.

The SAR Ice Constellation Backscatter Simulation Tool and Sea Ice Signature Database

Desmond Power [1], Dr. James Youden [1] , Nick Walker [2], Chris Williams [2] , Dr. David Barber [3] , Bruce Ramsay [4] , Kim Partington [5] , Matt Arkett [6] , Dr. Roger De Abreu [7] , Dr. Malcolm Davidson [8],
[1]C-CORE, CA
[2] eOsphere, UK
[3] University of Manitoba, CA
[4] Consultant
[5] Polar Imaging Limited, UK
[6] Canadian Ice Service, CA
[7] Canada Centre for Remote Sensing, CA
[8] European Space Agency, NL

Abstract

The mapping and monitoring of sea ice regions represents a key application for spaceborne synthetic aperture radar (SAR) missions. The all-weather day-and-night observation capability, coupled with the harsh arctic environment, often make radar the only reliable information source for operational services as well as providing a monitoring capability for science applications and climate change research. An important addition to this monitoring capability will be provided by the European Space Agency's Sentinel-1 C-Band SAR mission.

Over recent years there has been an increase in the range of different SAR sensor characteristics that are available from satellite platforms. This notably includes the range of frequencies that are available, in particular the increased availability of L- and X-band sensors (joining the more familiar C-Band systems) and the increase in the prevalence of multi-polarisation capabilities. This opens up the possibility of employing a "constellation" of satellites and exploiting the synergy between different SAR characteristics to achieve a better retrieval performance in terms of understanding what is being observed by the satellite. With respect to ice it is believed that this constellation approach will help to reduce the occurrence of ambiguities when attempting to separate important sea-ice classes, as well as for separating sea-ice from open water.

The work described here, which has been supported by ESA, has led to the development of a software tool (the Backscatter Signature Tool (BST) and its associated backscatter database) that allows the performance of different satellite sensor constellations to be evaluated for sea ice monitoring and to be compared against single satellite configurations. The tool allows the separability performance to be assessed quantitatively for the key ice and open water classes for a wide range of possible seasonal states and for a wide range of satellite parameters.

In addition to examining the added value of constellations, the BST is also expected to be of great benefit to the sea ice community in general for the understanding and analysis of sea ice signatures. The BST and its backscatter database will therefore be made available to the entire sea ice community. It is hoped that sea ice researchers will contribute to the legacy of the BST by building on the existing backscatter database and filling in the current gaps in BST signatures (particularly at X-Band and L-Band).

Notes

Day 3, Wednesday 20 June 2012

POSTERS

Future SAR missions (Sentinel-1, Radarsat Constellation Mission etc.)

Microwave Experiment Study of Shallow Sea Topography in Wind-Wave Tank

Xiaoqing Wang [1], Jinsong Chong [1], Zejun Li [1], Lei Liu [1]
[1]Institute of Electronics, Chinese Academy of Sciences, CN

Abstract

In the last several decades, we have seen a remarkable growth attempting to use SAR techniques to obtain shallow water depth data. But the detection technology is not operational at the moment. The SAR imaging theory we have cannot make proper explanations for some phenomenon such as underwater topography, which can be seen in deep water areas and in areas where current direction is parallel to the topography. So, more experiments have to be done to check the theory and make modification. The Maritime experiments are time-wasting. The meteorological and hydrographic conditions in the sea are uncontrollable. In our experiment, the wind-wave tank is used to create wind, current and wave under controlled environment. This article is divided into two parts. The first part mainly focuses on the design of shallow sea topography microwave experiments in wind-wave tank. Firstly, base on the fluid mechanics of current, the design of topography in water tank is discussed in order to make simulation of the real underwater topography environment. And then, the microwave experiment platform with multi-band and multi-polarization radar made by IECAS is introduced. With the design, experiments were performed at ShangHai Jiaotong University of China in Feb.2012. In the experiments, S, C, X and Ku band are used with full polarization. The second part gives out a brief analysis of the experimental data. Experimental results prove the efficiency of the discussion, and these create a foundation for future and more comprehensive experimental programs. Analyzing the initial experimental data, Doppler spectrum is getting wider with wind grown up. This disperses the energy of the radar backscatter, which means dynamic change of the backscatter is getting smaller with the wind growing up. And the experimental date also shows that the radar backscatter with upwind have better results.

Methodology and techniques

See the Sea - Multi-User Information System for Combined Analysis of Satellite Remote Sensing Data for World Ocean Investigations

Olga Lavrova[1], Marina Mityagina[1], Evgeny Loupian[1], Tatiana Bocharova[1], Ivan Uvarov[1]
[1]Space Research Institute of Russian Academy of Sciences , RU

Abstract

The immensity and high variability of the world ocean make gathering information on processes and phenomena in it and the atmosphere above it a rather difficult task. Therefore, the importance of ocean observations from space can hardly be overestimated. Currently, the application of satellite information is constantly broadening and large archives of ocean remote sensing data and related information products are being accumulated in various data centers. The obvious trend is an avalanche-like volume growth of isolated data and data products archives. There is a dramatic gap between a large number of satellite observation instruments available today and systems providing means for efficient processing and analysis of such data for complex interdisciplinary scientific purposes. The distributed satellite information service system See the Sea (STS) being developed by IKI RAS will not only provide the access to the data archives built in IKI RAS but also offer tools for producing different information products based on satellite data that can aid scientific investigation of processes and phenomena in the world ocean. STS is aimed at solving various tasks related to the study of processes in the ocean including interaction of the ocean and

atmosphere, currents, internal waves, eddies, pollution, etc. STS provides tools for joint analysis of different satellite data (VIS, IR, SAR), as well as metocean and ship location data. The key features of STS will be the possibility to work simultaneously with satellite information of different types and perform their complex analysis. This will facilitate large-scale investigations in the framework of scientific and educational programs and innovation projects. The development of system See the Sea is supported by Russian Foundation for Basic Research project 11-07-12025_ofi-m-2011. Satellite radar data provided by European Space Agency within Bear 2775 and C1P.6342 projects.

Re-thinking Statistical Based Segmentation of Sea Ice

Anthony Doulgeris [1]
[1]University of Tromsø, NO

Abstract

This presentation highlights problems found when applying recent advanced statistical analysis techniques for polarimetric SAR data to sea ice studies. Specifically, the resulting segments were not as solid as expected and the overall image still looked speckly and mixed. Possible causes are discussed and potential solutions are explored and demonstrated with preliminary real-world results. Generic and automated methods to analyse radar images of sea ice are important for meteorological studies and as input to global climate models, for safe ship navigation and structural engineering in ice covered waters, and for human endeavours and hunting in remote communities. Synthetic aperture radar images are advantageous because they operate both day and night and are not significantly influenced by atmospheric and weather conditions. The frequent availability of images over the Arctic and the desire for near-realtime operational products drives the need for automated processing methods. However, there is no standard method of analysis and polarimetric SAR techniques are still under active research. The main complication of using SAR images is that we have signal variations due to the changing target medium as well as variations due to radar speckle. Measured image data has been shown to be non-Gaussian in statistical distribution and is usually modelled as a product between a random texture term and a random speckle noise term. Several model families have been suggested and demonstrated in the literature and applied to multi-look complex (MLC) image analysis in order to achieve smoother, less speckled, results. The most applicable methods for automated segmentation are based on unsupervised clustering algorithms, because no ground truth data is required. The most advanced algorithm incorporates a very flexible non-Gaussian U-distribution model for the texture variable, uses the most accurate matrix log-cumulant techniques for parameter estimation, and incorporates statistical goodness-of-fit testing to determine an appropriate number of clusters. Although this method has been successfully applied to various PolSAR images of agricultural fields, forestry and glaciers, it produced unsatisfactory, very fragmented and still speckly segmentation results when applied directly to sea ice images. Sea ice analysis is a difficult problem because sea ice has a very complicated structure, having both thermodynamic growth as well as active dynamic mechanisms of development. Remotely sensing different types of sea ice is also a very narrow problem setting in comparison to the broader application of, for example, distinguishing between water, grassland, forest or urban areas. For sea ice SAR imaging, geometric effects, from orientations of blocks in a rubble field for example, may be larger than the differences between ice types. Hence, the pixel to pixel variation can appear to have extremely different polarimetric properties and causes very fragmented image segmentation results. Large scale regions are readily observed by eye, because of in-built smoothing mechanisms in the human visual processing systems. The fragmented clustering result is not strictly incorrect, as it reflects real polarimetric SAR differences at a very fine scale, but it is not the desired result when trying to simplify the image through segmentation. The large scale regions are actually visible through the fragmented results by looking at average mixture proportions of one class over another in different areas of the speckly, mixed segmentation. This hints that certain ice types may really only be defined by large scale properties rather than fine details. This concept is the same for urban areas which are really only defined at a larger scale, because urban consists of a mixture of buildings, roads, cars, trees and grass at the finer scale. So the problem now becomes how to make the clustering algorithms incorporate such large scale smoothing for sea ice analyses. Several smoothing approaches are investigated. The obvious method of large scale multi-look averaging is explored and does indeed achieve the regional smoothing, but at the expense of unwanted boundary effects due to blurring. Various adaptive multi-looking techniques exist, such as the modified Lee filter, but these produce pixel data with a continuous range in the degree of smoothing (equivalent number of looks) and cannot be incorporated directly into rigorous non-Gaussian statistical modelling. One new method is explored that uses goodness-of-fit testing to achieve dynamic multi-looking without blurring class boundaries and while mostly

retaining a consistent number of looks. The results are encouraging but still exhibit some small degree of blurring due to the statistical nature of the tests. Another approach explores applying the advanced clustering algorithms directly in the single look complex (SLC) image. Although the speckle variation is much higher with the original SLC data, using Markov random fields (MRF) to incorporate contextual smoothing achieves very smooth results. The MRFs are employed in a probabilistic sense that should does not blur distinct class boundaries. This SLC clustering may directly give a suitable resulting segmentation, or may be used to find the major classes, before performing a dynamic multi-look averaging to enhance the class contrast without crossing class boundaries. Subsequent MLC clustering may then achieve the desired result. The clustering problem and these solutions are demonstrated for real PolSAR imagery of sea ice from the Fram strait and north of Svalbard. The images were obtained with the support of the Fram Centre "Polhavet" project and the clustering approach forms only the first stage of more detailed sea ice analyses in the future.

Wave retrievals and applications

The Measurement of Surface Waves by Spaceborne SAR, Airborne SAR and Buoy Along the Coast of Hainan

Jian Sun [1]
[1]Ocean University of China 238 Songling Road, CN

Abstract

It has been well established that Synthetic Aperture Radar (SAR) images over the ocean can provide surface wave information only if there are stripes concerning surface waves, especially swell, in SAR image. SAR image data can be used quantitatively to retrieve surface wave parameters if the SAR is calibrated and a suitable SAR wave retrieval model is available. The retrieval scheme follows the procedure of former author Sun & Kawamura (2009). The 180¡ãdirectional ambiguity is overcome by considering that the waves propagate to the coast when studying the waves near the coastal region. Moreover, there is distortion of the surface wave stripes due to the strong nonlinearity caused by the orbital wave motions, especially for the wind waves. The result of this distortion is that there is a loss of information beyond a cut-off wavenumber and waves with wavelengths shorter than a certain length propagating in the azimuthal direction are not mapped onto the SAR image directly. We assume that the waves which can be seen on SAR images near the coastal region is swell instead of wind waves by assuring that the wind is not blowing to the island through checking the Quickscat wind field at that time. In this paper, the ocean wave spectra and the associated wave parameters are retrieved from the airborne and spaceborne SAR images which are acquired nearly simultaneously near the east coast of Hainan during the flight experiment of application at land and sea. The wave parameters from SARs are compared with the observation from Waverider buoy over the study site. The wave spectrum is derived by the inversion of quasi-linear transform which relate the ocean wave spectrum to the SAR image spectrum. The errors of retrieval wave propagation direction of waves for both SARs are less than 20¡ãand the errors of the wave height, wave length and wave period is less than 20%, which shows the good agreement of SAR wave parameters with in-situ observation. The off shore breaking is also shown in SAR multi-polarization images. The intensity of wave breaking stripe is proportional to the signal to noise ratio of SAR spectrum. The results can be used to evaluate the performance of ocean wave observation by spaceborne and airborne SAR.

Seafloor Topography Modelling in Northern Adriatic Sea Using Synthetic Aperture Radar

Federico Filipponi [1], Andrea Taramelli [1], Francesco Zucca [2]
[1]ISPRA , IT
[2]University of Pavia, IT

Abstract

Underwater bottom topography may be visible on Synthetic Aperture Radar (SAR) images through the radar signature of ocean surface currents. Using SAR images and a limited number of echo soundings it is possible to constructs accurate depth maps, greatly reducing the costs of bathymetric surveying. Based on shallow water bathymetry synthetic aperture radar (SAR) imaging mechanism and the microwave scattering imaging model for oceanic surface features, we are working to develop a new method for shallow water depth retrieval from space-borne SAR images. Shallow waters in the northern part of Adriatic sea may represent favorable depth condition for underwater bottom topography estimation testing over large area, using SAR imagery, although such area does not show strong tidal currents. Strategy for northern Adriatic Sea seafloor modeling is presented, using the Bathymetry Assessment System (BAS). Evaluation is conducted using SAR imagery from different satellite platforms and in multitemporal framework, in cooperation with echo soundings from bathymetric surveying. Two monitoring sites supply in situ data, such as water level, current flow, wind velocity and direction. Physical conditions evaluation in the study site supports selection of the best SAR images for depth estimation. Multisensor approach will give the possibility to evaluate differences in bottom topography estimation from sensor with different characteristics.

Ocean Wave Measurements using a Cross-Track Interferometric SAR Technique

Akitsugu Nadai [1]. Toshihiko Umehara [2], Seiho Uratsuka [2]
[1]National Institute of Information and Telecommunications Technology, JP
[2]Applied Electromagnetic Research Institute, JP

Abstract:

The cross-track interferometric SAR technique is widely utilized to the topography measurement of the earth crust. However this technique is not utilized to the ocean surface very much. In this paper, the ability of the interferometric SAR technique is used to measure the ocean waves by measuring the topography of ocean surface.

The current method of ocean wave measurement by SAR is based on the analysis of the spatial pattern on the intensity image. However, the intensity of each ocean wave component strongly depends on the geometric relation between the directions of wavenumber vector and the illumination. So, the intensity of spectral density of intensity does not directly related to the intensity of spectral density of ocean waves. Moreover, ocean waves are a kind of moving targets with not only its propagation but also the existent of ocean currents. The position change of ocean waves in synthetic aperture time influenced the intensity and sharpness of ocean wave patterns. As a result, the estimation of true spectra of ocean waves is difficult.

If the cross-track interferometric SAR technique can measure the topography of ocean surface, the ocean waves can be analyzed from the topography. However, the influence of the motion still remains. In this paper, the ocean waves is analyzed using the ocean topographies observed by the Pi-SAR[1], that is the airborne interferometric SAR developed by National Institute of Information and Communications Technology and Japan Aerospace Exploration Agency.

The Pi-SAR observation experiment was done with the cross-track interferometric SAR mode at the northwestern sea off Okinawa. In this experiment, the Pi-SAR observed same ocean area with different illumination directions. The spectra of ocean waves are obtained as the 2-dimensional spectra of topographies of ocean surface and the intensity images. Moreover, the sea truth data was obtained by the ocean wave measurement on the surface buoy near the observation area.

In this Okinawa observation experiment, the strongest peak on the spectrum of intensity image differs with the illumination (flight) direction (Fig. 1). It represents that the spectral intensity of the intensity image is determined not only by the intensity of wave components but also by the relation between the wavenumber vector of ocean waves and the illumination direction. On the other hand, the strongest peak on the spectrum of the topography of ocean surface corresponds to the dominant wave component, regardless of the illumination direction. This result shows that the spectra of topography of ocean surface are independent to the geometry between the illumination and wavenumber vector of ocean waves. It is because the tilt-modulation effect and the hydrodynamic-modulation effect, those make the ocean wave pattern on intensity images, depend on the geometry between ocean wave crest and illumination direction of SAR. The topography of ocean surface represents directly the surface elevation. Therefore, it was shown that the measurement of ocean wave by interferometric SAR is effective.

The results represent the ability of cross-track interferometric SAR technique to measure the ocean waves. It also represents the effectiveness of cross-track interferometric SAR technique to the topography of ocean surface. In these days, there are some plans of the satellite ocean altimeter using the cross-track interferometric SAR technique. This result may become one of the feasibility studies of such a new type ocean altimeter.

Internal Waves

A Study of Inversion Simulation of Internal Wave with Multi-polarization SAR

Jinsong Chong [1], Bing Duan [1]
[1]Institute of Electronics, Chinese Academy of Sciences, CN

Abstract

The complexity and randomness on the time and space of internal wave (IW) make it becomes one of the difficult problems in the field of marine research. Internal wave in South China Sea is extraordinary active. Therefore, we face urgent demands of studying internal wave. Since the amplitude of internal wave is very large and it may cause huge fluctuation, internal wave could bring serious influence for the ocean projects and ships. Synthetic aperture radar (SAR) is a major sensor to study internal wave. From 1970's, it obtains many SAR images of internal wave and provides abundance of data for studying internal wave. Now, the fluid dynamics model of inversion method of internal wave commonly uses the one-dimensional KdV equation under two density stratifications approximation model of ocean. However, the inversion method has no relationship with polarization. In fact, we get the multi-polarization SAR images of ALOS and find that the inversion amplitudes of interval wave of different polarization are not same. More accurate inversion of internal wave parameters has important impact on the conduct of marine activities. To verify the result and find rule of inversion of multi-polarization SAR internal wave, we use the M4S software and emulate radar cross section of ocean interval wave. In this paper, we presume some parameters for the simulation process. In our simulation, the depth of water is 1500m and the depth of upper layer is 100m. The given value of amplitude of internal wave is 40m. The radar bands of observe interval wave are C, L and X. The wind speeds are 2, 4, 6 and 8 m/s. The wind directions are 0, 45, 90, 135 and 180 degree. The incident angles are 23 and 30 degree. According to the relation between current and these parameters, we could compute the simulative current. Then, we use the M4S software emulates radar cross section of ocean interval wave and compute inversion result of simulative interval wave. At last, we compute the difference between the given value and inversion result. In the preliminary result, we could obtain the conclusions that the inversion amplitudes of multi-polarization SAR internal wave are not consistent and the amplitude changes with band, wind speed, wind direction or incident angle changes.

ASAR-Based Statistics of Oceanic Internal Waves in the Barents Sea

Igor Kozlov [1], Vladimir Kudryavtsev [1], Johnny Johannessen [2], Bertrand Chapron [3], Alexander Myasoedov [1], Knut-Frode Dagestad [4]
[1]Russian State Hydrometeorological University, RU
[2]Nansen Environmental and Remote Sensing Centre, NO
[3]Ifremer , FR
[4]StormGeo , NO

Abstract

Results of oceanic internal waves (IW) study in the Barents Sea obtained through the processing of Envisat ASAR imagery for July-October 2007 are presented. In general more than 600 IW packets were identfied on 120 Envisat ASAR images. Maps of spatial distribution of main IW parameters, such as IW observational frequency, IW wave length, IW packet area and packet front length, number of waves in packets, propagation speed and direction were calculated. Interaction of tidal currents with bottom topography is suggested to be the main source of IW's generation for the most of observed packets. Maximum number of IW packets was identified to the north-west from Franz Josef Land. Assuming IW generation by tides, phase speeds of IW packets were defined. Using dispersion relation for IW Mode 1 and IW packet phase speeds obtained from SAR, estimate of mass content of upper mixed layer and its time evolution is given. Dependences of SAR IW contrast on background wind speed and direction, SAR imaging geometry, surface waves direction are presented and discussed. Funding for this research was provided by the Mega-grant of the Russian Federation Government to support scientific research under the supervision of leading scientist at RSHU, No. 11.G34.31.0078.

Study of Intensive Oceanic Internal Waves in the White Sea Based on In-Situ and Satellite ASAR Measurements

Igor Kozlov [1], Aleksei Zimin [1], Vladimir Kudryavtsev [1], Bertrand Chapron [2], Alexander Myasoedov [1]
[1]Russian State Hydrometeorological University, RU
[2]Ifremer , FR

Abstract

In this work we present an analysis of in situ and ASAR measurements of tidally induced intensive short-periodic internal waves observed on the shelf of the White Sea in summer 2008 and 2009. Main observation sites were located in the vicinity of the Solovetsky Islands and in the Gorlo Strait. Registration of short-periodic internal waves characteristics (amplitude, wave length, phase speed, propagation direction) was done using buoy-mounted thermistor chain and ADCP. Thermocline depth was obtained from towed CTD records. Vertical profiles of main hydrological characteristics were obtained from ship-borne CTD moorings. Analysis of in situ hydrographic data revealed a presence of a pronounced near-surface picnocline on which the trains of intensive nonlinear internal waves are generated. Registered internal waves trains were characterized by periods about 10-20 minutes, wave lengths about 300-500 m, phase speeds of 0.9-1.5 m/s and maximum amplitude up to 25 m. In situ records of internal waves parameters were then compared with spatial signatures observed in collocated Envisat ASAR images. Dependences of SAR IW contrast on thermocline depth and amplitude of internal waves, as well as on background wind speed and direction, SAR imaging geometry are presented and discussed. Additionally spatial statistics of oceanic internal waves in the White Sea as observed in Envisat ASAR imagery for 2010 is presented. Funding for this research was provided by the Mega-grant of the Russian Federation Government to support scientific research under the supervision of leading scientist at RSHU, No. 11.G34.31.0078.

Ocean current retrievals and applications

The Influence of Ship-Wake Turbulence on Radar Backscattering

Simon George [1], Adrian Tatnall [1]
[1]University of Southampton Astronautics Research Group, GB

Abstract

The surface layer of the ocean is a key region of turbulent mixing, forming a crucial part of the air-sea interaction boundary governing the exchange of heat, momentum and energy fluxes between the ocean and the atmosphere. Increasing scrutiny is placed on the impact of upper-layer turbulence and wave-breaking (i.e. whitecapping) on exchange of atmospheric CO2 and oceanic heat transfer and storage - measurement of turbulence in the ocean and improved understanding of the cause and character of turbulent phenomena are therefore vital, particularly from a climate change perspective. Small-scale turbulence in the near-surface layer of the ocean is commonly generated by internal oceanic processes, interaction with wind forcing or shear or due to interactions of currents with ocean bottom topography or man-made objects, and the improvement in spatial resolution achievable from high-resolution radars such as TerraSAR-X (2007) has led to increasing interest in the identification and measurement of small-scale ocean turbulence using Synthetic Aperture Radar (SAR). This paper discusses the results of ongoing research into the detection of small-scale turbulence in the near-surface region of the ocean by SAR and extraction of ocean turbulence parameters from simulated radar imagery. Smacll-scale turbulence at and near the sea surface is most commonly observed in SAR imagery as the turbulent wake present behind a moving surface vessel such as a ship. However, such disturbances may also be visible in the radar backscatter signatures of breaking waves, internal waves, upwelling, convection, and Langmuir circulations. According to Kitaigorodskii et al. (1983), turbulence causes a downward convection of wave energy – as such, turbulence near the sea surface causes dissipation of the energy of the short waves which cause resonant Bragg scattering with radar waves, and resulting in a flattening of the sea surface. Hence, in regions of turbulence and mixing near the ocean surface (e.g. in the turbulent wakes of ships), there is an observed decrease in radar backscattering and the wake region appears dark. As part of this research, fine-resolution turbulent wake flows were computed numerically using Direct Numerical Simulation and the interaction of small-scale wake turbulence with the free surface investigated. Radar imaging algorithms were used to process the resulting surface currents for a variety of ambient conditions to examine the impact of turbulent surface wake flows on simulated SAR and NRCS imagery. The results are presented for their ability to resolve turbulent structure from the resulting imagery and improve understanding of the relationships between small-scale turbulence and radar backscattering. Furthermore, the impact of turbulent dissipation on the computation of simulated wave spectra was examined and subsequent simulated radar imagery was applied through a numerical study. The results indicate that there are grounds for the application of turbulent dissipation of short wave energy into the source term used in the wave action computation, particular for ship wake cases. The appropriate theory and descriptions of the applied models was discussed for the legitimacy of operating for turbulent flow currents. The results display close relationships between surface flow parameters (such as velocity, vorticity, etc.) with the results from simulated Bragg NRCS, full surface NRCS and SAR imagery. The impact of ambient conditions, ship parameters and antenna characteristics were examined to evaluate the potential for observing wake turbulence under geophysical conditions. The impact of radar scattering was examined as a function of antenna characteristics to improve understanding of the impact of turbulent flow on the radar backscattering problem. These results permit extension of these relationships to a range of turbulent phenomena of both natural and man-made origin, and definition of desirable instrument parameters to measure and characterise ocean turbulence in the ocean surface layer.

Ship Wake Distortion as Indicator of Spatial Current Fine Structure

Olga Lavrova [1], Konstantin Sabinin [1], Marina Mityagina [1]
[1]Space Research Institute of Russian Academy of Sciences , RU

Abstract

Parameter determination of current fine structure is attempted for a case of ship wake distortion. In high resolution radar and optical images, one can clearly detect long narrow slick bands formed on the sea surface in result of discharges of waters containing surfactants (ballast water, bilge water or slops, fish processing wastewater, etc.). The slick bands are often subject to drift and distortion under the impact of currents related to eddy passages, internal waves, hydrological fronts and other phenomena. Many-year satellite monitoring of sea surface based on Envisat ASAR and ERS-2 SAR data of spatial resolution of 25-150 m has demonstrated numbers of small-scale eddies of diameters ranging hundreds of meters to tens of kilometers that are visualized in radar data also due to slick bands. Internal waves as well are manifested in radar data as alternating slick bands. Instances of the impact of various hydrological processes on ship wake patterns are discussed. In particular, ship wake distortions caused by small-scale eddies are analyzed, orbital current velocities in the eddies are determined from the distortion characteristics. A unique case of sharp distortion of a narrow slick wake of a moving ship manifested in an Envisat ASAR image obtained over the west Black Sea is discussed. A 2,3-km shift of the wake was observed along a rip band formed by internal solitons. It is suggested that the phenomenon was the result of interaction of two internal solitons that propagated towards each other from opposing directions. Estimates of the internal soliton non-linearity and orbital current velocities are made. The obtained results implicitly prove the suggested hypothesis about the origin of the phenomenon. The work is supported by Russian Foundation for Basic Research (projects ¹ 10-05-00428-a, 11-07-12025-ofi-m-2011) and the Russian Federal Thematic Programme “Scientific and scientific-educational professionals of innovative Russia” for 2009-2013. ASAR Envisat images are provided by the European Space Agency under project C1P.6342.

Ocean Dynamic Information Obtaining Based On Improved Phase Correlation Method

Haiqing Sun [1]
[1]Institude of Electronics,Chinese Academy of Sciences, CN

Abstract

Ocean surface information acquisition is one of the most important applications in the ocean remote sensing field. Ocean current distribution and wave transmission are vital constituent part of ocean dynamic information. An indispensable step to get the dynamic information through SAR sequential images is image matching. However, regular SAR image processing method handles the image as transient state, and can not get dynamic information. According to the relationship between SAR azimuth signal spectrum and azimuth visual angle, we get several sequential images which have the same time interval from one image using sub-aperture division method. The time interval between sequential images is very short, hence we believe there is approximately a rigid movement between these images. The time interval is so short that the sub-aperture images¡¯ relevance is very high, and the movement quantity between sequential images is very small. Furthermore, the most challenging problem of SAR ocean images matching is very heavy speckle noise. In conclusion, we need a matching algorithm that has a property of high matching precision and strong noise-robust. Among all the matching algorithms, Phase Correlation Method is well known by its low operation quantity, high calculation accuracy and noise-repress ability. Phase Correlation Method can be used on optical images very well which have tiny noise. However, the heavy speckle noise on SAR ocean images makes the method invalidate. Therefore we propose an improved Phase Correlation Method to deal with it. Experimental results show that the improved method presents 1/10 resolution accuracy and noise robustness. To obtain ocean surface current, we divide the images into small pieces and match the corresponding

pieces. According to the improved Phase Correlation Method, we know the movement quantity and direction, then the big scale feature (such as ocean waves) movement tendency can be obtained. With the sequential images interval time and image resolution already known to us, we can calculate the ocean current speed.

Oil Spill and Ship Detection

X-Bragg-Based Detection of Oil Spills Using Polarimetric SAR

Øystein Rudjord [1], Arnt-Børre Salberg [1]
[1]Norwegian Computing Center, NO

Abstract

Introduction Current oil spill detection methodology, as well as operational services, use single frequency, single polarization SAR images only, e.g., C-band VV- or HH-polarization. In such imagery, the oil slicks are often clearly visible; however, one of the main challenges is to discriminate oil spills from look-alikes. Typically the look-alikes arise from e.g. low-wind patterns, biogenic materials (e.g. algae), upwelling, ocean-currents, weather fronts, or rain cells. Multi-polarization SAR sensors have been studied the last decade as a means to improve the oil spill detection performance, in particular with respect to distinguishing between oil spills and biogenic look-alikes (Gade , et al., 1998; Migliaccio, et al., 2007; Migliaccio, et al., 2009; Nunziata, et al., 2011; Zhang, et al., 2011; Migliaccio, et al., 2011). For most of these studies, the Bragg model is used to describe the backscatter from the ocean surface (Ulaby, et al., 1986). However, this model fails to account for nonzero cross-polarization and depolarization. In order to extend the Bragg model to also account for these phenomena, and thereby cover a wider range of roughness conditions, the so called X-Bragg model is proposed (Hajnsek, et al., 2003). The X-Bragg model is derived by introducing a roughness disturbance obtained by tilting of the mean reflection plane. Method Three features from the X-Bragg model The X-Bragg model describes the statistical properties of the polarimetric SAR backscatter based on three variables: incidence angle, relative permittivity of the dielectric and surface roughness. Within the model it is possible to construct two features, R and Coh, which are dependent only on the surface roughness, and independent on the incidence angle and relative permittivity. Both surface roughness measures R and Coh describes the surface roughness using the surface tilt angle distribution parameters and not the backscatter amplitude. It is also possible to construct a feature, RP, which is only dependent on the incidence angle and relative permittivity, and independent on the surface roughness (Hajnsek, et al., 2003). We will here explore the potential of using these three features for oil spill detection. Estimating the relative permittivity The RP parameter is only dependent on the incidence angle and the relative permittivity of the dielectric. The incidence angle is known for a given SAR image, and may therefore be considered as a constant. It should therefore be possible to estimate the relative permittivity of the observed surface by measuring the RP feature in the image. It should be noted that this estimation is strictly speaking only valid for water (or other X-Bragg surfaces), since oil slicks are described by very different scattering mechanics. Also, due to the penetration depth of the C-band radar, estimating the relative permittivity of thin oil slicks may be influenced by the relative permittivity of the sea water. However, an estimate of the relative permittivity may assist in excluding non-water surfaces from low-wind zones. RP is real, while relative permittivity, ε is a complex parameter. A given value for RP therefore has no unique solution for ε, but rather defines a curve in the complex plane. We assume that RP is mostly sensitive to the amplitude of ε, and that the relative permittivity of water is one of the possible solutions. We therefore assume a linear parameterization of ε between $\varepsilon\_0=0$ and $\varepsilon\_w=69.34+32.43i$. The latter value is the relative permittivity of water at 5°C for 5.405 GHz radiation (C-band of Radarsat-2). Provided a value for RP, an estimate for ε may be found using a numerical root finding technique. Plotting RP as a function of ε, keeping θ constant, we find that RP is very suitable for estimating the relative permittivity for Bragg surfaces with low values of ε. However, in our case we are interested in the relatively high values for water (with $|\varepsilon|=77$), and we find that in this region the estimate of ε is oversensitive to variations in RP, making practical estimation of ε challenging. Experiments Oil spill in Radarsat-2 data The performance of the RP-

measure, R-measure and Coh-measure was evaluated on a Radarsat-2 quad-pol image covering various types of oil released in an oil-in-sea exercise in Norwegian waters on the 8th of June, 2011 by the Norwegian Clean Seas Association for Operating Companies (NOFO). The image contains plant oil, emulsion and crude oil. It also contains a black area of unknown status (but it is not oil). Clearly, all oil slicks have a high contrast to the surrounding sea water in the SAR backscatter image. From the results we find that the RP-measure distinguishes the oil spills from the background, but also emphasizes the dark patch of unknown origin. The R-measure puts different contrast on the three different oil slicks, with plant oil being the slick with the weakest contrast and crude oil the one with highest contrast. This is contrary to the VH-image that gives the plant oil slick the highest contrast and crude oil the lowest. The Coh-measure provides an almost perfect image for oil spill detection. It enhances all three oil slicks and suppresses ocean phenomena. However, the measure does not provide any means to distinguish the type of oil. Look-alike in SIR-C data We demonstrate the performance of the three features on biogenic look-alikes. We evaluate R, RP and Coh estimated for a SIR-C image acquired in 1994, containing a surface film of an alcohol-like liquid, simulating a biogenic slick. From our results it is clear that for all the three features, the look-alike slick is suppressed and has a very weak contrast. Conclusion We have presented three features for oil spill detection based on the X-Bragg model for polarimetric SAR. We have demonstrated that they are sensitive to oils spills, but when applied to biogenic slicks they all provide a lower contrast value than for oil slicks. Hence, we may use these features to enhance oil slicks and suppress natural biogenic slicks. For operational services this is desirable since the purpose is to report oil slicks only, and not natural biogenic slicks or other look-alikes. One of the features we have proposed, the RP-measure, only depends on the relative permittivity of the surface, and could in principle be used to estimate the relative permittivity of the surface. However, our studies show that the estimate of the relative permittivity would be oversensitive to variations in the RP-measure. The next step will be to combine these features to a multi-variate oil spill discrimination approach. References Gade , M., Alpers, W., Masuko, H. & Kobayashi, T., 1998. Imaging of biogenic and anthropogenic ocean surface films by the multifrequency/multipolarization SIR-C/X-SAR. J. Geophysical Research, 103(C9), pp. 18851-18866. Hajnsek, I., Pottier, E. & Cloude, S. R., 2003. Inversion of surface parameters from polarimetric SAR. IEEE Trans. Geosci. Remote Sens., 41(4), pp. 727-744. Migliaccio, M., Gambardella, A. & Tranfaglia, M., 2007. SAR polarimetry to observe oil spills. IEEE Trans. Geosci. Remote Sensing, 45(2), pp. 506-511. Migliaccio, M. et al., 2009. The PALSAR polarimetric mode for sea oil observation. IEEE Trans. Geosci. Remote Sens., 47(12), pp. 4032-4041. Migliaccio, M. et al., 2011. A multifrequency polarimetric SAR processing chain to observe oil fields in the Gulf of Mexico. IEEE Trans. Geosci. Remote Sens., 49(12), pp. 4729-4737. Nunziata, F., Migliaccio, M. & Gambardella, A., 2011. Pedestal height for sea oil slick observation. IET Radar Sonar Navig., 5(2), pp. 103-110. Ulaby, F. T., Moore, R. K. & Fung, A. K., 1986. Microwave remote sensing: Acitve and passive. Dedham, Mass.: Artech House, Inc.. Zhang, B., Perrie, W., Li, X. & Pichel, W. G., 2011. Mapping sea surface oil slicks using Radarsat-2 quad-polarization SAR image. Geophys. Res. Lett., Volum 38, pp. L10602, doi: 10.1029/2011GL047013.

Ship Detection by Using L-Band SAR

Oshimura Koichi [1]
[1]JAXA, JP

Abstract

The Advanced Land Observing Satellite-2, ALOS-2, will provide new opportunities for spaceborne monitoring of vessel traffic and fishing activities. ALOS-2 has the L-band SAR instrument, PARSAR-2 and the satellite-AIS(Automatic Identification System) receiver, SPAISE-2. PALSAR-2 has the Spotlight mode (1 to 3 m), Stripmap mode (3 to 10 m) and ScanSAR mode (350km swath and 490km swath), which will provide a good performance for ship detection. The difference of 3m resolution SAR image among L-band, C-band and X-band are analyzed. The ship detection capabilities of 490km wide swath L-band SAR image are also analyzed.

Long Term Satellite Monitoring of the Oil Spillages in the South-Eastern Baltic Sea

Marina Mityagina [1], Olga Lavrova [1], Andrey Kostianoy [2]
[1]Space Research Institute of Russian Academy of Sciences , RU
[2]P.P. Shirshov Institute of Oceanology, Russian Academy of Sciences , RU

Abstract

The results of long-term satellite monitoring of the Baltic Sea aimed to reveal sea surface pollutions by oil as well as manifestations of biogenic and anthropogenic surface films are summarised and reported. The Baltic Sea ecosystem undergoes growing human induced impacts, especially associated with an increasing oil transport and production. One of the main tasks in the ecological monitoring of the Baltic Sea is an operational satellite detection of oil spills, determination of their characteristics, establishment of the pollution sources and forecast of probable trajectories of the oil spill transport. Operational satellite monitoring of the south-eastern Baltic Sea, as an important component of the environment monitoring, was performed in June 2004 – November 2005 on the base of daily remote sensing (AVHRR NOAA, MODIS, QiuckSCAT, ENVISAT ASAR, ERS-2 SAR and RADARSAT SAR imagery) of oil spills, sea surface temperature (SST), suspended matter, chlorophyll concentration, mesoscale water dynamics, wind and waves. This work was performed by the team from Space Research Institute of RAS jointly with our colleagues from Institute of Oceanology of the Russian Academy of Sciences and specialists from Marine Hydrophysical Institute of Ukraine National Academy of Sciences under a pilot project initiated by Oil Company LUKOIL and aimed to the complex monitoring of the south-eastern Baltic Sea, in connection with a beginning of oil production at continental shelf of Russia. Starting from 2009 up to the present moment a satellite survey of the central and south-eastern Baltic is carried out by the Space Radar Laboratory of the Space Research Institute of RAS. The main attention is focused on the detection of oil pollution as well as biogenic and anthropogenic surfactant films. The basic data are high resolution radar images obtained by advanced synthetic aperture radar ASAR on board Envisat satellite of the European Space Agency. Remotely sensed data in visual and IR bands taken by sensors Envisat MERIS, Terra/Aqua MODIS and NOAA AVHRR nearly simultaneously with the ASAR images, are involved into consideration in order to facilitate the discrimination between different types of surface pollutants, to understand a comprehensive figure of meteorological and hydrodynamic processes in test areas, and to reveal factors determining pollutants spread and drift. The results obtained in 2004-2005 were compared with the up-to-date situation. Namely the comparison of the number, individual sizes and location of ship-induced oil spillages, as well as total area of the oil pollution were carried out. It can be concluded that the situation with the anthropogenic oil pollution in the Baltic Sea have much improved last years. May be it is a result of increased control of various organizations in local countries on the water surface pollution. The illegal ship discharges as well as outflows of local rivers and Kaliningrad channel continue to be the main sources of the oil pollution. The ship discharges traditionally take place at an anchorage point near the Baltiisk, along the main navigation routes near the Gotland Island, to the north of the Gdansk bay and in the vicinity

of ports of Klaipeda, Liepaja, Ventspils and Gdansk. The work is partially supported by RFBR grants 10-05-00428, 11-07-12025-ofi-m-2011 and 11-05-12047-ofi-m-2011 and the Russian Federal Thematic Program "Scientific and scientific-educational professionals of innovative Russia".

Oil Spill Detection: Operational Service and Perspectives

Guillaume HAJDUCH [(1)], Nicolas Longépé [(1)], Jean-Yves Lebras [(1)], Pascal Lozac [(1)]
[(1)]CLS , FR

Abstract

OIL SPILL DETECTION: OPERATIONAL SERVICE AND PERSPECTIVES G.Hajduch(1), N.Longépé(1), JY. Le Bras(2), P. Lozac'h(1) (1) CLS, Plouzané, France (2) CLS, Ramonville Saint-Agne, France Abstract The European Maritime Safety Agency (EMSA) has been providing the operational CleanSeaNet service for marine oil spill detection and surveillance of European waters since April 2007. This kind of service is now a worldwide leading example of the capabilities of space based technologies in order to prevent pollutions. The purpose of this paper is to present the status of such a space based service and its possible capabilities and evolutions (1) by using additional earth observation products in routine and near real time, (2) by addressing other service areas and (3) by improving identification of possible polluter either offline or in near real time. From one hand, most of the operational oil spill detection service is now performed using C-Band SAR sensors (Envisat, Radarsat-1, Radarsat-2). On the other hand the two constellations of X-Band sensors (Cosmo SkyMed and TerraSAR-X) allow performing additional observation on the area of interest and to improve the revisit time. The optimal use of those sensors requires a precise knowledge of the backscattering in X-Band in order to estimate the local wind conditions at high resolution collocated with the potential spill observation. In addition the characteristics of those sensors must be evaluated with respect to their adequacy with the contrast between clean and polluted sea area. We will present results on those two aspects illustrated on real data. The characteristics of the illegal discharges in the European waters are pretty well known. The behavior of the polluter in other regions of the globe has still to be evaluated in order to evaluate the relevance of deploying a systematic oil spill detection service. We will present results of such a demonstration service in the Indian Ocean and the analysis of the operational performances like the delivery delay of the oil detection report from the radar acquisition on the area of interest, taking benefit of a network of ground receiving station. Finally, we will present new methods for the identification of polluters. First of all we will present results of identification based on Satellite AIS. Second, we will illustrate the benefit of using offline analysis together with near real time analysis of SAR acquisitions in order to improve the identification of potential polluters. We will show that suspicious behavior of vessel identified on archive products may be beneficial for near real time analysis. This paper will be illustrated by concrete cases along the French Atlantic coast, and in Indian Ocean. Acknowledgement These studies are partially funded by (1) the European Commission under Framework Program 7 (FP7) SEA-U project no. 263246 (2) the ANR POLHSAR project (3) a dedicated project (SIPOL) and (4) by French Maritime Affairs, the national contact point of EMSA Some Cosmo SkyMed products used in this study were provisioned through the ASI/CSK Principal Investigator program. References R0 Donald R. Thompson, Jochen Horstmann, Alexis Mouche, N.S. Winstead, Raymond E Sterner, Frank Monaldo, "Comparison of high-resolution wind fields extracted from TerraSAR-X SAR imagery with predictions from the WRF mesoscale model", JOURNAL OF GEOPHYSICAL RESEARCH, doi:10.1029/2011JC007526 R1 V. Kerbaol, F. Collard, P. Leilde, and F. Parthiot, Improved oil spill detection service over the French ZPE: developments and results, SEASAR 2006, ESA/ESRIN, Frascati, 23-26 Jan. 2006 R2 "Enhancing the effectiveness of the law enforcement chain in combating illegal discharges", February 2011, EMSA workshop report R3 Girard-Ardhuin, F.; Mercier, G.; Collard, F.; Garello, R, Operational Oil-Slick Characterization by SAR imagery and Synergistic data, IEEE J. Oceanic Engin., Vol 30.(3), pp. 487-495, Jul. 2005

A Review of the Key Research Questions That Need to be Answered to Better Exploit Satellite Borne SAR Sensors for Vessel Detection and Maritime Security

Nick Walker, Armando Marino [1], Irena Hajnsek [2]
[1]ETH Zurich , CH
[2]German Aerospace Center , DE

Abstract

There is a growing requirement for improved maritime surveillance and satellite-borne synthetic aperture radar (SAR) can play an important role for this application, specifically relating to vessel detection and classification. Furthermore SAR sensors with increasingly advanced characteristics (resolution, polarisation, noise levels, swath width etc.) offer the prospect of improved detection and classification performance if suitable algorithms can be developed to exploit these richer sources of information. In this paper the authors review what they believe the key technology questions are that need to be answered in order for new and future SAR systems to be maximally exploited for vessel detection & classification. Questions will include reference to: the relative merits of different polarimetric modes, the relative merits of different radar frequencies, performance and robustness with respect to sea-state, and the best matching of sensor with regard to application and vessel size. Where, for each of these topics specific attention will be given to the algorithms that appear to offer the most promise for delivering improved performance. It is the intention that this paper will act as an invitation for other groups to pose their own questions and suggest their own answers.

DOLPHIN - Improved Ship Detection

Annekatrien Debien [1]
[1]KSAT , NO

Abstract

DOLPHIN, an FP7 project, focuses on the improvement of existing ship detection techniques for the purpose of setting up a state-of-the-art maritime surveillance system, tailored to the user needs. Three user domains have therefore been defined, who use ship detection and tracking algorithms in a different manner: Traffic Safety, Fisheries Control and Border Surveillance. Each of these domains use a different set of algorithms to aid the users in their decision making. In the validation phase, the decision support modules will be tested with several scenarios. There are two scenarios relevant for Norway: Traffic Safety in the Northeast Passage, and a Joint Operational Scenario in the Barents Sea. Over the years to come, it is expected that the North East Passage in the Arctic Sea will open up due to global warming. In recent years, some ships have tried to sail through the North East Passage when the ice extent of the North Pole is at its lowest, in fall. This route would be of great economic importance for commercial shipping, and the ice extent in the North East Passage is monitored carefully. Although the traffic density in the North East Passage is low, and restricted to favourable conditions in August and September, it presents an interesting validation scenario for the Traffic Safety DSM, due to the presence of ice, and the remoteness of the location, making coastal radars useless. However, due to the ice, this route presents many dangers, and the setup of a regular, reliable monitoring system of ships and ice in the area would be favourable for the users of this area. The Joint Operational Scenario in the Barents Sea focuses on the three Decision Support Modules together. - Border Surveillance: Customs reported issues with vessels coming into Norwegian waters without previous warning. Increased monitoring of entrance zones for unidentified vessels is necessary to tackle this problem. - Traffic Safety: in summer, ship traffic increases in the Barents Sea, and sea ice melts leaving many drifting ice floes which can collide with ships. This requires ice floe identification and ship and ice berg tracking in order to increase safety at sea. - Fisheries Control: suspicious activities take place in the Barents Sea with regards to illegal fishing: ships meeting each other at sea before heading towards the coast and reporting their catches.

Operation System Design for Satellite-Based Oil Spill Monitoring

Chan-Su Yang [1], Tae-ho Kim [1], Ouchi Kazuo [2]
[1]Korea Ocean Research & Development Institute , KO
[2]National Defense Academy of Japan , JP

Abstract

In recent years, the oil spill detection over sea surface and similar oil material filtration are attracting much attention from the ecological point of view, and synthetic aperture radar (SAR) is considered as an effective way of monitoring such phenomenon due to the day-and-night and all weather observation capability. In South Korea, there were two oil spill accidents that threatened our ocean environment in 2007 and 2011, and gave us to feel keenly the need of satellite remote sensing. Therefore, we have developed a system to detect oil spills and to bring benefit to the current oil combating system using satellite data. In this paper, we will introduce a design concept for satellite-based oil spill monitoring system, and give some results of applications through the prototype system. The prototype consists of three modules: SAR oil detection module, SAR scattering module (MoM), and Oil prediction module. To supplement SAR¡¯s weakness, the last two modules are used to compare with the backscattering signals calculated from a numerical model and the predicted locations of spilled oil from currents and winds obtained in near real time. As an example, results of the oil slick detection experiment by multi-frequency space borne SARs are reported. On December 7, 2007, an oil tanker was wrecked in the Yellow Sea off the Korean west coast, spilling over 12,000 tons of crude oil, and causing considerable damage on the coastal environment. In order to analyze the impact of the oil spill, we acquired 4 sets of multi-frequency spaceborne SAR images, including TerraSAR-X X-band data, ENVISAT ASAR and RADARSAT-1 C-band data, and ALOS-PALSAR L-band data. We also computed, as a preliminary study, the backscatter radar cross sections (RCS) based on the Integral Equation Method (IEM) and the Method of Moments at three microwave frequencies for different wave damping ratios by oil slick. In this paper, we describe the present status of the study on oil slick detection, and suggest the possible future direction to be taken.

A Hybrid Approach using SAR Image Segmentation and Classification Applied to Low Backscatter Regions Detection in Southeastern Brazil

Patrícia C. Genovez [1], Corina da Costa Freitas [1], Nelson Francisco Favilla Ebecken [2], Cristina Bentz [3], Ramon Morais de Freitas [1], Luciano Vieira Dutra [1], Enrico Pedroso [4]
[1]INPE , BR
[2]UFRJ , BR
[3]CENPES/PETROBRAS , BR
[4]HRT , BR

Abstract

Automatic oil detection systems have been developed to improve SAR image interpretation. The processing chain is carried out in oceanic areas, emitting an alarm when low backscatter regions (dark spots) are detected like an oil slick suspect. These oil detection systems are generally composed by four (4) main steps: 1) image pre-processing; 2) low backscatter regions detection; 3) feature extraction; 4) oil and look-alike classification. The low backscatter regions detection is an essential stage in the processing chain, considering that without the geometry of the slicks the oil and look-alikes classification is unfeasible. Numerous efforts have been made to produce a completely automatic system, but there isn't a procedure totally satisfactory applied to all SAR image. The detection of the low backscatter regions depends on the environmental conditions and the parameters of the sensor at the moment of the image acquisition, as summarized below: i) the contrast between the slick and the background; ii)electrical properties of the surface; iii) the wavelength of the signal emitted by the RADAR; iv) wind intensity; v)acquisition geometry; vi) polarization, and; vii) speckle noise. In this context, this work presents the methodology proposed to develop a hybrid system, combining automatic and semi-automatic procedures able to detect low backscatter regions in SAR imagery. The proposed methodology were organized in seven (7) stages as follow: 1) images subset selection; 2) pixel spacing and filter definition; 3) image partition into proper regions using region growing segmentation techniques; 4) features extraction, exploratory analyses and feature selection, using data mining techniques; 5) low backscatter regions detection using automatic clustering algorithm; 6) decision rules to indicate the procedure like automatic or semi-automatic, and; 7) validation of the proposed method. For this purpose, twelve (12) SAR images with different levels of complexity were acquired by the RADARSAT-1 and RADARSAT-2 satellites over the Southeastern Brazilian Coast. The set of ten (10) images were used to develop the methodology and the other two images were used to validate the proposal. All automatic clustering results were compared through metrics with the reference images (Phantons) made manually by the interpreter. The main metric were calculated combining elements of the confusion matrix and was named "Accuracy of the Dark Spots". This metric considers the number of pixels correctly classified as dark spot, divided by the number of pixels correctly classified as dark spot summed with the errors of inclusion and omission. In spite of the proposed method had been able to detect low backscatter regions with different complexity levels in different image subsets, it didn't achieve good results for all analyzed examples. Considering that in the scientific community there isn't a wide agreement about the operational use of fully automatic methods, the development of a hybrid system, including decision rules able to conduct the images for one automatic or semi-automatic processing, was an interesting approach. The potential of these rules to improve the automation process was indicated. Nevertheless, more samples to return more robust rules are recommended in order to be widely applied to all SAR images acquired.

Multi-polarization X-band data for oil and target detection

Domenico Velotto [1], Ferdinando Nunziata [2], Susanne Lehner [1]
[1]German Aerospace Center (DLR), DE
[2]Università degli Studi di Napoli "Parthenope" , IT

Abstract

TerraSAR-X (TS-X) and Tandem-X (TD-X) multi-polarization data are used to identify oil slicks and man-made targets over the ocean surface. For the purposes of this study the co-polarized channels combination has been chosen, i.e. HH&VV. The correlation between the selected channels is estimated through the co-polarized phase difference standard deviation (CPDstd). In the CPDstd domain oil slicks and targets are characterized by high values in contrast with low values of the surrounding ocean surface. Oceanic features characterized by weak damping properties, i.e. look-alikes like biogenic slicks, show values comparable with the one measured over slick free areas. This behaviour lies in the fact that slick-free ocean surface, imaged in moderate wind condition and normal incidence angle, follow a Bragg type scattering, while oil slicks and targets follow a non-Bragg scattering mechanisms. Exploiting the aforementioned physical behaviour, the proposed processing chain allows to: 1) distinguish oil slicks from a broad class of look-alike; 2) detect targets over the ocean surface. Experiments, accomplished over a wide dataset of X-band Single look Slant range Complex (SSC) HH&VV channel combination, show the effectiveness of the proposed processing chain.

Ocean wind retrievals and applications

Estimating errors in the determination of the wind fields from SAR using external direction information

Stefano Zecchetto (1), Francesco De Biasio [1]
[1]National Research Council of Italy , IT

Abstract

In several studies and projects about the wind retrieval from SAR, external wind direction information are used in order to derive the wind speed from the backscatter radar data. Since the wind fields is a two variable function, i.e. it depends both from the wind speed and direction, this is equivalent to impose the value to one of the two independent variables. We believe that an estimate of the possible errors produced by such approaches should be carried out,focusing on coastal areas where the wind is usually less well reproduced by the atmospheric models. In the last years we developed a methodology, based on the 2-D continuous wavelet approach, to infer the wind fields from SAR without using any external wind direction information: taking the wind fields derived using this methodology as the benchmark (despite its shortcomings that will be illustrated), we present here some comparisons obtained using both the ECMWF global model and the Limited Area atmospheric Models wind directions in areas located in the Mediterranean Sea. The SAR data used are the Envisat Wide Swath images.

Investigation of a Winter Monsoon Wind front over the South China using Multi-Sensor Satellite and Weather Radar Data and a Numerical Model

Werner Alpers [1], Knut-Frode Dagestad [2], Wai Kin Wong [3], Pak Wai Chan [3]
[1]University of Hamburg, DE
[2]Nansen Environmental and Remote Sensing Center, NO
[3]Hong Kong Observatoty, CN

Abstract

During the winter monsoon season in South East Asia, high wind events often occur over the South China Sea (SCS) near the Chinese coast, which give rise to sharp wind fronts. During these events, cold air from Siberia, Mongolia or northern China advances southward over the Chinese Continent, reaching the Chinese coast and advancing further over the SCS. Usually these events occur in the form of cold air outbreaks and are associated with a sudden freshening of the wind from a northerly direction and a sudden drop in air temperature. Such cold air outbreaks, called in Hong Kong northerly surges, have been studied extensively using conventional meteorological data, and recently also by using satellite data, in particular high resolution synthetic aperture radar (SAR) (Alpers et al., 2012). In this paper we investigate for the time a high wind event over the SCS which is not associated with a cold air break, but with a freshening of the winter monsoon wind due to the merging of two high pressure areas over the Chinese Continent. This freshening or "replenishment" of the northeast monsoon gives rise to similar strong winds over the SCS and the generation of similar sharp wind fronts with embedded rain cells as cold air outbreaks. However in this case, the wind blows from a northeasterly direction and is not associated with a sudden drop in air temperature in Hong Kong, since the cold air has been warmed on its way over the warm waters of the Strait of Taiwan. The satellite data we are using are from the scatterometer onboard the European MetOp satellite, called ASCAT, the synthetic aperture radar (SAR) data onboard the European Envisat satellite, called ASAR, the imaging multi-spectral radiometers (vis/IR) onboard the Japanese geostationary satellite MTSAT-1R, and the SSM/I onboard the American DMSP F-15 satellite. Furthermore, we use data from the weather radar of the Hong Kong Observatory and meteorological data from weather stations and weather charts. We have compared these multi-sensor data with simulations carried out with the newly developed meso-scale atmospheric model of the Hong Kong Observatory, called AIR forecast model system (Wong, 210). The comparison shows that the SAR-derived and the simulated wind fields agree quite well over the open ocean, but disagree considerably near the coast, which we attribute to the limited representation of the coastal topography in the model. Thus this investigation can be used to verify the AIR forecast model system with respect to near-surface wind predictions and for improvement of the model physics in the future. Detailed knowledge of high wind speed events associated with the winter monsoon is of great importance for the numerous off-shore activities in the South China Sea. We were also able to study the time evolution of the frontal system since we had available time series of weather radar images and cloud images from the MTSAT-1R geostationary satellite, two maps of the near-surface wind fields from ASCAT, and two maps of liquid water content from SSM/I. The comparison of the MTSAT-1R and the weather radar time series reveals that, at the early stage of the development of the frontal system, the southward motion of the rain band follows closely to the motion of the cloud front. However, at later stages, the southward motion of the rain band partially decouples from the motion of the cloud line leading to a fall back of the rain band behind the cloud line. References Alpers, W., W. K. Wong, K.-F. Dagestad, and P. W. Chan, "A northerly winter monsoon surge over the South China Sea studied by remote sensing and a numerical model," Int. J. Rem. Sens., 2012 (in press). W.K. Wong, "Development of Operational Rapid Update Non-hydrostatic NWP and Data Assimilation Systems in the Hong Kong Observatory," The 3th International Workshop on Prevention and Mitigation of Meteorological Disasters in Southeast Asia, 1-4 March 2010, Beppu, Japan.

Using Surface Pressure Measurements to Improve Tropical Cyclone Surface Wind Retrievals from SAR

Ralph Foster [1]
[1]University of Washington , USA

Abstract

Using Surface Pressure to Improve Tropical Cyclone Surface Wind Retrievals From SAR Ralph Foster Applied Physics laboratory University of Washington 1013 NE 40th St Seattle, WA, 98105-6698 Jerome Patoux Department of Atmospheric Sciences University of Washington Box 351640, Seattle, WA, 9895-1640 Chris Wackerman General Dynamics Jochen Horstmann NURC LONG-TERM GOALS The calibration and validation of surface wind and stress retrievals from oceanic synthetic aperture radar (SAR) imagery is especially difficult in tropical cyclone (TC) conditions. The geophysical model functions (GMFs) that characterize the radar backscatter in terms of the near-surface wind vector for different viewing geometries are currently poorly characterized for the very high wind and strong ocean surface wave conditions that are present in all TCs. These problems are worse for low incidence angles. A key problem is that reliable wind vector observations in very high winds are rare. In contrast, surface pressure observations are quite reliable and common from, for example, drop sondes and buoys. Our long-term goal is to develop a novel methodology to use surface pressure observations and a planetary boundary (PBL) model for calibration and validation (Cal/Val) of SAR GMFs in TC conditions and to produce scene-wide wind vector retrievals that are most consistent with the image backscatter, the GMF and the PBL model. OBJECTIVES The objectives of this research are to (1) develop the methodology for deriving TC SLP fields from first-guess surface wind vector estimates based on various GMF formulations and surface wind direction estimates; (2) Use these SLP fields to derive surface wind vector retrievals that are, in a least-squares sense, a scene-wide optimal surface wind retrieval that is consistent with the observable linear features in the SAR image, the GMF and the PBL model; (3) Develop an optimization scheme that seeks the minimum adjustment to the surface wind vector field that will minimize the difference between observed (e.g. via drop sondes or buoys) and SAR-derived bulk pressure gradients across the image. The optimized surface wind field can then be used either to assess or adjust the GMF. APPROACH GMFs describe the average radar backscatter from the sea surface in terms of the surface wind speed and the viewing geometry (incidence and azimuth angles). Scatterometers obtain multiple approximately simultaneous looks at multiple different viewing geometries (at least fore and aft looks) at the same patch of the sea surface. The incidence angles are known, so it is possible to estimate the most likely wind speed and azimuth angle (i.e. wind direction) that best explains to the separately measured radar backscatters from the different viewing geometries. As compared to routine scatterometer wind vector retrievals, the standard method for obtaining surface wind vectors from SAR imagery is very difficult. The same GMFs are used, but there is only a single viewing geometry for each wind vector cell. Wind directions are estimated by identifying linear features in the imagery at scales ranging from ~0.5 km to 2-4 km wavelengths. These linear features are assumed to be the surface imprint of PBL coherent structures that roughly align with the surface wind (Foster, 1997; 2005; Morrison et al., 2005; Lorsolo et al. 2008; Zhang et al. 2008; Ellis and Businger, 2010). These linear features cannot be identified throughout the entire SAR scene (which is commonly about 450 by 450 km), so wind directions are interpolated between the identified linear features using different methods. These directions and the backscatter are input to the GMF and wind speeds are retrieved. Our research is performed in collaboration with Chris Wackerman of General Dynamics (GD) and Jochen Horstmann of NATO Undersea Research Centre (NURC). In addition, Roland Romeisser of RASMAS, Univeristy of Miami, has developed a method to remove the "scalloping" noise that is common in ScanSAR images. GD and NURC have developed separate methods for estimating wind directions. The GD and NURC wind directions have been merged into a single wind direction product and incorporated into a new processing system (WiSAR) that produces surface wind vector maps at 1 km spacing. WiSAR has been installed and is being run by Mike Caruso at the Center for Southeastern Tropical Advanced Remote Sensing (CSTARS, Hans Graber director). We use the WiSAR wind vector fields as input to our SLP pattern and SLP-filtered surface wind retrieval system. Because the pressure gradient force is a dominant term in the PBL momentum budget, the imprint of the surface stress field can be used to estimate the surface pressure gradient field through the use of a diagnostic PBL model. In its simplest form, PBL model assumes that the mean advective forces are relatively small and that the flow is neutrally-stratified and barotropic. The standard PBL model includes the effects of thermal winds, boundary layer stratification, a gradient wind correction for curved flow and momentum entrainment across the boundary layer top. In tropical cyclones, the nonlinear momentum terms are of leading order, comparable to the pressure gradient forcing. We significantly improved the nonlinear dynamics representation in terms of a modified gradient wind correction for TC conditions,

which added a second tuning parameter to the PBL model. We also developed and included an important correction for the inherent radial dependence of boundary layer depth in a strong swirling vortex consistent with the vortex boundary layer model developed in Foster (2009). Once the pressure gradient fields have been obtained from the surface winds and the PBL model, a least-squares optimization technique is used to find the best-fit, zero-mean surface pressure pattern that matches the pressure gradient field. If pressure observations are available, the average difference between them and the zero-mean field is the least-squares optimal estimate of what is effectively the integration constant that results from converting pressure gradients into a pressure field. The premise of using pressure data for SAR wind Cal/Val is based on the following fact: Even without using ancillary data to set the absolute value of the pressure field, the bulk pressure gradient (BPG) between any two points in the SAR-derived pressure field is the optimal estimate of that pressure difference derived from the SAR imagery. Hence pressure differences are more useful than point-by-point pressure comparisons assessing the quality of surface wind retrievals. The derived SLP patterns may be used as inputs to the PBL model to re-derive an "SLP-filtered" surface wind field. This product is a scene-wide estimate of the surface wind vectors that enforces consistency between the all of the wind vectors and the pressure fields. We have extensively documented this overall methodology and the high quality of our SLP fields and derived wind vectors using QuikSCAT and ASCAT scatterometer wind vector data in several papers (Patoux et al. 2003; 2008; 2011). Our applications to TC conditions with SAR wind vectors have shown that both the directions and speed in the SLP-filtered winds can be significantly changed from the raw input winds. In particular, the GMFs in TC conditions work best when the surface winds are across the radar beam and work poorly when the radar beam looks either up- or down-wind. The SLP-filtered winds "fill-in" the low wind holes near the TC core in these up- and down-wind regions. They can also fill in regions in the SAR WiSAR product that have been masked due to rainy conditions or for being out of range of the GMFs. Prior to the ITOP field campaign, we had only a handful of good SAR cases to study with near-in-time in situ data (dropsondes and stepped-frequency microwave radiometer, SFMR, surface wind speeds). Examination of these cases has shown that the SLP-filtered wind speeds are a major improvement over the input wind speeds. A qualitative inspection of the wind directions suggests that they are more realistic than the input directions, which tend to have too little inflow in the inner core region. However, validation of wind directions is currently on-going using data from the ITOP experiment. We now describe how a SAR-derived pressure field can be used to calibrate the surface winds. We pose the Cal/Val problem as an optimization problem in which we seek the minimum adjustment to the surface vector field that will minimize the difference between the SAR BPG and that derived from observations. A first-guess surface wind vector field from SAR is produced by WiSAR from which we calculate a first-guess surface pressure field. Given multiple surface pressure observations within this field, e.g. from dropsondes or aircraft-deployed buoys, we can calculate multiple, M= N*(N-1)/2, BPGs within the image. The cost function to be minimized is the RMS difference between the SAR-derived BPGs and the observations along with constraints on the corrections to the wind field so that the optimization procedure does not impose unreasonable wind vector corrections. Each optimization step adjusts the surface wind vectors and recalculates the surface pressure field and the BPGs. The optimization treats the U and V components of the SAR winds separately since their error characteristics are approximately independent and Gaussian (Freilich, 1997). The computation cost is nontrivial because each step in the optimization requires a new nonlinear surface pressure field in order to evaluate the cost function. It should be emphasized that since surface pressure fields are integral properties of the surface vector wind fields, wind adjustments must occur over a broad spatial region rather than just locally near the pressure data. Thus, even though we use point wise pressure data, they imply wind corrections at a large number of wind vector cells. RESULTS To date we have focused on improving the PBL model and on producing SLP-filtered surface winds from the SAR images. Only a few simple iterations of the optimization scheme have been attempted. Much of the research involved a collection of historical Canadian RadarSAT-1 SAR images from the Hurricane Watch Program provided through an announcement of opportunity by the Canadian Space Agency, NOAA, NASA and CSTARS. From this collection, we examined a number of typhoons and hurricanes. The methodologies were developed and improved using these data prior to the ITOP field program. We will focus the presentation on the ITOP data from three images of Western pacific typhoons that span the range from a weak Cat-1 typhoon to a Cat-5 super-typhoon and from excellent in situ data to no in situ data. Typhoon Malakas, 22 Sep, 2010, 20:30 UTC At the time this image was acquired, Malakas had just reached typhoon strength. It also has the best in situ data coverage of any of the images. The C-130 aircraft was within the SAR scene at the time of acquisition for very complete storm survey between 20:00 to 01:00 (23rd) UTC that included 31 drop sondes and SFMR winds. Because the storm was a weak Cat-1, the wind speed range was within reach of the standard GMF, CMOD5N. The image was acquired in HH polarization, so we had to apply the Thompson polarization correction using the parameter α = 0.8. The storm center was in the low incidence angle region of the image, so saturation was an issue. The C-130 aircraft data were mapped to the SAR image using a two-step process. First, we used the NOAA Hurricane Research Division (HRD) flight-level storm center estimates to find the best-estimate eye location

for the complete C-130 storm survey. Similarly we calculated the eye location for each time along the drop sondes' descents. From these, we calculated the distance and azimuth from the storm center for each individual SFMR or sonde measurement. An initial estimate of the storm center at the SAR overpass time was interpolated from the HRD best track. Adjusted latitudes and longitudes relative to this center were calculated from the instantaneous distances and azimuths. The HRD center estimate at the overpass time can differ from the center directly estimated from the SAR image due to errors in the flight level estimates, tilt in the storm with height and the possibility of multiple near-surface circulation centers due to complex inner core dynamics. So, a final constant translation to be applied to all of the adjusted data locations is obtained from the difference between the SAR-estimated and HRD centers. The C-130 flight track normalized to the SAR overpass time is shown in Figure 1. Figure 2a shows the input wind field using the merged GD/NURC wind directions and the CMOD5N GMF. This is a descending pass and the low incident angles are along the right edge of the image. The winds were retrieved on 1 km pixels. The white vectors are spaced 30 km apart and have uniform length. The superposed black vectors are 10 m wind directions from the C-130 drop sondes. The sonde surface wind speeds are plotted as white-outlined boxes with the same colormap as the SAR wind speeds; they should fade into the background if the speeds agree. Figure 2c shows the derived SLP pattern normalized using the drop sonde splash pressures, which are shown a color shaded white-outlined boxes. The SLP-filtered winds are shown in Figure 2b. Note the significant changes in both wind speed and direction between the SLP-filtered winds and the raw CMOD5N input winds. The SAR wind speeds are compared with the SFMR surface wind speed estimate in Figure 3a. The GMF for the SFMR surface wind speeds is calibrated to produce approximately 1-min average winds; SAR wind speeds represent 10-min averages. The SAR winds are multiplied by 1.2 to compensate for the differences in GMF calibration. Both the raw and SLP-filtered speeds compare well, but the SLP-filtered winds track SFMR better. A first check on the SAR-derived SLP is shown in Figure 3b. The C-130 flight-level data include an estimate of the surface pressure below the aircraft. The SAR SLP underneath the C-130 track the C-130 surface pressures quite well. The best test of the methodology is shown in Figure 4a. The SAR SLP pattern is normalized to the drop sondes. However, the relatively small scatter shows that the shape of the pressure pattern is good. A better test is shown in Figure 4b, which compares the pressure differences between all pairs of sonde surface pressures with the corresponding SAR SLP pressure differences. If the shape of the retrieved pressure pattern is accurate, the slope of the best fit line should be unity, which we find to be the case. The in situ data confirm that the SAR-derived SLP pattern agrees well with the drop sonde data. Overall, the comparison between the SAR SLP field and the SLP-filtered winds with the C-130 data shows that the methodology has worked very well in this case. There are evident issues with the wind retrievals in the low incidence angles (northeast side of the storm). In these cases the CMOD5N model (with polarization conversion) could not match the backscatter and selected the closest match to the backscatter for the given viewing geometry. Because the SLP-filtering acts as a scene-wide retrieval, it finds that slightly different wind directions are a better overall fit to the inputs. The GMF in high winds and low incidence angles is very sensitive to the wind direction. If the SLP method is viable, we can use the SLP-derived wind directions to improve the CMOD5N wind retrievals. We use the SLP-filtered directions as inputs to CMOD5N and produce a new wind field iteratively. The results are shown in Figure 5. Figure 5a shows the raw input winds. The dark blue patch to the northeast of the storm center is the region of no CMOD5N retrieval. Figure 5b shows the result of a single iteration using SLP-filtered directions and Figure 5c shows the result of a second iteration. Note that the region of no solution shrinks after each iteration. Typhoon Megi 15 October, 2010 21:00 UTC Typhoon Megi was a very small, very strong typhoon that propagated very rapidly across the Pacific. The compact size presents a major challenge to the PBL model used in the SLP retrieval, and the results show the further research is needed to improve its performance for very intense storms. At the time the image was acquired, the C-130 aircraft was dispatched from Guam to deploy a string of buoys across the predicted path of the storm. It made a mini survey of the storm on its return flight about six hours after the satellite overpass during which time the storm propagated about 100 km to the west. So, there is much less in situ data and the measurements were made in a different location and at a later time. However, according to the JMA best track, the storm strength did not increase significantly during this time. The aircraft data were adjusted to the SAR image time as described above; the adjusted track is shown in Figure 6. The input and SLP-filtered surface winds are shown in Figure 7ab and the SLP field is shown in Figure 7c. The small size of Megi relative to Malakas is evident. The SFMR wind speeds are plotted on Figure 7ab using the same colormap as the SAR winds, and they evidently agree better with the SLP-filtered winds than with the raw CMOD5N winds. However, the sonde surface wind and splash pressures have larger disagreement with the SAR winds and SLP. The SFMR surface winds and C-130 flight-level surface pressure estimates are compared to the raw and SLP-filtered SAR winds in Figure 8a. The agreement is best for the SLP-filtered winds on the first SW-to-NE transect of the eye and on the final eye-to-SE transect. But, due to the time difference between the overpass and the aircraft survey, it is difficult to determine which transects are most representative. The SAR/C-130 surface pressure comparison in Figure 8b suggests that the PBL model in the

pressure retrieval system is having difficulty capturing the very strong pressure gradients in this very compact storm. The scatter plots of pressure differences between the sonde splash pressures and the SAR SLP are consistent with too weak pressure gradients in this case (Figure 9). Improving the model's performance in compact storms is a focus of the research during the follow-on grant. Typhoon Megi 17 October, 2010 21:41 UTC This image captured Megi near the time that it reached super-typhoon status and just before it made landfall on Luzon. JMA estimated a central pressure of 885 mb and peak winds of 64 m/s. A C-130 drop sonde from about 9 hours earlier measured 85 m/s. This flight was the closest in time to the satellite overpass, but the JMA best track showed that the storm was continuing to deepen by at least 12 mb. Hence, for this case we do not have reliable in situ data for comparison even as it represents the most severe possible challenge to wind and pressure retrieval due to its small diameter and extreme strength. A major issue with the high wind behavior of C-band GMFs in high winds is they become multi-valued, with high and low estimates of wind speed. Usually we use the lower wind speed ambiguity. In this case however, it was not possible to generate a reasonably deep SLP field from this image. So, a small number (fewer than 200 pixels) of high wind ambiguities replaced the lower ambiguities in the inner core region. The criteria were that the radius from the eye had to be less than 35 km and the high ambiguity could not be more than 60 m/s stronger than the low ambiguity. The input winds, SLP-filtered winds and SLP are shown in Figure 10. The pressure field was normalized using the sonde splash pressures from the C-130 flight from 9 hours earlier without correction for further storm intensification. The most interesting feature of this case is the suggestion of a double eyewall in the SLP-filtered winds. Validating this structure is the focus of current research. Partial Summary of Drop Sonde Results Figure 11 show a summary from four Atlantic hurricanes and two cases from ITOP (excluding Megi) of the drop sonde splash pressure differences and SAR-derived pressure differences. Overall the agree is quite good, although further research should reduce the scatter. Also, the Megi results are inconsistent with these other cases, which suggest that further research is needed to improve the PBL model performance for the cases of small and intense storms. Summary Overall, the SLP-filtered surface wind fields appear to be an important improvement over the standard surface wind retrieval methods for tropical cyclones. We are continuing to validate the methodology and to improve the central PBL model used in the pressure gradient estimates.

REFERENCES Ellis, Ryan S Businger 2010: Helical circulations in the typhoon boundary layer. J. of Geophys Res 115, D06205, doi:10.1029/2009JD011819 Foster RC 1997: Structure and energetic of optimal Ekman layer perturbations, J Fluid Mech., 333, 97-123. Foster, R. C., 2005: Why rolls are prevalent in the hurricane boundary layer. J. Atmos. Sci., 62:2647–2661. Foster RC 2009: Boundary-layer similarity under an axi-symmetric, gradient wind vortex. Bound.-Lay Meteorol. 131 321-344. Freilich, MS 2001: Validation of Vector Magnitude Datasets: Effects of Random Component Errors, J Atmos. Ocean Tech, 14, 695-703. Lorsolo S, J L. Schroeder, P Dodge, F Marks Jr. 2008: An Observational Study of Hurricane Boundary Layer Small-Scale Coherent Structures, Mon Wea Rev. 136, 2871-2893 Morrison, I., S. Businger, F. Marks, P. Dodge, and J. A. Businger, 2005: An observational case for the prevalence of roll vortices in the hurricane boundary layer. J. Atmos. Sci., 62:2662–2673. Mourad PD and RA Brown 1990: Multiscale large eddy states in weakly stratified planetary boundary layers, J. Atmos. Sci., 47, 4, 414-438 Patoux J, RC Foster and RA Brown, 2003: Global pressure fields from scatterometer winds, J Appl Meteorol., 42 813-826. Patoux, J Foster RC and RA Brown 2008: An evaluation of scatterometer-derived ocean surface pressure fields, J Appl. Meteor. Clim. 47, 835-853. Patoux, J, RC Foster and RA Brown, 2011: Cross-validation of scatterometer measurements via sea-level pressure retrieval, submitted to J Geo Phys. Res. Wurman J and Winslow 1998: Intense Sub-Kilometer-Scale Boundary Layer Rolls Observed in Hurricane Fran, Science, 280 555-557. Zhang, J. A., K. B. Katsaros, P. G. Black, S. Lehner, J. R. French, and W. M. Drennan, 2008: Effects of roll vortices on turbulent fluxes in the hurricane boundary layer. Bound-Layer Meteor. 128, 173-189.

Wind Measurements in the Ferry Box System for Validation of SAR Wind Gradients

Birgitte Furevik [1], Knut-Frode Dagestad [2], Kai Sørensen [3], Uta Brandt [3]
[1]Norwegian Meteorological Inst. , NO
[2]Storm GEO , NO
[3]Norwegian Institute for Water Research , NO

Abstract

Wind from Synthetic Aperture Radar (SAR) often show very strong gradients at offshore flow conditions along the Norwegian coast. Wind from SAR may be very useful in near-coastal weather forecasting, if we are able to verify the observed gradients and further use SAR to verify the high resolution numerical weather prediction models (grid size

~1km). In the FjordVind project (partly financed by the Norwegian Space Center JOP-17.11.3) two wind sensors was mounted onboard M/S Trollfjord in March 2011. M/S Trollfjord is a passenger ship on the route "Hurtigruten" between Bergen on the west coast of Norway to Kirkenes in Northeast. The wind recordings are logged in the FerryBox system. From a longer time period, it is possible to collect a number of cases like presented in Furevik, Johannessen and Sandvik (2002) SAR-retrieved wind in Polar Regions – Comparison with in situ data and atmospheric model output, IEEE TGRS, vol. 40(8), and this way obtain more documentation of the performance of SAR winds in coastal regions. The wind sensors are placed symmetrically on each side of the mast on the top deck of the ship and show a correlation of 0.87 with each other and practically no bias for the 1 minute recordings. There are few in situ stations to validate the ship measurements against, but the available observations indicate that the measurements are good for strong winds but may be less reliable at low winds. SAR wind speed has been calculated from Envisat ASAR Wide Swath images with the CMOD4 algorithm with wind direction taken from a NWP model (HIRLAM). The mean wind speed from SAR over 4 years are compared to corresponding averages of wind speed from HIRLAM. The agreement is good offshore, but shows some deviation on the coast, where the measurements from Trollfjord is the only source of data for validation. The available measurements along the ship track have been averaged and are compared to the SAR and model mean wind maps. However, since the ship passes only every 5-6 days, it will take a few years to collect a data set large enough for validation of the mean wind speed. The poster will show the preliminary results.

On the Generation of Higher Level Wind Products from Level 2 SAR Wind Products

Alexis Mouche [1], Fabrice Collard [1], Nicolas Longépé [1], Bertrand Chapron [2], Knut-Frode Dagestad [3], François Vandenberghe [4], Solène Jousset [1]
[1]CLS , FR
[2]Ifremer , FR
[3]StormGeo AS, NO
[4]NCAR , USA

Abstract

Since the launch of ENVISAT in 2002, a substantial amount of acquisitions have been made in wide swath mode, providing a very good coverage of many coastal regions. In parallel, much effort has been devoted to improving the inversion of sea surface winds from SAR imagery, and Level 2 SAR winds are now routinely produced by several groups. This work aims to investigate different leads to take benefit of this historical data set of SAR winds. In particular we show how SAR can be used to characterize complex coastal wind regimes at high resolution, and we compare this to atmospheric models such as WRF in order evaluate their performances. The spatial coverage as well as the irregular revisit time of SAR sensors is considered as inadequate for direct use of SAR winds in operational weather forecasting or for assimilation into numerical forecast models. We propose here an alternative method: to develop a transfer function which can prescribe (emulate) a high resolution wind field from a given lower resolution weather forecast model field. Such a transfer function (or emulator) can be trained to learn particular wind conditions of specific coastal regions by co-locating a large historical dataset of model and SAR derived wind fields. Once developed, this emulator can then be used in real time, or even forecast situation, to emulate the high resolution wind fields from the coarse model output, without the need for additional real time SAR data.

An Experiment for High Speed Retrieval by ENVISAT-ASAR Cross-Polarized Observations

Guo Jie [1], He Yijun [2]
[1]Yantai Institute of Coastal Zone Research,Chinese Academy of Sciences , CN
[2]School of Marine Sciences , CN

Abstract

Sea surface wind vector is an important physical parameter for understanding of atmospheric dynamics, air-sea interactions, and climate. There are three satellite sensors can be used measure wind vectors from space, such as radiometer, altimeter, and synthetic aperture radar (SAR). Among them, SAR has advantage as it has high spatial resolution, large coverage and can observe sea surface independent of cloud cover. Generally, there are two approaches for wind vectors retrieval by co-polarization SAR measurements. The first one is based on the analysis of spectral features of SAR imagery [1]. It uses an empirical linear relation to evaluate wind speed from azimuth cut off frequency. The Second method retrieves wind vector from geophysical model function (GMF). The GMF is derived from scatterometer observations, which is a function of wind speed, relative wind direction and radar incidence angle [2, 3]. However, the single polarization SAR image has some limitations to obtain ocean surface wind. For example, the wind direction has to be known from external sources, inaccurate wind directions are able to cause wind speed retrieval errors. Moreover, conventional GMFs are saturated under high wind conditions. Zhang et al. (2011) found that the normalized radar cross sections (NRCS) in co-polarization and cross-polarization are different; the latter is independent of radar incidence angles and wind directions, but is quite linear with respect to wind speeds. Based on this special characteristic, a new method to retrieve high wind speed using RADARSAT-2 cross-polarization hurricane SAR imagery was present by Zhang biao et al. (2012). Hwang et al. (2011) compared satellite quad-polarization measurements with the composite surface Bragg (CB) theory. They also found the cross-polarization data are more sensitive to wind speed compared to theoretical prediction, thus retrieval of high winds is more accurate. [4]. In this paper, we provide a new method to retrieve wind vector by ENVISAT ASAR Dual-Polarization data. As they have differences in the equipment itself, different calibration and noise floor between RADARSAT-2(-35dB) and ENVISAT (-22¡«-25dB). We use 12 of ENVISAT ASAR images (VV-VH polarization) data (Medium resolution), pixel spacing is 75 m, 100¡Á100 pixels as a unit of account. As there are no buoys observations can be collocated with SAR images, we use Advanced Scatterometer data to match up with them (766 data). The spatial and time differences between SAR and ASCAT measurements are 0.15¡ã and 1 hour. We use 424 sampling point of data set (wind speed >8 m/s) to fit relation between the cross-polarization normalized radar cross section (NRCS) and wind speed at 10-m height (see equation 1). ¦Ò=0.24*U10-25.51 (1) Where ¦Ò is cross-polarized NRCS, U10 is wind speed. We use ASAR data to retrieve wind speed and to retrieve wind direction by CMOD5(we use start wind speed and wind direction of ASCAT to remove blur)that compare with ASCAT data to verify equation (1) yield average absolute bias, average absolute error, and root-mean-square error of 0.05m/s, 1.13m/s, and 1.41m/s, respectively. The wind direction is -0.16¡ã, 13.04¡ã, and 16.16¡ã, respectively. We found that when the wind speed <15m/s is not good by equation 1 as noise floor. In a word, the high wind speed retrieves by equation 1 is feasible from ENVISAT ASAR (VV-VH polarization) data.

Sea Ice Retrievals and Applications

Classification, Concentration Estimation and Seasonal Trend Analysis of Arctic Sea Ice Using RADARSAT-2

Saba El-Hilo [1], Tom Zagon [2], Don Isaacs [2], Gordon Staples [1], Matt Arkett [2], David A. Clausi [3], Christian Nadeau [1]
[1]MDA Corporation , CA
[2]Canadian Ice Service , CA
[3]University of Waterloo , CA

Abstract

We present a processing chain that derives sea ice information from co- and cross-polarized (HH and HV) ScanSAR Wide RADARSAT-2 (RS-2) synthetic aperture radar (SAR) images. Our processing chain focuses on several sea ice charting problems: i) Sea ice mapping i.e., separating sea ice from open water. ii) Sea ice type mapping, the segmentation of ice regions into regions containing consistent ice types, such as Multi-Year ice (MYI) and First-Year ice (FYI). iii) Automatic calculation of total and ice-type specific concentration, and iv) seasonal trend analysis of sea ice over an area of interest. The sea ice-water separation and sea ice classification output is used for the ice concentration calculations, which in turn is used for the seasonal trend analysis. The goal of the seasonal trend analysis is to provide the capability to monitor sea ice concentration changes over time for a specific area to help determine the start and end of the ice season. Our sea ice classification is performed using a multichannel data fusion algorithm designed for sea ice-water separation and sea ice classification. The algorithm uses co- and cross polarized RS-2 SAR images and image texture features. We demonstrate that using the SAR backscatter alone has limited capability in separating sea ice from water and that combining backscatter information with texture features improves sea ice-water separation and ice typing. The texture features are second-order parameters derived from the gray level co-occurrence matrix (GLCM), which describe the spatial organization of the backscatter and can be used to describe sea ice information within the image. In this work, three textural parameters derived from the GLCM were examined: entropy, dissimilarity, and contrast. Each of the three texture features are computed over four different directions resulting in a total of 12 texture features. We performed texture statistics analysis on selected regions from a set of six RS-2 images that span several months to assess the universality of the examined texture parameters and their dependence on environmental conditions and seasonal effects. The results of our analysis demonstrate the capability of the GLCM texture statistics in separating water from sea ice and that ice can be uniquely identified using the texture parameters. The co-polarized channel was used for calculating the texture features whereas the backscatter information from the cross-polarized channel was used in our classification process. Our technique performs ice classification using a per pixel supervised scheme. Feature vectors for sea ice and water were computed in terms of the texture parameters and comprised of the mean value for each of the features yielding distinct vectors that act as signatures for sea ice and water. Classification is then performed by assigning each pixel to the class with the minimum Euclidean distance from each feature vector. As for the estimation of the total ice concentration, it is performed using a spatial filtering approach that attempts to estimate the percentage of ice pixels within a region. The input to the spatial filtering process is the water and sea ice segmentation result. The output of the spatial filtering is a colour-coded ice concentration image that emulates the manual ice chart concentration levels traditionally used by an ice analyst, such those generated by the Canadian Ice Service. We present our classification results along with the ice concentration images and perform the validation by comparing the results to manually generated ice charts created by an expert ice analyst. The ice concentration information is also used to produce seasonal charts that demonstrate the change of ice concentration over a period of time and is also presented here. We compare our results to other techniques which include a semi-automated threshold method and a Wishart classifier, previously developed at MDA. Moreover, we present some of the challenges related to both sensor and environmental characteristics associated with computer-assisted SAR sea ice classification techniques.

Integrated studies of multi-polarimetric SAR over sea ice

Nick Hughes (1), Anthony Doulgeris (2), Torbjørn Eltoft (2), Sebastian Gerland (3), Richard Hall (4), Mari-Ann Moen (2), Angelika Renner (3),
(1)Norwegian Meteorological Institute, NO
(2)University of Tromsø, NO
(3)Norwegian Polar Institute, NO
(4)Kongsberg Satellite Services, NO

Abstract:

In Tromsø, Norway a number of institutions including the Norwegian Meteorological Institute, Norwegian Polar Institute, the University of Tromsø, and Kongsberg Satellite Services, collaborate on research of remote sensing of Arctic sea ice, ranging from data acquisition, through research and development of new products, to dissemination of sea ice information products. This poster presents some of the work done with remote sensing and collection of validation data during the April 2012 cruise of the Norwegian Polar Institute on board the Norwegian coastguard icebreaker KV Svalbard. Three Radarsat-2 fine resolution quad-polarisation scenes were acquired on consecutive days (11-13 April 2011) over drifting sea ice north-west of Nordaustlandet, Svalbard. It was possible to position the ship within all three images, which in turn were also located under the ground tracks of the ESA CryoSat-2 radar altimeter on two of the days. Validation data included ice stations with drill hole and coring measurements of the ice and snow properties, a routine shipboard ice log, and thickness measurements by sledge and helicopter-borne electro-magnetic (EM) induction. These different datasets have now been combined, and a comparison of the results is shown here.

Research currently being conducted collaboratively by the Tromsø institutions, and utilising this combined data set, includes; classification of multi-polarisation SAR for detection of different types of new and first-year sea ice, improvements to automated image segmentation algorithms, development of high resolution sea ice drift and object tracking, and estimation of sea ice thickness. The objectives of these studies are to provide improved information on sea ice parameters that can be used to improve polar climate process understanding, operational model forecasts, to assess how the environment is changing, and for maritime users who require the information to assist in navigation.

Towards Automatic Classification of Sea Ice Using Dual-Polarisation SAR Data in an Operational Environment

Frode Dinessen [(1)], Nick Hughes [(1)]
[(1)]Norwegian Meteorological Institute , NO

Abstract

The Norwegian Ice service produces ice charts of the Arctic area from east Greenland to Novaja Semilija every weekday based on a manual interpretation of satellite data. The main data used are dual polarization Radarsat-2 data in ScanSAR wide mode. Four scenes are acquired each weekday utilizing the satellite morning pass. Data are analysed during the day and ice charts are issued at the end of the workday. A demand for more frequently updated ice information leads to a desire to supplement the ice charts with automatically generated analysis. In this study we have derived statistical information from the Radarsat -2 images based on the classification in the ice chart. The analysis takes into account the large incident angle in wide swath data. The information is then used as input to an automatic classification routine for separating water and sea ice. The routine has been tested on several Radarsat-2 datasets from last winter season and the results of this work are presented.

Field Campaigns for Sea Ice Detection Using Multi-frequency and Multi-polarization SAR

Chan-Su Yang [1], Hiroyuki Wakabayashi [2]
[1]Korea Ocean Research & Development Institute , KO
[2]Nihon University , JP

Abstract

We present several of our field experiments on sea ice detection and its scattering properties in the fjords Kongsfjorden and van Mijen, Spitsbergen, and in the sea of Okhotsk using multi-frequency and multi-polarization SAR data such as ENVISAT ASAR, TerraSAR-X, PALSAR, COSMO-SkyMed, and RADARSAT-2. In May of 2009 and 2010, snow and sea ice measurements were conducted over the two fjords, Svalbard, and in February 2012 at Saromako (Lake Saroma), the third largest lake of Japan located on the north-eastern shore of Hokkaido, separated from the Sea of Okhotsk by a 20 km-long sandbar (only 150-500 m wide) allowing seawater inflow through a narrow opening. The first theme describes measurements of fast ice in the fjord Kongsfjorden, Spitsbergen, in the Svalbard Archipelago, on May 23, 2009. Seasonal fast ice is an important feature for Svalbard fjords, both concerning the physical environment and the ecosystem since it grows seaward from a coast and remains in place throughout the winter. Ice thickness, snow and ice properties, and wind speed were measured, and SAR (Synthetic Aperture Radar) data was simultaneously observed two times from ALOS-PALSAR (L-band). The ice thickness was 25-35cm while the thickness of ice floe, broken from fast ice was 10-15cm. The average level of salinity was 1.9-2.0ppt during the melting period. The polarimetric data is used to extract H/A/alpha parameters of fast ice, ice floe, snow and glacier, and was classified into 18 classes from those parameters. It was found that the area of fast ice represents the surface scattering which means low and medium entropy surface scatters such as Bragg and random surfaces, but the fast ice covered with snow belongs to a zone of low entropy surface scattering like snow-covered land surfaces. The results will be contributed to variable interpretation of the interrelationships between H/A/alpha parameter and the scattering processes of sea ice. The van Mijen Fjord is well shelter from the open sea by Aksel©ªya. Further, the island hinders the easterly winds to empty the fjord for winter ice. Thus the ice conditions are stable throughout the year and very minor ridging is observed. Riding is mainly observed close to the mouth of the fjord (L©ªset, 1998; H©ªyland; 1999, 2000). We measured mainly the thickness of snow and sea ice in the ridging region and the first-year sea ice area with a thickness of 70 to 100 cm. In addition, dielectric constants of ice and snow were measured at Saromako. Analyses including comparisons with SAR data are under investigation and will be presented.

Classification of Sea Ice Types in ENVISAT SAR Images Using Automated Algorithms

Stein Sandven [1], Natalia Zakhavtkina[1], Vitaly Alexandrov[1]
[1]Nansen Environmental and Remote Sensing Center , NO

Abstract

Sea ice in the Central Arctic has been classified in Synthetic Aperture Radar (SAR) images from ENVISAT using a neural network based algorithm and a Bayesian algorithm. Since different sea ice types can have similar backscattering coefficients at C-band HH-polarization, it is necessary to use textural features in addition to the backscattering coefficients. The analysis revealed that the most informative texture features for classification of multiyear, deformed first-year, level first-year ice and nilas/open water are correlation, inertia, cluster prominence, energy, homogeneity, and entropy, as well as third and fourth central statistical moments of image brightness. The optimal topology of the neural network, trained for ENVISAT Wideswath SAR sea ice classification, consists of nine neurons in input layer, six neurons in hidden layer and three neurons in output layer. The classification results for a series of 20 SAR images, acquired in the central part of the Arctic Ocean during winter months were compared to expert analysis of the images. The results of the neural network classification show that the average errors compared with the expert analysis amount to 15%, 17%, and 20% for level first-year, deformed first-year and

multiyear ice, respectively. Use of the Bayesian algorithm shows similar classification results as the NN method for the three ice types when the resolution in the classified images is 2400 m for both methods. The Bayesian method is pixel-based and can provide higher resolution in the classified image and therefore better capability to identify leads. Development of automated algorithms will improve exploitation of SAR data from Sentinel-1 in ice monitoring services.

Other

SOPRANO Demonstration-Service for the Delivery of SAR Ocean Demo-Products from ESA SAR Data

Marcus Engdahl [1], Alexis Mouche [2], Fabrice Collard [2], Manuel Goacalou [2], Romain Husson [2], Romain De Joux [2], Vincent Kerbaol [2]
(1)ESA , IT
(2)CLS , FR

Abstract

The Soprano web-service has been set up within the framework of ESA-funded R&D-projects developing Wind-, Wave- and Surface-Current retrieval from SAR data. The poster will describe the Soprano web-service including available demo ocean product types, spatio-temporal coverage of the available products, download statistics etc

On Physical Principles of Characterization of Algae Bloom using SAR

Stanislav Ermakov [1], Irina Sergievskaya [1], Ivan Kapustin [1], Tatiana Lazareva [2]
[1]Institute of Applied Physics, RU

Abstract

Intensive algae bloom is a serious threat for the ecology of inland waters and shelf areas. Satellite optical and IR methods used to monitor eutrophication areas have significant limitations in operation, in particuar, under cloudy sky conditions. A very effective all-weather tool for ocean remote sensing is satellite SAR. In spite of some evidence that algae bloom areas can be detected using SAR the physical mechanisms of the action of phytoplankton on the radar return is not understood yet.This work aims to understand beter such mechanisms. The influence of algae bloom (phytoplankton) on X-band radar backscattering from surface wind waves has been studied in field experiment on the Gorky Water Reservoir. Samples of biogenic film from the water surface and volume water samples with phytoplankton have been collected simultaneously and nearly co-located with radar probing of surface wind waves. Phytoplankton biology as well as total phytoplankton concentration and its variations in the studied area were analyzed in laboratory. It is obtained that the intensity of X-band radar backscattering decreased monotonically with phytoplankton concentration in the upper water layer. The surface and volume samples have been used to study the damping of gravity-capillary waves in laboratory, the film elasticity and effective water viscosity values and their dependencies on phytoplankton concentration have been obtained. The increase of effective water viscosity and the film elasticity due to phytoplankton are shown to be the main physical mechanisms of enhanced wind wave damping, and, correspondingly, of radar backscatter depression. The depression of radar return due to enhanced water viscosity and film elasticity has been calculated theoretically for the conditions of the experiment, theory and observations are found to be in good agreement. Since both the film elasticity and effective viscosity depend on phytoplankton concentration the latter can be potentially estimated from SAR observations.

On the Use of Multi-Frequency SAR Data to Improve the Monitoring of Intertidal Flats on the German North Sea Coast

Martin Gade [1], Kerstin Stelzer [2], Jörn Kohlus [3],
[1] Universität Hamburg, DE
[2] Brockmann Consult GmbH, DE
[3] Landesbetrieb für Küstenschutz, Nationalpark und Meeresschutz Schleswig Holstein, DE

Abstract

High-resolution multispectral remote sensing data from satellite-borne optical sensors are already being used for the classification of sediments, macrophytes, and mussels on exposed intertidal flats in the German Wadden Sea. Since the use of those sensors in northern latitudes is strongly limited by clouds and haze, we included synthetic aperture radar (SAR) data, allowing for an observation of intertidal flats that is independent of cloud coverage and daytime. The data acquired at different radar bands (L, C, and X band, from ALOS PALSAR, ERS SAR, Radarsat-2 and ENVISAT ASAR, and TerraSAR-X , respectively) have been used to analyse their potential for crude sediment classification on dry-fallen intertidal flats and for detecting benthic fauna such as blue mussel or oyster beds.

The integration of SAR data into an existing classification system results in a significant improvement of the classification of different surface types, particularly of mussel or oyster beds. We demonstrate that mussel and oyster beds can be detected at all deployed frequency bands, i.e. by all sensors used. In this frame, our statistical, multi-temporal analyses provided most promising results. The joint processing of SAR images of various sensors, working at different radar frequencies, has shown that surface roughness parameters can be obtained through the inversion of the Integral Equation Model (IEM), even when the input data were acquired at different times and from different platforms. The information gained from the optical and SAR sensors, along with in-situ observations, is used to improve an existing classification system.

In addition to the routine sediment classification, for the first time, data from the high-resolution TerraSAR-X are used to demonstrate that residuals of former settlements and agricultural areas, lost during storm surges in the 14th and 17th centuries, can be detected from space. This finding has provided a completely new application field for SAR data, since such residuals haven't been observed on satellite imagery so far, and the analysis of TerraSAR-X data has already enhanced the knowledge about land use residuals, which were so far unknown. The SAR data are complemented by aerial photographs and in-situ data.

Notes